

UNIVERSITY OF ALBERTA

Characterization of Active Glucose Oxidase Langmuir-Blodgett Films

by

Xiaodong Zhang



A thesis submitted to the Faculty of Graduate Studies and Research in partial fulfillment of the requirements for the degree of **Master of Science**.

Department of Chemistry

Edmonton, Alberta

Fall, 1996



National Library
of Canada

Acquisitions and
Bibliographic Services Branch

395 Wellington Street
Ottawa, Ontario
K1A 0N4

Bibliothèque nationale
du Canada

Direction des services
d'acquisitions et
bibliographiques

395, rue Wellington
Ottawa (Ontario)
K1A 0N4

Your file *Voire référence*

Our file *Notre référence*

The author has granted an irrevocable non-exclusive licence allowing the National Library of Canada to reproduce, loan, distribute or sell copies of his/her thesis by any means and in any form or format, making this thesis available to interested persons.

L'auteur a accordé une licence irrévocable et non exclusive permettant à la Bibliothèque nationale du Canada de reproduire, prêter, distribuer ou vendre des copies de sa thèse de quelque manière et sous quelque forme que ce soit pour mettre des exemplaires de cette thèse à la disposition des personnes intéressées.

The author retains ownership of the copyright in his/her thesis. Neither the thesis nor substantial extracts from it may be printed or otherwise reproduced without his/her permission.

L'auteur conserve la propriété du droit d'auteur qui protège sa thèse. Ni la thèse ni des extraits substantiels de celle-ci ne doivent être imprimés ou autrement reproduits sans son autorisation.

ISBN 0-612-18343-2

Canada

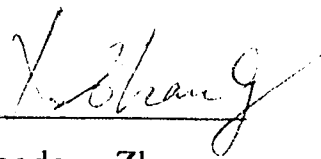
UNIVERSITY OF ALBERTA

Library Release Form

Name of Author: Xiaodong Zhang
Title of Thesis: Characterization of Active Glucose Oxidase
Langmuir-Blodgett Films
Degree: Master of science
Year this Degree Granted: 1996

Permission is hereby granted to the **University of Alberta Library** to reproduce single copies of this thesis and to lend or sell such copies for private, scholarly, or scientific research purposes only.

The author reserves all other publication and other rights in association with the copyright in the thesis, and except as hereinbefore provided, neither the thesis nor any substantial portion thereof may be printed or otherwise reproduced in any material form whatever without the author's prior written permission.

Author's Signature: 

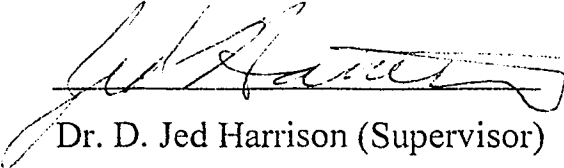
Xiaodong Zhang
607F, Michener Park
Edmonton, Alberta
Canada T6H 5A1

Date: *Sept 5, 1996*

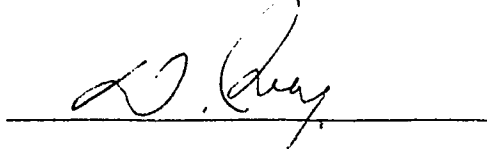
UNIVERSITY OF ALBERTA

Faculty of Graduate Studies and Research

The undersigned certify that they have read, and recommend to the Faculty of Graduate Studies and Research for acceptance, a thesis entitled **Characterization of Active Glucose Oxidase Langmuir-Blodgett Films** submitted by **Xiaodong Zhang** in partial fulfillment of the requirements for the degree of **Master of Science**.


Dr. D. Jed Harrison (Supervisor)


Dr. Mark McDermott


Dr. Doug Ivey

Date: *Aug 29, 96*

ABSTRACT

The research undertaken during the course of this program was concerned with the characterization of active glucose oxidase Langmuir-Blodgett (LB) films.

Active glucose oxidase LB films were prepared and characterized by area-surface pressure isotherms, ellipsometry, electrochemistry activity, quartz crystal microbalance (QCM), transmission electron microscopy (TEM) and atomic force microscopy (AFM) techniques.

The LB films of glucose oxidase modified with glutaraldehyde gave a thickness of 45 Å/layer by ellipsometry. The activity of the modified glucose oxidase LB film is 4 times that of conventional bovine serum albumin (BSA) film.

The QCM study results in a area/molecule of 5611 Å² and 5723 Å² for modified glucose oxidase and native glucose oxidase, respectively. They are in reasonable agreement with the known hydrodynamic radius of glucose oxidase, 5800 Å². The surface pressure-mass isotherms from the QCM are independent on the initial surface concentration and more reliable than the surface pressure-area isotherms.

Both TEM and AFM images of modified glucose oxidase in the films show a continuous, long stranded "snake-like" shape, with some short branches attaching different strands to each other. There appears to be local order, with a parallel pattern. Overall, the LB films of glucose oxidase is locally ordered, but somewhat porous, and can not be regarded as a truly dense packed monolayer. However, the film is close to a monolayer in thickness.

ACKNOWLEDGMENTS

First and foremost, I would like to express my sincere gratitude to Dr. D. Jed Harrison, my supervisor, for his support and guidance to this project, for his encouragement and patience throughout the course of this work, and for his careful editing of the manuscript.

I am deeply indebted to a host of people involved in every aspect of this study. Mr. R. Sherburn and Dr. Ming H. Chen were very helpful at the TEM specimen preparation and the TEM microscopy. I would like to thank Dr. Randy Mikula, Dr. Ken Westra, and Mr. George D. Braybrook for their assistance with the technical problems involved with the AFM. I also thank Dr. M. Palcic for use of, and assistance with, the ultrafiltration apparatus, the Alberta Microelectronic Centre for use of the ellipsometer and the frequency counter, and CANMET for use of AFM instrument.

My committee members, Dr. D. Jed Harrison, Dr. Mark McDermott, and Dr. Doug Ivey, are sincerely acknowledged for their effort and time.

Each member of Dr. Harrison's research group is acknowledged.

Finally, I thank my wife, Jie, for her continued support and enthusiasm in all my endeavor.

TABLE OF CONTENT

CHAPTER	PAGE
1. INTRODUCTION.....	1
1.1 Glucose sensor.....	2
1.2 Active Langmuir-Blodgett (LB) films of glucose oxidase.....	7
1.2.1 Langmuir-Blodgett technique.....	7
1.2.2 Various methods used for preparing enzyme films.....	9
1.2.3 Previous study of active glucose oxidase.....	10
1.3 Quartz crystal microbalance (QCM).....	12
1.4 Ellipsometry.....	15
1.5 Transmission electron microscopy.....	19
1.6 Atomic force microscopy.....	23
1.7 Summary.....	26
1.8 References.....	27
2. CHARACTERIZATION OF LANGMUIR-BLODGETT FILMS OF GLUCOSE OXIDASE.....	33
2.1 Introduction.....	33
2.1.1 Application of the microbalance.....	37
2.1.2 The dimensions of glucose oxidase.....	38

2.2 Experimental section.....	40
2.2.1 Material used in this experiment.....	40
2.2.2 Glucose oxidase modification reaction.....	42
2.2.3 Langmuir trough.....	43
2.2.4 Film thickness measurement.....	45
2.2.5 Quartz crystal microbalance.....	46
2.2.6 Activity measurement.....	50
2.3 Results and discussion.....	51
2.3.1 Film thickness measured by ellipsometry.....	51
2.3.2 Area per molecule from pressure-area isotherms.....	55
2.3.3 Area per molecule from mass-area isotherms.....	66
2.3.4 Activity of Langmuir-Blodgett film of modified glucose oxidase.....	72
2.4 Conclusions.....	76
2.5 References.....	79

3. TRANSMISSION ELECTRON MICROSCOPY (TEM) AND ATOMIC FORCE MICROSCOPY (AFM) STUDY OF GLUCOSE OXIDASE FILMS.....	81
3.1 Introduction.....	81
3.2 Experimental.....	83

3.2.1 Preparation of glucose oxidase LB films.....	83
3.2.2 Preparation of TEM specimen.....	85
3.2.3 Preparation of AFM sample.....	87
3.2.4 TEM and AFM equipment.....	87
3.3 Results and discussions.....	88
3.3.1 Blank silicon substrate TEM images.....	88
3.3.2 TEM images of modified glucose oxidase.....	88
3.3.3 TEM images of native glucose oxidase.....	96
3.3.4 AFM images of modified glucose oxidase.....	102
3.4 Conclusions.....	108
3.5 References.....	109
4. CONCLUSIONS.....	111
4.1 Summary of the study on the LB films of glucose oxidase.....	111
4.2 Future research directions.....	115
4.3 References.....	116

LIST OF TABLES

TABLE	PAGE
1. Native and modified GO LB film thickness by ellipsometry.....	52
2. Area/molecule, \AA^2 , extrapolated from isotherms of native glucose oxidase.....	59
3. Area/molecule, \AA^2 , extrapolated from modified glucose oxidase isotherms.....	60
4. Data of absorbance measured for native glucose oxidase.....	61
2b Area/molecule from pressure-area isotherms.....	63
5. Area per molecule of native and modified GO measured by QCM.....	67
3b Summary of area/molecule from pressure-area isotherms and pressure-mass isotherms.....	71
6. Current density with glucose concentration.....	73

LIST OF FIGURES

FIGURE	PAGE
1.1 The optical system of an ellipsometer.....	18
1.2 Ray paths in the electron microscope (a) under microscopy conditions and (b) diffraction conditions.....	20
1.3 Schematic diagram of AFM imaging mode.....	25
2.1 Schematic of enzyme reaction.....	35
2.2 Schematic diagram of Langmuir trough.....	44
2.3a Schematic of QCM.....	47
2.3b Modified oscillator circuit of QCM.....	48
2.4a Isotherm of native glucose oxidase.....	56
2.4b Isotherm of modified glucose oxidase.....	57
2.5 Plot of absorbance at 450 nm <i>vs</i> concentration of native glucose oxidase.....	62
2.6 Area/molecule <i>vs</i> surface concentration of native and modified GO from pressure-area curves.....	64
2.7a Area per molecule measured by QCM as a function of surface pressure.....	68
2.7b Plot of surface pressure <i>versus</i> area per molecule.....	69

2.8	Current density as a function of glucose concentration.....	74
3.1	Shadowing used to determine thickness.....	86
3.2a	TEM image of silicon substrate. not dipped in subphase.....	89
3.2b	TEM image of the same silicon substrate as in Fig 3.2a with a magnification of 27,000.....	90
3.3a	TEM image of silicon substrate dipped in subphase.....	91
3.3b	TEM image of silicon substrate dipped in subphase with a magnification of 234,000.....	92
3.4a	TEM image of one layer modified glucose oxidase LB film coated at a surface pressure of 30 mN/m (5.54 mg/ml).....	93
3.4b	TEM image of one layer modified glucose oxidase LB film coated at a surface pressure of 30 mN/m (4.20 mg/ml).....	94
3.5	TEM image of one layer modified glucose oxidase LB film coated at a surface pressure of 30 mN/m (5.54 mg/ml) with a magnification of 234,000.....	97
3.6a	TEM image of one layer modified glucose oxidase LB film coated at a surface pressure of 30 mN/m (5.71 mg/ml) with a magnification of 109,000.....	98
3.6b	TEM image of one layer modified glucose oxidase LB film coated at a surface pressure of 30 mN/m. The solution was not filtered with a magnification of 234,000.....	99

3.7a TEM image of one layer native glucose oxidase LB film coated at a surface pressure of 30 mN/m (4.01 mg/ml) with a magnification of 109,000.....	100
3.7b TEM image of one layer native glucose oxidase LB film coated at a surface pressure of 30 mN/m (4.01 mg/ml) with a magnification of 26,000.....	101
3.8a Top view AFM image of one layer modified GO LB film coated at 30 mN/m.....	103
3.8b Two dimensional view AFM image of one layer modified GO LB film coated at a surface pressure of 30 mN/m.....	104
3.9a Top view AFM image of blank silicon substrate shadow coated with Pd/Pt alloy.....	106
3.9b Two dimensional view AFM image of blank silicon substrate shadow coated with Pd/Pt alloy.....	107

CHAPTER 1

INTRODUCTION

A sensor is an input transducer to an electronic system that converts a physical or chemical signal to an electrical signal [1]. A chemical sensor, defined by the International Union of Pure and Applied Chemistry (IUPAC), is a device that transforms chemical information, ranging from the concentration of a specific sample component to total composition analysis, into an analytically useful signal. The chemical information may originate from a chemical reaction of the analyte or from a physical property of the system investigated [2].

IUPAC states that a chemical sensor contains two basic functional units: a receptor and a transducer. The receptor transforms the chemical information about the sample into a form of energy which may be measured by the transducer. The transducer then transforms the energy into a useful analytical signal. Most chemical sensors also contain a separator which is, for example, a membrane. The selectivity of a sensor is usually contributed by this separator [3].

Chemical sensors may be classified according to the operating mechanism of the transducer. J. Janata has divided them into four groups: thermal sensors, mass sensors, electrochemical sensors, and optical sensors [4]. Another term, biosensors, is often seen in the literature. However, the principle of the transducer on which they are based is, in general, common to

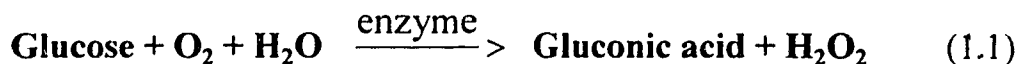
these four groups of chemical sensors. Biosensors are differentiated due to the use of biological elements, e.g., enzymes, in their receptors, and to the fact that they are used for biologically important analyses. For example, generally the transducer of the glucose sensor is an electrode, while the receptor is an enzyme, glucose oxidase.

1.1 Glucose sensor

There are about 30 million people throughout the world affected by diabetes [5]. Diabetes is now considered to be the third leading cause of death in first-world countries [1, 2]. Moreover, there is no known cure for diabetes, and all therapeutic measures are aimed at limiting the disease and relieving the patient's symptoms [6]. The most powerful and reliable antidiabetic agent known is insulin, which facilitates the metabolism of glucose that is the major end product of carbohydrate digestion. Because the glucose level in the bloodstream of a diabetic fluctuates considerably in response to ingestion of foodstuffs, activity level, and so on, the amount of insulin injected has to be adjusted accordingly or the patient may suffer severe reactions. For those insulin-dependent diabetics, therefore, it is very important to know the glucose concentration in the blood before each injection. This has spurred the development of glucose sensors.

As early as in 1962, Clark and Lyons described the determination of glucose by oxidizing it using glucose oxidase enzyme [7], which is the basis of virtually all glucose sensors and analyzers. As shown in equation (1.1),

glucose is catalyzed by the enzyme to gluconic acid in the presence of dissolved oxygen.



The concentration of glucose was determined by electrochemically measuring the extent of oxygen consumption with a Clark-type oxygen electrode [8]. The oxygen electrode consisted of a Ag anode and a Pt cathode coated with a hydrophobic gas selective membrane. Oxygen in the sample diffuses through the membrane and is reduced at the cathode. A few years later, Updike and Hicks developed a miniature glucose sensing electrode immobilized with glucose oxidase enzyme using the same principle [9]. Although the method was extended by Gough *et al.*[10] and others [11], it suffered from two drawbacks. First, the method had a high background, because the detected O₂ signal changed from high to low when glucose was present. Secondly, the relationship between the signal and the concentration of glucose became nonlinear when a large amount of glucose was present, because oxygen transport through the membrane was the limiting reagent of the reaction.

Another approach is to determine the rate of hydrogen peroxide production in reaction (1.1), reported by Guilbault *et al.* and others [12-15]. Hydrogen peroxide was electrochemically measured at a potential of about +0.7 V *versus* a saturated calomel electrode (SCE) as shown in equation (1.2).



This is the least complicated and most commonly employed detection mechanism for miniaturized glucose sensors [1].

The devices used in clinics for glucose concentration measurement fall into three main categories [16]. The first type is the dip-stick that performs *in vitro* measurement in blood samples or urine specimens. The glucose level can be read by comparing the colour developed due to the reagents on the strip with a chart or from the electrical current generated. The second type is the bench-top analyzer, most of which are based on the amperometric detection of hydrogen peroxide formed at an electrode coated with a glucose oxidase membrane. The glucose analyzers are very reliable and are used in routine clinical practice. The third type is the implantable glucose sensor for continuous monitoring of glucose concentration. The implantable glucose sensor is a goal for the future rather than an existing product.

The use of a long term implantable glucose sensor can eliminate the need for diabetic patients to prick their fingers several times every day to obtain blood samples. Moreover, glucose sensors could lead to an artificial pancreas, which includes not only a glucose sensor but also an insulin delivery system, which automatically administers the amount of insulin based on the feedback signal from the sensor [17-20]. The need for such a closed loop system has spurred research interest.

In 1974, Albisser *et al.* reported the implementation of a closed-loop glycaemic control system, which consisted of a glucose analyzer, a minicomputer and peripherals, an insulin delivery pump, and intravenous

catheters to interface with a patient [17, 18]. The system had been improved by Shichiri *et al.* in the 1980's [19, 20] by using a needle type sensor.

Considerable efforts in this field have been directed toward the design of implantable glucose sensors including the pioneering work of Shichiri *et al.* in the 1980's. Harrison *et al.* have implanted a miniature glucose sensors in dogs and the sensors functioned for more than a week [21]. Implantation of glucose sensors in dogs and rats has also been performed by Reach and Wilson [22]. Pickup [23], Wilson [24] and Harrison [25] have also implanted glucose sensors in humans.

Most implantable glucose sensors also rely on the electrochemical measurement of hydrogen peroxide generated by oxidation of glucose, which is catalyzed by the glucose oxidase enzyme as shown in equations (1.1) and (1.2). The configuration of many implantable glucose sensors comprises a Pt electrode, inner membrane, an enzyme layer, and outer membrane [22]. Ideally both inner membrane and outer membrane are selective, i.e., permeable to the concerned chemical while eliminating interferences. In fact, it is impossible to find a membrane that is absolutely selective in a very complex sample like blood. This is why two types of membranes are often used for inner and outer membranes to reduce interferences from different species.

When this sensor is implanted, glucose in the body first diffuses through the outer membrane, is catalyzed by the enzyme into hydrogen peroxide, which then permeates through the inner membrane and is detected on the Pt electrode. The inner layer needs to be selective to H_2O_2 , while the

outer layer must be selective to glucose and oxygen. The membrane used for the outer layer is important, because it must also prevent degradation of the enzyme and electrode in the biological environment, and be biocompatible as well. Biocompatibility has been defined as the ability to perform with an appropriate host response in a specific application. In other words, after implantation, a biostable environment should be rapidly formed that will be compatible with the sensor's function [22].

Several materials have been suggested for the outer membrane of implantable glucose sensors, including polyurethane [19, 26, 27], cellulose and cellulose acetate [14, 28, 29], and the perfluorinated ionomer Nafion [1, 21, 30, 31, 32]. Nafion-encapsulated glucose sensors were pioneered by Harrison *et al.* and have demonstrated superior performance both *in vitro* and *in vivo* to others in terms of response time, reproducibility and biocompatibility [31, 32, 33].

The inner layer of glucose oxidase is still the key component of a glucose sensor. Therefore, preparing active glucose oxidase films is especially important, because it provides the rapid response, high sensitivity and most of the selectivity of the glucose sensor. The understanding gained in this work may potentially lead to the development of more efficient inner layers for glucose sensors.

1.2 Active Langmuir-Blodgett films of glucose oxidase

1.2.1 Langmuir-Blodgett Technique

The Langmuir-Blodgett technique for transfer of films at the air-water interface to a solid substrate is a powerful means of obtaining organized, densely packed assemblies for a variety of applications [34, 35].

Langmuir described, in 1920, the process of transferring a floating insoluble monolayer to a solid surface by raising the solid through a monolayer-covered liquid surface. If the monolayer (e.g., a fatty acid) is under sufficient surface pressure that the molecules are close together, and the solid is clean and wetted by the liquid, the monolayer is transferred quantitatively to the solid. Langmuir demonstrated this behaviour with the aid of several simple tests based on the motion of floating talc particles or threads. He also demonstrated, by the same methods, that the attachment of the monolayer is strongly dependent on the nature of the solid. Sometimes the monolayer will float off the solid if it is reinserted into the water; in other case, the deposited film will adhere so strongly that only chemically destructive treatments, such as high-temperature oxidation or etching of the underlying solid, will remove it [36].

In order to affect a transfer, the monolayer must be under a finite surface pressure. Since the transfer process is critically dependent on the surface pressure, it is generally desirable to maintain a constant pressure as film is removed from the water surface. A variety of techniques can be applied for this purpose.

The most commonly used, of course, is Langmuir's original method [36]; because of its extensive application by Blodgett, this technique is often named the Langmuir-Blodgett method. A clean wettable solid is placed in the water before a monolayer is spread, and then drawn up through the surface after formation of the film. Alternatively, the clean, dry slide may be lowered into the water through the already-formed monolayer and then withdrawn. If the solid is water-wettable, no monolayer is deposited while the slide is passing downward through the liquid-gas interface, but only when it moves upward out of the water.

The preparation and nature of protein and enzyme films at the air-water interface have been the subject of continued investigation [37, 38, 39] since the original studies of Langmuir and Schaeffer [40], Groter [41], and others [42, 43]. It is believed that proteins that are spread at low surface concentration (less than 1 mg/m^2) are denatured at the interface through disruption and unfolding of the tertiary structure. Incomplete unfolding when concentrated films of an enzyme are prepared (greater than 1 mg/m^2) is thought to explain their retention of activity. Using the Langmuir trough, the subphase and surface composition, as well as the surface pressure can be controlled. Consequently, the LB technique provides a means of preparing oriented enzyme films with an increased accessibility of activity sites compared to other immobilization techniques. Further, many enzymes are known to self-aggregate *in vivo* where they are most stable, while others are most stable in the crystalline form. Densely packed protein films prepared by

using the LB technique may resemble these forms. Consequently, LB films may offer a means to stabilize immobilized enzymes.

1.2.2 Various methods used for preparing enzyme films

Beside the early work of Langmuir and others [37-43] on proteins spread on the air-water interface, relatively little has been reported regarding formation of enzymatically active LB films of pure enzyme [44, 45]. Much more work has focused on protein-lipid films formed by adsorption of protein from the subphase onto lipid films spread on the surface [46-52]. LB films consisting of alternative lipid and enzyme layers show activity in the case of some enzymes but not others [49-52]. Adsorption of *penicillin* onto LB films of stearic acid on a pH-sensitive electrode has been used as a means of preparing a *penicillin* sensor. Films of glucose oxidase have been prepared by covalent bonding onto an LB film of surfactant predeposited on SnO₂ [53, 54], as well as by adsorption of glucose oxidase to a lipid layer at the air-water interface prior to deposition on a solid [55, 56]. These latter methods form active films that generate H₂O₂ in the presence of glucose and O₂, but even monolayer coatings exhibit relatively low sensitivity and response times of several minutes. Hydrophobic lipid or surfactant layers are densely packed and poorly permeable to many ions and molecules [57], so that the presence of the lipid layer probably accounts for the poor sensing characteristics.

Improved response times have been reported for films prepared by first forming a water insoluble enzyme-lipid complex before spreading the compound on the subphase [58]. Unfortunately, this method dilutes the

enzyme density in the film, and deposits thicker than two monolayers have not been accomplished.

When the current is limited by the amount of enzyme, as it is for the monolayer films discussed here, increasing the amount of enzyme will increase sensitivity. Also, to increase a sensor's longevity it is desirable to have a significant reservoir of enzyme in the films [59]. Sun *et al.* reported a method of direct preparation of active glucose oxidase film, which showed that up to at least 10 monolayers can be deposited, providing rapid response time and increased electrochemical sensitivity to glucose relative to the lipid-glucose oxidase films prepared by the LB technique [60].

1.2.3 Previous study of active glucose oxidase

The purpose of this study is to characterize the preparation of active LB films of glucose oxidase prepared without the use of additional surfactants, following the procedure of Sun *et al.* [60]. The film properties of glucose oxidase have been studied by using ellipsometry, quartz crystal microbalance (QCM), electrochemical activity, transmission electron microscopy (TEM) and atomic force microscopy (AFM). The results of Sun *et al.*'s studies are summarized below.

Native enzyme LB film activity of glucose oxidase is poor, as determined by electrolysis of H_2O_2 produced by reaction with glucose oxidase and O_2 . This is thought to be due to denaturing of the enzyme at the air/water interface. A modified enzyme can be prepared by reaction with glutaraldehyde before spreading it on the subphase [60]. This treatment

results in LB films on Pt substrates that are 5 - 10 times more active, depending on the glutaraldehyde reaction conditions. Normally monomolecular layers are formed by using glucose oxidase modified by reaction with glutaraldehyde for 24 hours at 5 °C, followed by ultrafiltration to remove oligomers before spreading on the subphase [60]. These modified films exhibit an activity similar to conventional bovine serum albumin immobilized enzyme electrodes and a response time of less than 3 seconds.

Deposition at a surface pressure of 30 mN/m onto silicon substrate was reported to give a film thickness of 48 Å/layer, compared to 30 Å/layer for the native glucose oxidase [60]. Films of ultrafiltered, modified glucose oxidase appeared smooth at 70,000 times magnification using scanning electron microscopy (SEM). LB films of modified glucose oxidase that is not ultrafiltered showed even greater activity and were apparently thicker, however SEM showed these films have an island structure, so that the mass deposited was greater than for a true monolayer [60].

Homogeneous assays of the glutaraldehyde treated enzyme showed about 89% of the activity of the native enzyme, with minimal change in selectivity. Gel electrophoresis of the native enzyme using denaturing conditions gave only the 80,000 Dalton subunit, while the modified enzyme showed the presence of 11% subunit, 60% holoenzyme, and 29% oligomers of the enzyme when first reacted for 24 hours at room temperature in 2.5% glutaraldehyde [60]. The results indicate an increased resistance to denaturing following inter- and intra-molecular cross-linking with glutaraldehyde [60].

In the present work, the quartz crystal microbalance was used to determine the mass of material deposited in the Langmuir films so as to develop surface concentration - area isotherms for the Langmuir films on the subphase surface. The normal procedure, which is to measure surface pressure - area isotherms, was used by Sun *et al.*. However, it is not satisfactory, since the enzyme apparently dissolves into the subphase as the surface pressure increases. The other probes used in this study to characterize the transferred LB films were atomic force microscopy, transmission electron microscopy and ellipsometry. These tools helped evaluate the micro- and macroscopic order of the deposited films and described in the following sections.

1.3 Quartz Crystal Microbalance (QCM)

The quartz crystal microbalance (QCM) is a piezoelectric device capable of extremely sensitive mass measurements. It oscillates in a mechanically resonant shear mode by application of an alternating, high frequency electric field using electrodes which are usually deposited on both sides of the disk [61].

The mass sensitivity arises from a dependence of the oscillation frequency on the total mass of the usually disk shaped crystal, its electrodes, and any materials present at the electrode surface. These devices have been used for many years to measure the masses of films in various types of deposition processes [62]. To the extent that the density of the deposit is

known, the thickness may be calculated, so these devices are used in a number of commercial film thickness monitors. Years ago it was thought that these crystals would not oscillate in liquids, due to excessive energy loss to the solution from viscous effects. Later, Konash and Bastiaans [63] and Nomura [64] demonstrated the use of the QCM in the liquid environment for the determination of mass changes at the crystal surface. These reports made clear the potential utility of the QCM for accurate, in situ determinations of extremely small mass changes of the crystal electrodes or films deposited on them. A very important type of QCM application is the use of the QCM in an electrochemical context to monitor mass changes at electrodes. The first in situ application of the QCM to electrochemical problems was to determine Cu (2) and Ag (1) by electrodeposition [65, 66]. In addition, many other applications of QCM were reported, such as the study of monolayer and multilayer depositions and dissolutions, mass transport in polymer films on electrodes, corrosion processes at electrodes, electrolysis deposition, and mass changes caused by protein adsorption [67].

Sauerbrey was the first to recognize that the QCM could be used to measure mass changes at the crystal surface [68]. He demonstrated the extremely sensitive nature of these piezoelectric devices towards mass changes at the surface of the QCM electrodes. He also described their differential radial mass sensitivity and correlated this with the radial distribution of the vibration amplitude. The results of his pioneering work in this area are embodied in the Sauerbrey equation (1.3).

$$\begin{aligned}
\Delta f &= - (f_0 / t_q \rho_q) \Delta m \\
&= - (2 n f_0^2 / (\rho_q \mu_q))^{1/2} \Delta m \\
&= - (f_0 / N \mu_q) \Delta m \\
&= - C_f \Delta m
\end{aligned}
\tag{1.3}$$

where Δf is the observed frequency change (Hz), f_0 is the resonant frequency of the fundamental mode of the crystal, Δm is the change in mass per unit area (g cm^{-2}), ρ_q ($=2.648 \text{ g cm}^{-3}$) is the density of quartz, μ_q ($=2.947 \times 10^{11} \text{ g cm}^{-1} \text{ s}^{-2}$) is the shear modulus of quartz, N ($=1670 \text{ kHz mm}$) is the frequency constant for quartz, n is the number of the harmonic at which the crystal is being driven (i.e. 1 for the fundamental, 3 for the third harmonic, etc.) and C_f is a constant typically referred to as the sensitivity factor for the crystal employed for the measurement, which depends on the thickness, and therefore, the fundamental frequency. For a 5 MHz crystal operated in its fundamental mode, C_f is $56.6 \text{ Hz } \mu\text{g}^{-1} \text{ cm}^2$, so that a uniformly distributed mass increase of $1 \mu\text{g cm}^{-2}$ would result in a frequency decrease of 56.6 Hz. The sensitivity factor is a fundamental property of the QCM crystal. Thus these mass sensors do not require calibration. This ability to calculate the mass sensitivity from first principles is a most attractive feature of these devices.

For a 9 MHz crystal in its fundamental mode ($n=1$)

$$\begin{aligned}
C_f &= 2 n f_0^2 / (\rho_q \mu_q)^{1/2} \\
&= 2 \times 1 \times (9 \times 10^6)^2 / (2.648 \times 2.947 \times 10^{11})^{1/2} \\
&= 183.38591 \times 10^6 \text{ Hz g}^{-1} \text{ cm}^2 \\
&= 183.38951 \text{ Hz } \mu\text{g}^{-1} \text{ cm}^2
\end{aligned}$$

It is worth pointing out that the term Δm in the Sauerbrey equation is an areal mass change with units of g cm^{-2} . Couching the equation in this way emphasizes the necessity of film uniformity for the quantitative evaluation of mass changes from frequency changes. It also emphasizes that the mass sensitivity per unit area does not depend on the electrode geometry. In other words, it is the film thickness which determines the frequency change, not its total mass. The Sauerbrey equation shows the linear dependence of Δf on Δm and on f_0^2 , and the linear increase in sensitivity which accompanies the use of higher harmonics (i.e. frequency change dependence with n). The negative sign shows that increases in mass correspond to decreases in frequency.

1.4 Ellipsometry

Ellipsometry is an optical sensing technique conventionally used for measuring the dimensional change and other properties of thin films under static or very slowly changing circumstances [69].

Ellipsometry has been recommended for film thickness measurements because it is non-destructive and can be accurate with thin films [70, 71]. Semiconductor industries have used it routinely for measuring the thickness

of thin films on silicon wafers. It has also been used to study the growth of surface oxides during corrosion, passivation and electrodeposition. The application of ellipsometry has also been extended to medical and biological science, such as for studies on adsorption of proteins on a surface. Weir *et al.* report using an ellipsometer for high speed sensing of thin films and surfaces [69].

As an optical technique, ellipsometry involves illuminating the surface of a sample with a monochromatic light of known wavelength and polarization. The state of polarization changes after reflection can be measured and used to determine the thickness of the film on the sample.

Two parameters, $\tan \psi$ and Δ , are used to represent the polarization state of light [72]. $\tan \psi$ is the ratio of the reflection coefficient for the light component polarized in the plane of incidence to that for the component polarized normal to the plane of incidence. The reflection coefficients can be calculated from the incidence angle and the optical properties of the media. Δ is the relative phase difference between the light component polarized in the plane of incidence and the component polarized normal to the plane of incidence. The relationship between these two parameters and film thickness can be described by the Drude equations (1.4) and (1.5) [73].

$$\Delta - \Delta' = \frac{4\pi \cos \varphi \sin^2 \varphi (\cos^2 \varphi - \alpha)}{\lambda (\cos^2 \varphi - \alpha)^2 + \alpha^2} \left(1 - \frac{1}{n^2}\right) d \quad (1.4)$$

$$\psi - \psi' = \frac{2\pi \sin 2\psi' \cos \varphi \sin^2 \varphi \alpha_1}{\lambda (\cos^2 \varphi - \alpha)^2 + \alpha_1^2} (1 - n^2 \cos \varphi) \left(1 - \frac{1}{n^2}\right) d \quad (1.5)$$

In these equations, Δ , ψ , are the values obtained in the presence of the film whereas Δ' , ψ' are the values obtained on the bare substrate. φ , λ , n , d are the angle of incidence, the wavelength of the incident light, refractive index of the film, and the thickness of the film, respectively. α and α_1 are defined by equations (1.6) and (1.7).

$$\alpha = \frac{n_1^2 - k_1^2}{(n_1^2 + k_1^2)^2} \quad (1.6)$$

$$\alpha_1 = \frac{2n_1 k_1}{(n_1^2 + k_1^2)^2} \quad (1.7)$$

where n_1 and k_1 are the refractive index and extinction coefficient of the substrate.

The optical system of an ellipsometer is shown in Figure 1.1 [71, 74]. A monochromatic, polarized laser beam is projected onto the surface of a sample after being converted into circularly polarized light by a quarterwave plate (QWP). The reflected beam is elliptically polarized because of the changes occurring in the amplitude and phase of both the parallel and perpendicular oscillating light components as a result of the presence of a thin

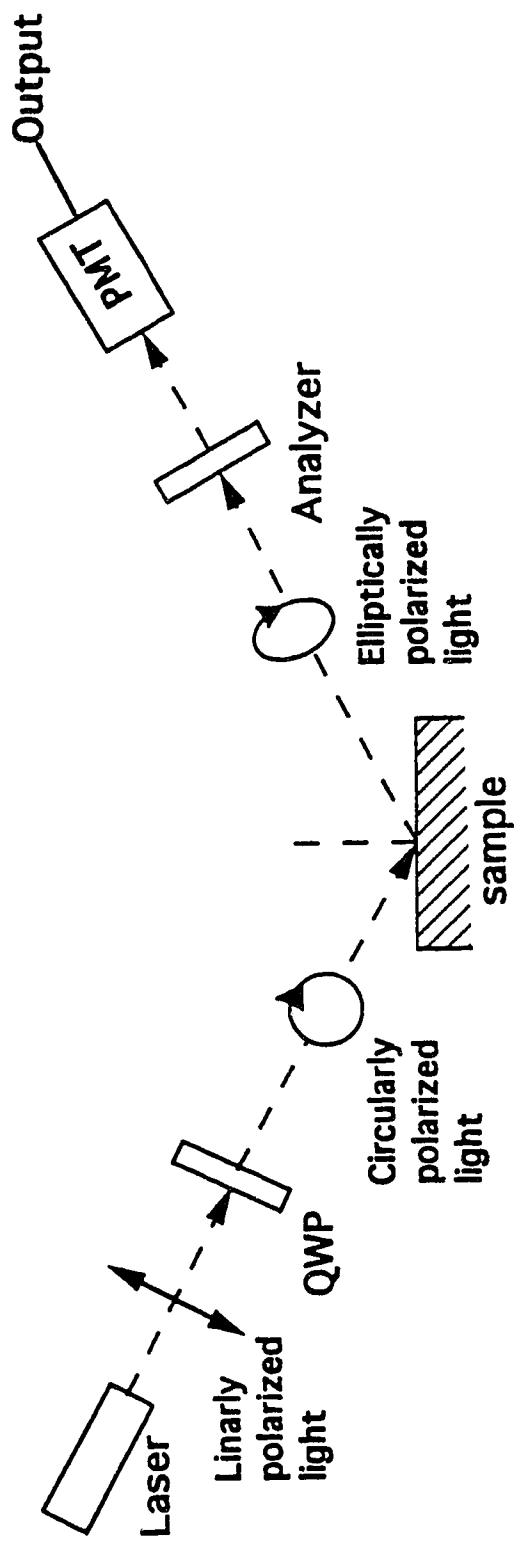


Figure 1.1 The optical system of an ellipsometer [71, 74].

film or the substrate itself. After polarization measurement by an analyzer the signal is detected by a photomultiplier tube (PMT) and then sent to a computer for a series of calculations to determine n and d from $\tan \psi$ and Δ .

1.5 Transmission Electron Microscopy

The electron microscope is now a well-established research tool both in the biological and physical chemistry domains. An electron microscope consists of an electron gun and an assembly of lenses as shown in Figure 1.2 [75] (this is an about 30 years old design). The ray paths are depicted in a microscope employing three stages of magnification and a single condenser lens system for illuminating the specimen. The lenses may be either of the magnetic or electrostatic type, although, due to the development of electronically stabilized sources of current and beam voltage, the magnetic lens is nowadays used almost exclusively because of its smaller optical aberrations and its freedom from the usual troubles associated with high voltages. In modern high resolution instruments the use of three stages of magnification (objective, intermediate lens and projector), often with a double condenser lens illuminating system, has become a fairly standard design.

The most critical component of a magnetic lens is the soft-iron pole-piece, which produces an axially symmetric magnetic field for focusing the electrons. The rest of the lens is a magnetic yoke containing the windings for

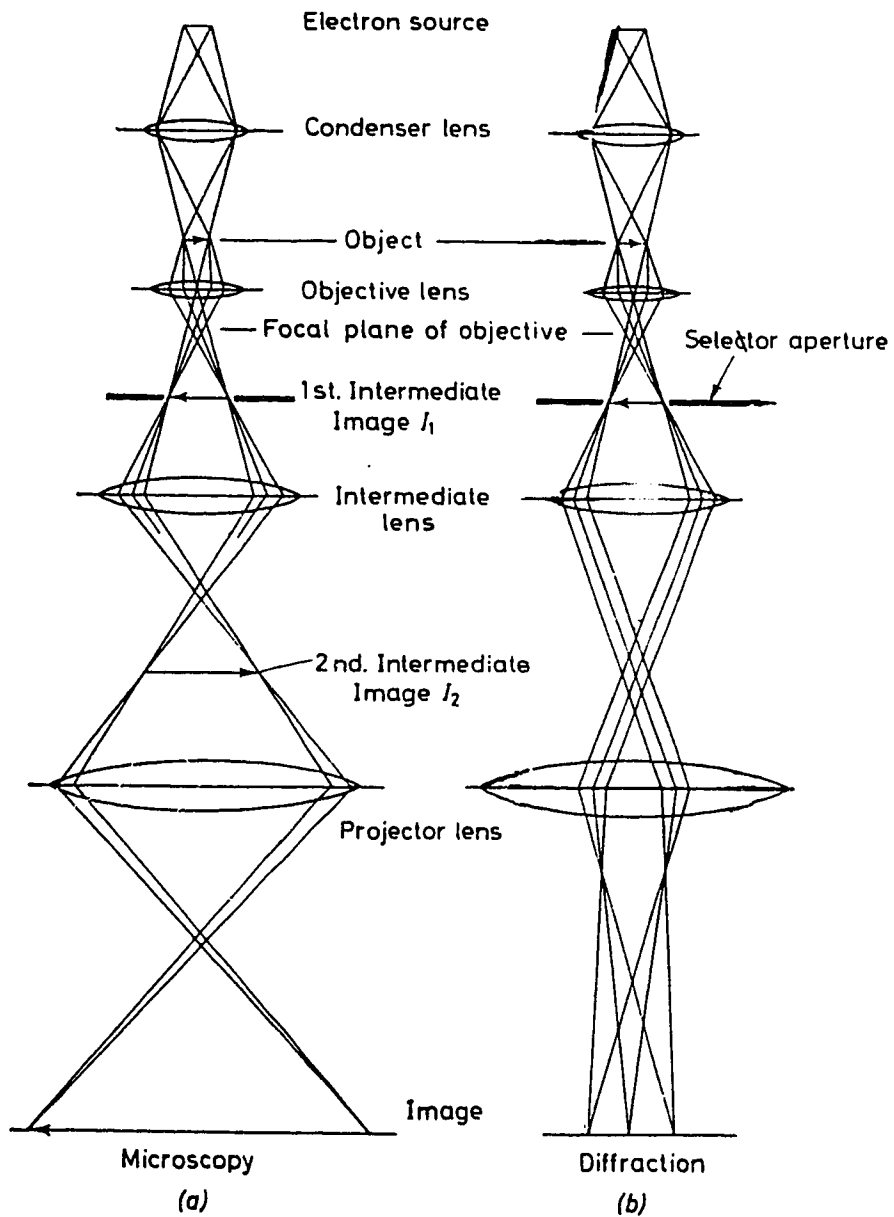


Figure 1.2 Ray paths in the electron microscope (a) under microscopy conditions and (b) diffraction conditions [75].

energizing the lens with d.c. current and varying the focal length of the pole-piece system. The specimen to be examined by transmission of electrons is placed near the entrance to the bore of the objective lens pole-piece, the design and perfection of which most influences the electron optical performance of the microscope. The magnified image I_1 (Figure 1.2) produced by the objective is called the first intermediate image. This serves as an object for the intermediate lens which produces a second intermediate image I_2 , and this is magnified further by the projector lens to produce the final image on the fluorescent viewing screen. The photographic plate for recording the image is placed immediately below this. Typical approximate magnifications produced by the various stages are: objective lens x 25, intermediate lens x 8, projector lens x 100.

Thus a total magnification of about 20,000 is obtained on the viewing screen, which is a convenient magnification for examination of many defects in crystalline materials. Since the specimen is usually in a fixed position in the objective pole-piece bore, the magnification of this stage is fixed. The final magnification may be varied by regulating the energizing currents of either the intermediate or projector lenses.

A very important part of a TEM experiment is the specimen preparation. There are many specimen preparation methods for different materials, such as electrolytic polishing, chemical polishing, vacuum evaporation or deposition, section or replication, etc.. The basic requirements for TEM specimens are simple: the two sides should be approximately parallel, thin (500 - 5000 Å) and have clean surfaces [75, 76]. A replication

method was used to prepare the glucose oxidase TEM specimen, since it is suitable for examining a surface of a bulk, fractured or etched sample.

The replication procedure includes shadowing with a heavy metal layer, followed by coating a thin (1000 - 2000 Å) layer of carbon film, then etching away the original substrate. Shadowing will improve the TEM image contrast since the vacuum evaporation of a heavy metal layer produces a high density, electron scattering layer. Deposition of metal only on one side of high features and not in the valleys results in enhanced topological imaging. It should be noted that contrast enhancement by shadowing is only applicable to bright-field imaging and the shadowing layer must precede application of a carbon support film to be meaningful [77]. The films coated with metal and carbon layers are then peeled off the substrate, by use of an etchant, then transferred onto a support grid.

It should be noted that the attainable resolution of a replica never approaches that of a directly observed specimen. The replication procedure may deform the sample during metal deposition or substrate stripping, leading to artifacts in the final carbon replica. Much care is required in preparing replica and interpreting their images [77].

1.6 Atomic Force Microscopy

The atomic force microscope (AFM) can be operated in many ways. These different approaches provide a variety of capabilities for imaging different types of samples and generating a wide range of information. Imaging modes (sometimes referred to as "scan modes" or "operating modes") are the methods that are used to move the AFM probe over the sample surface and sense the surface in order to create an image. There is a continuum of possible imaging modes, due to differing interactions between the probe tip and sample, as well as the detection scheme used [78]. The AFM operates by measuring the forces between the probe and sample. These forces depend, in part, on the nature of the sample, the distance between the probe and sample, the probe geometry, and any contamination on the sample surface.

The published technological applications of AFM already include atomic-scale friction measurements, imaging of magnetic fields above thin-film recording heads, imaging of polymers, and imaging of photoresist on silicon. AFM can also be used on a large and important class of systems: nonconductors covered with aqueous solutions. This class includes many important systems in biology, medicine, and technology; from mitochondria in cytoplasm to painted ships in seawater. The AFM obtains images fast enough (a few seconds per image) to even observe many biological and chemical processes in real time [79].

A schematic diagram of AFM imaging is shown in Figure 1.3. The laser light is focused on a cantilever and bounces off toward a photodiode. The photodiode detects the deflection of the cantilever by sensing the position of the reflected beam. In operation a feedback loop keeps the position of the reflected beam and hence the force on the sample constant. This is accomplished by moving the sample up and down with the z-axis of the piezoelectric translator as the sample is scanned underneath it with the x-and y-axes [79].

In our application, there are limitations of imaging proteins by AFM. First is lack of light, well-characterized tips on the cantilevers. Secondly, a more fundamental limitation is the protein motion in water. This may be minimized by imaging in more viscous fluids, or by lowering the temperature proteins could be imaged at temperatures near freezing in water, or for the ultimate in resolution, to liquid nitrogen temperature or below; AFMs have already been operated in cryogenic fluids [80].

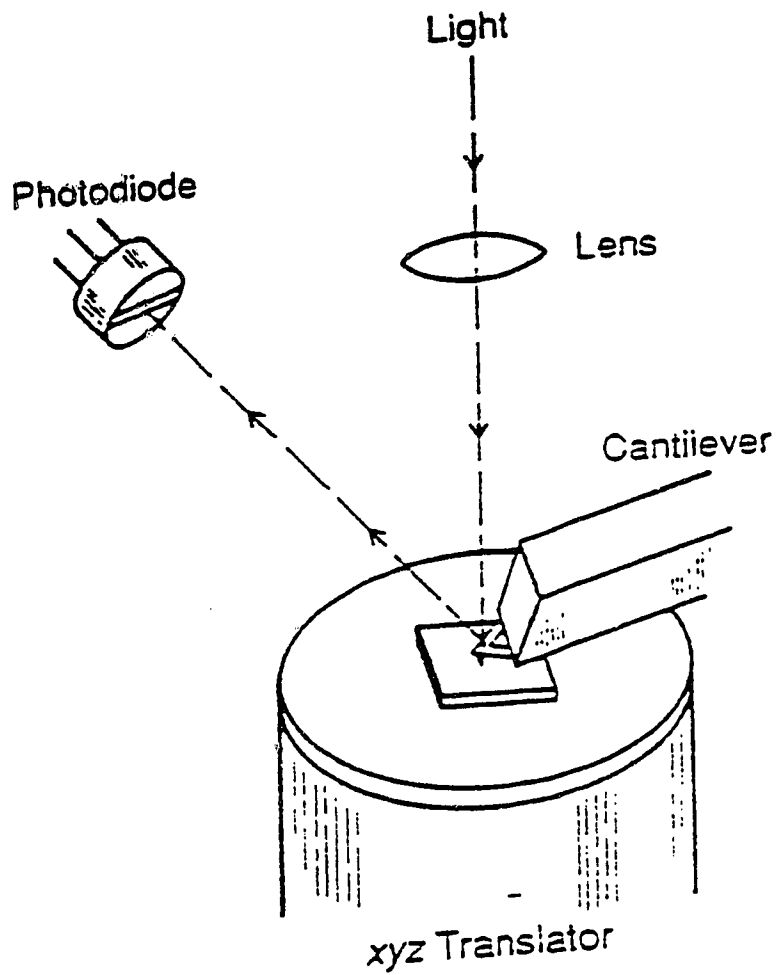


Figure 1.3 Schematic diagram of atomic force microscopy imaging mode [79].

1.7 Summary

The research undertaken during the course of this program, and described herein was directed toward the characterization of active glucose oxidase films prepared using the LB technique using the QCM, ellipsometry, TEM and AFM. The fundamental nature of the enzyme films at the water/air interface was also addressed in this research. The overall work is divided into two independent studies presented in Chapter 2 and Chapter 3.

In Chapter 2, the nature of both native and modified glucose oxidase Langmuir films was addressed through study of the Langmuir trough isotherms. LB films of native and modified glucose oxidase were prepared and characterized by ellipsometry, QCM and electrochemical activity measurements. Comparisons between the native glucose oxidase and glucose oxidase modified with glutaraldehyde LB films were discussed. The modified films have much higher activity and greater thickness. Measurement of the true area per molecule was made possible using the QCM technique.

TEM images of both native and modified enzyme LB films and AFM images of modified films are presented in Chapter 3. The goal of this chapter was to understand the structure of the glucose oxidase LB films on a molecular scale, using TEM and AFM imaging.

Chapter 4 draws conclusions from the work presented in the thesis, and gives some suggestions for future research in this area.

1.8 References

1. Turner, R. F. B., *Toward an Implantable Glucose Sensor for the Artificial Beta Cell*, Ph. D. thesis, University of Alberta, **1990**.
2. Hulanicki, A.; Glab, S.; Ingman, F., *Pure & Appl. Chem.*, **1991**, *63*, 1247-1250.
3. Fan, Z., *Ph.D thesis*, University of Alberta, **1994**
4. Janata, J., *Principles of Chemical Sensors*, Plenum press: New York, **1989**
5. Powers, M. A., *Handbook of Diabetes Nutritional Management*, Aspen publishers: Rockville, MD, **1987**, 3.
6. Solomon, I., in *The Encyclopedia Americana*, International Edition, *Vol. 9*, Grolier Inc.: Danbury, CT, **1981**, 51-53
7. Clark, L. C.; Lyons, C., *Ann New York Acad. Sci.*, **1962**, *102*, 29-35.
8. Clark, L. C., *Trans. Am. Soc. Artif. Intern. Organs*, **1956**, *2*, 41-47.
9. Updike, S. J.; Hicks, G. P., *Nature*, **1967**, *214*, 986-988.
10. Gough, D. A.; Leypoldt, J. K.; Armour, J. C., *Diabetes Care*, **1982**, *5* (3), 190-198.
11. Kondo, T.; Ito, K.; Ohkura, K.; Ito, K.; Ikeda, S., *Diabetes Care*, **1982**, *5*(3), 218-221.
12. Guilbault, G. G.; Lubrano, G. J., *Anal. Chim. Acta*, **1972**, *60*, 254-255.
13. Guilbault, G. G.; Lubrano, G. J., *Anal. Chim. Acta*, **1973**, *64*, 439-455.
14. Clark, L. C.; Duggan, C., *Diabetes Care*, **1982**, *5*, 174-180.
15. Yao, T., *Anal. Chim. Acta*, **1983**, *148*, 27-33.

16. Pickup, J. C.; Shaw, J.; Armstrong, D. J., *Biosensors*, **1987**, *3*, 335-346
17. Albisser, A. M.; Leibel, B. S.; Ewart, T. G.; Davidovac, Z.; Botz, C. K.; Zingg, W., *Diabetes*, **1974**, *23*, 389-396.
18. Albisser, A. M.; Leibel, B. S.; Ewart, T. G.; Davidovac, Z.; Botz, C. K.; Zingg, W.; Schipper, H.; Gander, R., *Diabetes*, **1974**, *23*, 397-404.
19. Shichiri, M.; Kawamori, R.; Goriya, Y.; Yamasaki, Y.; Nomura, M.; Hakui, N.; Abe, H., *Diabetologia*, **1983**, *24*, 179-184.
20. Shichiri, M.; Kawamori, R.; Hakui, N.; Yamasaki, Y.; Abe, H., *Diabetes*, **1984**, *33*, 1200-1202.
21. Moussy F.; Harrison, D. J.; O'Brien, D. W.; Rajotte, R. V., *Anal Chem.*, **1993**, *65*, 2070-2077.
22. Reach, G.; Wilson, G. S., *Anal. Chem.*, **1992**, *64*, 381A-386A.
23. Pickup, J., *TIBTECH*, **1993**, *11*, 285-291.
24. Poitout, V.; Moatti-Sirat, D.; Reach, G.; Zhang, Y.; Wilson, G. S.; Lemonnier, F.; Klein, J. C., *Diabetologia*, **1993**, *36*, 658-663.
25. Yu, C., *M. Sc. thesis*, University of Alberta, **1996**
26. Yamasaki, Y., *Medical Journal of Osaka University*, **1984**, *35*, 25-34
27. Moatti-Sirat, D.; Capron, F.; Poitout, V.; Reach, G.; Bindra, D. S.; Zhang, Y.; Wilson, G. S.; Thevenot, D. R., *Diabetologia*, **1992**, *35*, 224-230.
28. Thevenot, D. R., *Diabetes Care*, **1982**, *5*, 184-189.
29. Ikeda, S.; Ito, K.; Kondo, T.; Ichikawa, T.; Yukawa, T.; Ichihashi, H., *Proc. Chem. Sensors*, **1983**, *17*, 620-625.

30. Turner, R. F. B.; Harrison, D. J.; Rajotte, R. V.; Baltes, H. P., *Sensors and Actuators*, **1990**, *B1*, 561-564.
31. Harrison, D. J.; Turner, R. F. B.; Baltes, H. P., *Anal. Chem.*, **1988**, *60*, 2002-2007.
32. Turner, R. F. B.; Harrison, D. J.; Rajotte, R. V., *Biomaterials*, **1991**, *12*, 361-368.
33. Harrison, D. J.; Daube, K. A.; Wrighton, M. S., *J. Electroanal. Chem.*, **1984**, *163*, 93-115.
34. Roberts, G. G. *Adv. phys.*, **1985**, *34*, 475, and **1983**, *4*, 131.
35. Kuhn, H. *Thin Solid Films* **1983**, *99*, 1.
36. Gaines, G. L., *Insoluble Monolayers at Liquid-Gas Interfaces*, **1966**
37. Miller, I. R.; Bach, D., *Surf. Colloid Sci.* **1977**, *7*, 185.
38. James, L. K.; Augenstein, L. G., *Adv. Enzymol. Relat. Subj. Biochem.* **1966**, *28*, 1.
39. Adamson, A. W., *Physical Chemistry of Surfaces*, 4th ed.; J. Wiley: New York, **1982**; *Chapter 3*.
40. Langmuir, I.; Schaefer, V. J., *Science* **1937**, *85*, 76; *J. Am. Chem. soc.* **1938**, *60*, 1351 and 2803.
41. Gorter, E., *Trans. Faraday Soc.* **1937**, *33*, 1125.
42. Cheesman, D. F.; Davies, J. T., *Adv. Protein Chem.*, **1954**, *9*, 439.
43. Bull, H. B., *Adv. Protein Chem.* **1947**, *3*, 95.
44. Benjamins, J.; DeFeister, J. A.; Evans, M. T. A.; Graham, D. E.; Phillips, M. C., *Faraday Discuss. Chem. Soc.* **1975**, *59*, 218.

45. Adams, D. J.; Evans, M. T. A.; Mitchell, J. R.; Phillips, M. C.; Rees, P. M., *J. Polym. Sci., Part C: Polym. Symp.* **1971**, *34*, 167.
46. Fromherz, P., *Nature* **1971**, *231*, 267.
47. Quin, P. J.; Dawson, R. M. C., *Biochem. J.*, **1969**, *113*, 791, **1969**, *115*, 65, and **1970**, *116*, 671.
48. Fromherz, P. *FEBS Lett.* **1970**, *11*, 205.
49. Steinemann, A.; Lauger, P., *J. Membr. Biol.* **1971**, *4*, 74.
50. Fromherz, P. *Biochim. Biophys. Acta*, **1971**, *225*, 382.
51. Peters, J.; Fromherz, P., *Biochim. Biophys. Acta*, **1975**, *394*, 111.
52. Fromherz, P.; Marcheva, D., *FEBS Lett.*, **1975**, *49*, 329.
53. Anzai, J.; Furuya, K.; Chen, C.; Osa, T.; Matsuo, T., *Anal. Sci.* **1987**, *3*, 271.
54. Tsuzuki, H.; Watanabe, T.; Okawa, Y.; Yoshida, S.; Yano, S.; Koumoto, K.; Komiyama, M.; Nihei, Y., *Chem. Lett.*, **1988**, *8*, 1265.
55. Sriyudthsak, M.; Yamagishi, H.; Moriizumi, T. *Thin Solid Films*, **1988**, *160*, 463.
56. Moriizumi, T., *Thin Solids Films*, **1988**, *160*, 413.
57. Porter, M. D.; Bright, T. B.; Allara, D. L.; Chidsey, C. E. D., *J. Am. Chem. Soc.*, **1987**, *109*, 3559.
58. Okahata, Y.; Tsuruta, T.; Kuniharu, I.; Ariga, K., *Langmuir*, **1988**, *4*, 1373.
59. Gough, D. A.; Lucisano, J. Y.; Tse, P. H. S., *Anal. Chem.*, **1985**, *57*, 2351.
60. Sun, S.; Ho-Si, P. H.; Harrison, D. J., *Langmuir*, **1991**, *7*, 727-737.

61. Buttry, D. A., In *Electroanalytical Chemistry*, Bard, A. J., Ed., Marcel Dekker: New York, **1991**, 17, 1-85.
62. Lu, C.; Czanderma, A. W.; eds., *Applications of Peizoelectric Quartz Crystal Microbalances, Methods and Phenomena, Vol. 7*, New York, **1984**.
63. Konash, P. L.; Bastiaans, G. J., *Anal. Chem.*, 52, 1929, **1980**.
64. Nomura, T., *Anal. Chim. Acta*, 124, 81, **1981**.
65. Nomura, T.; Nagamune, T.; Izutsu, K.; West, T. S., *Bunseki Kagaku*, 30, 494, **1981**.
66. Nomura, T.; Iijima, M., *Anal. Chim. Acta*, 131, 97, **1981**.
67. Ebara, Y.; Okahata, Y., *Langmuir*, **1993**, 9, 574-576.
68. Sauerbrey, G., *Z. Phys.*, 155, 206, **1959**.
69. Weir, K.; Chitaree, R.; Grattan, K. T. V.; Palmer, A. W., *High Speed Sensing Using an Ellipsometer for Investigation of Thin Films and Surfaces*.
70. Carlin, C. M.; Kepley, L. J.; Bard, A. J., *J. Electrochem. Soc.*, **1985**, 132, 353-359.
71. Collins, R. W.; Kim, Y. T., *Anal. Chem.* **1990**, 62, 887A-900A.
72. Passaglia, E., in *Ellipsometry in the Measurement of Surface and Thin Films*, Passaglia E; Stromberg, R. R.; Kruger, J.; Eds.; National Bureau Standards: Washington, D. C., **1963**, 1-4.
73. Heavens, O. S., *Optical Properties of Thin Solid Films*, Dover Publications: New York, **1965**, 95-154.

74. Gaertner Scientific Corp., *User Manual of Two Wavelength Ellipsometers L125B and L126B*, Chicago, IL.
75. Hirsch, P. *et al.*, *Electron Microscopy of Thin Crystals*, **1977**.
76. Reimer, L., *Transmission Electron Microscopy*, **1989**.
77. Vadimsky, R. G.; *Electron Microscopy. Polymers*, **1980**, Vol. 16, Part B, 185-235.
78. TopoMetrix Corporation, *User manual of AFM imaging modes*, **1993**.
79. Drake, B.; Prater, C. B.; Weisenhorn, A. L.; Gould, S. A. C.; Albrecht, T. R.; Quate, C. F.; Cannell, D. S.; Hansma, H. G.; Hansma, P. K., *Imaging Crystals, Polymers, and Processes in Water with the Atomic Force Microscope*, *Science*, **1989**, Vol. 243, 1586-1589.
80. Kirk, M. D.; Albrecht, T. R.; Quate, C. F., *Rev. Sci. Instrum.*, 59, 833, **1988**.

CHAPTER 2

CHARACTERIZATION OF LANGMUIR BLODGETT FILMS OF GLUCOSE OXIDASE

2.1 Introduction

Glucose oxidase is used commercially for various applications. Industrially it has been used in the production of gluconic acid and in food preservation. One of the most important applications is in biosensors, for quantitative determination of glucose in body fluids, foodstuff, beverages and fermentation liquor [1]. The enzyme (glucose oxidase) from *Aspergillus niger* is a glycoprotein with a high-mannose type carbohydrate content contributing 10 to 16% of its molecular weight [2, 3]. The carbohydrate moieties are N and O-glycosidically linked to the protein [4, 5]. Enzymatic removal of 30% [4] and 95% [6] of the carbohydrate content did not significantly affect the catalytic activity or the stability. The enzyme is highly specific for β -D-glucose, with other monosaccharides being oxidized at much lower rates [7, 8].

The mechanism of the glucose oxidase reaction has been extensively studied and a detailed reaction scheme has been proposed [9, 10, 11, 12, 13,

14]. As seen in Figure 2.1, the reaction can be divided into two separate steps, the oxidation of substrate with the corresponding reduction of the enzyme and the subsequent re-oxidation of the enzyme in the oxidative half-reaction [1].

As mentioned in Chapter 1, active LB films of glucose oxidase can be prepared directly by spreading a modified form of the enzyme at the air-water interface and transferring to a substrate using LB techniques. In this chapter, the glucose oxidase films were transferred to silicon (Si), platinum (Pt) and gold (Au) substrates following the method reported by Sun *et al.* [15]. Silicon provides a good substrate for ellipsometry, Pt is the active substrate for sensors, and Au is the metal present on the quartz crystal microbalance. The properties of both native and modified glucose oxidase films were characterized using the Langmuir trough, the QCM, the ellipsometer and by measuring the electrochemical activity. In this chapter, the QCM study is reported. A quartz crystal stability test was done as well, to choose a practical set of procedures for performing the QCM measurement. The goal of this chapter is to characterize the glucose oxidase films spread on the subphase of the trough and any effect spreading has on the enzyme activity. We then correlate all experimental results to the Langmuir-Blodgett film structure of both native and modified glucose oxidase.

Although there have been extensive studies of the properties of protein films at the air-water interface, many questions still remain unanswered. In particular, there is uncertainty regarding the structure of protein molecules in adsorbed films. It is not clear whether an adsorbed film consists of a monolayer of unfolded protein molecules, or molecules in various degrees of

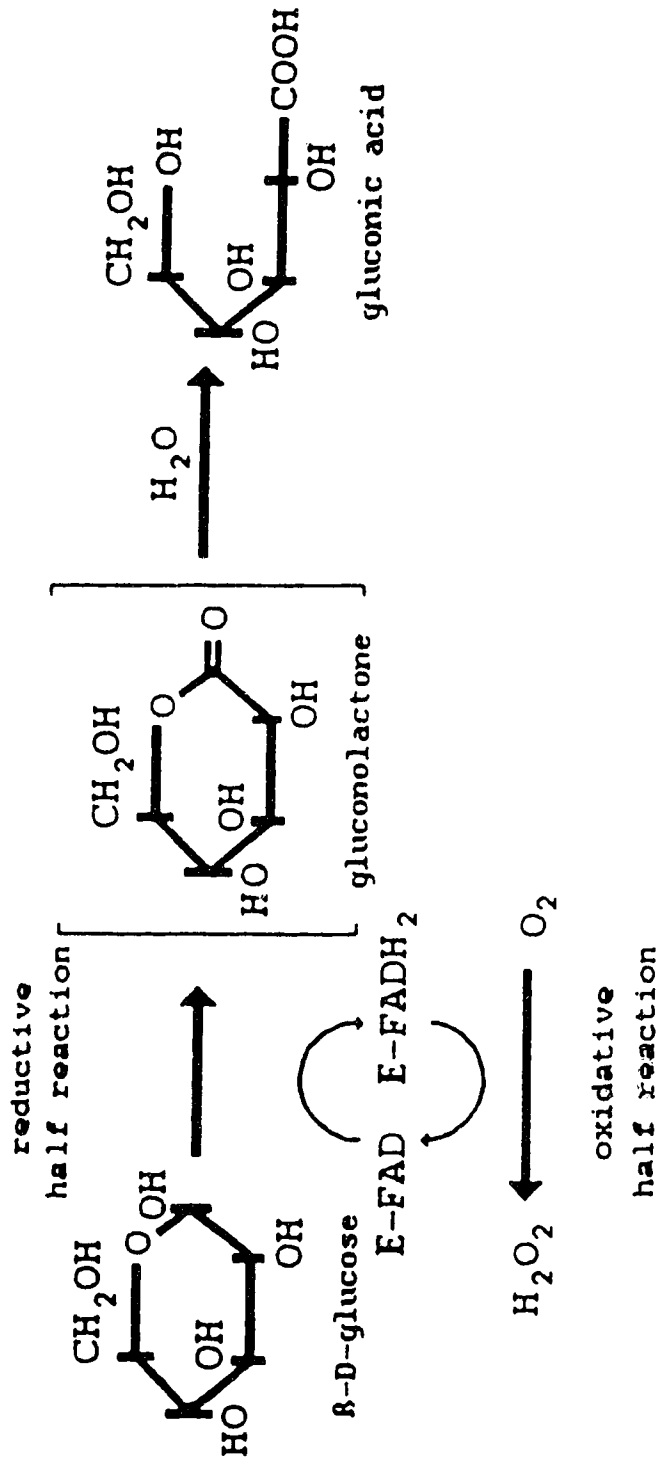


Figure 2.1 The enzymatic reaction catalyzed by glucose oxidase. The product of the reductive half reaction, δ -gluconolactone, hydrolyzes spontaneously to gluconic acid. The reduced FADH_2 is re-oxidized by molecular oxygen in the oxidative half reaction [1].

unfolding. Recently, it was shown that some adsorption properties of proteins can be related to their tertiary and quaternary structures, and that the type of adsorbed film may be changed when the conformation of the adsorbing molecule is altered by denaturing [16].

A large fraction of all studies of enzyme structure and function have been done in relatively pure aqueous solutions [16]. The reason is obvious: this is the situation which is most manageable experimentally. While such studies provide a great deal of information about enzyme behaviour, many of the results may be misleading as to the role and properties of most enzymes in their actual cellular environment.

Unfortunately, only relatively few enzyme studies have been made in situations which mimic cellular conditions. Of that small fraction which have been conducted at interfaces, most have involved films at an air-water surface; and most of these have dealt primarily with the processes of adsorption or the determination of molecular weights rather than investigating those factors which affect biological activity. The tremendous advance in the understanding of protein structure in solution and the crystalline state during the last two decades unfortunately has not been paralleled by a similar increase in the knowledge of their interfacial configuration. Present knowledge stems mainly from the measurement of surface pressure, surface potential and the rheological properties of spread and adsorbed films at air-water and oil-water interface. Certain generally acceptable conclusions have been drawn from this extensive work on the interfacial properties of proteins.

For instance, it is thought that at the air-water interface, and probably also at the oil-water interface, a protein can form two types of film [17]:

(a) A dilute film, in which all the molecules are in the same extensively unfolded (i.e. denatured) state. There is minimal interaction between the adsorbed molecules. Such unfolding under conditions where a protein has minimal interaction with other protein molecules appears to completely destroy enzyme activity.

(b) A concentrated film, which may contain only native and unfolded molecules, or molecules in many different degrees of unfolding.

2.1.1 Application of the microbalance

The quartz crystal microbalance (QCM) is a small mechanical resonator which can vibrate at very high frequencies (ca. 1-100 megahertz). As is true for all mechanical resonators, the resonant frequency is partially determined by the mass of the resonator (mass increases lead to frequency decreases, and *vice versa*). This mass dependent resonant frequency forms the basis of the use of QCM's as chemical sensors [18]. The basic principles of this device were introduced in Chapter 1.

An area per molecule was calculated based on the geometric electrode area, the mass change and the enzyme's molecular weight. In our case, the film is deposited on both sides of the quartz crystal. The Δm was calculated using the following equations (2.1) and (2.2).

$$\Delta f = -2c_f \Delta m \quad (2.1)$$

$$\text{and } \Delta m = -\Delta f / 2 c_f$$

$$= -\Delta f / 366.77182 \quad (2.2)$$

in unit of mg / cm²

We used a molecular weight for glucose oxidase of 160,000 Dalton, so the weight of 1 molecule glucose oxidase = 160,000 / 6.0221367 x 10²³ in unit of g/molecule, and 2656.8643 x 10⁻¹⁶ in unit of μg/molecule. Combining with the Δm determined from the frequency experiment, the calculation of Area /molecule was performed using the following equation (2.3):

$$\text{Area/molecule} = 2656.8643 \times 10^{-16} / \Delta m \text{ (cm}^2\text{/molecule)}$$

$$= 2656.8643 / \Delta m \text{ (\AA}^2\text{/molecule)} \quad (2.3)$$

2.1.2 The dimensions of glucose oxidase

The dimensions of glucose oxidase are of particular importance to analysis of the following experiments. The literature presents a number of values which will be discussed here.

The dimensions of glucose oxidase from *Aspergillus niger* were estimated in terms of the hydrodynamic radius to be 43 Å [19]. Using an electron micrograph technique, Vainshtein *et al.* have estimated the dimensions of crystalline glucose oxidase from *penicillium vitale* to be 50 x 50 x 70 Å [20]. From the hydrodynamic radius, an area per molecule of 5800 Å² would be predicted for a densely packed Langmuir film, while the area predicted by the dimensions of the *penicillium vitale* strain, assuming an

ellipsoidal shape, range from 2000 to 2750 Å² depending on the direction of the major and minor axis relative to the surface normal.

Glucose oxidase from *Aspergillus niger* is a homodimer of molecular weight 150,000 to 180,000 Dalton containing two tightly bound flavin adenine dinucleotide (FAD) molecules [7]. Approximate dimensions of a glucose oxidase crystal are 60 x 52 x 37 Å for a compact spheroid monomeric enzyme molecule. The corresponding dimensions for the dimer are 60 x 52 x 77 Å [1]. The dimer form is the result of strong hydrogen bonds or salt bridges. Dissociation of the subunits is possible only under denaturing conditions and is accompanied by the loss of the cofactor FAD [21]. The molecule is dominated by two separate structural domains. Contacts between molecules forming the dimer are confined to a long, narrow stretch [1]. The predicted area per molecule from this crystal structure ranges from 2450 Å² to 3465 Å² depending on the direction of the major and minor axis relative to the surface normal.

The area per molecule from the hydrodynamic radius gives the largest value of the above three predicted values. The dimensions from the electron microscope study by Vainshtein *et al.* was obtained from a different source of glucose oxidase, crystalline glucose oxidase from *penicillium vitale*. The area per molecule predicted from this data is much less than the values of hydrodynamic radius and the crystal structure of glucose oxidase from *Aspergillus niger*. Technically, the electron diffraction method is less definitive than the X-ray technique used to estimate the crystal structure of glucose oxidase from *Aspergillus niger*. Therefore the crystal structure of

glucose oxidase from *Aspergillus niger* was selected to compare with our experiment results, because it was from the same source of enzyme and used the more reliable X-ray technique.

It is more difficult to select between the crystal structure data and the hydrodynamic radius result. The crystal structure data would be the better choice if the LB film is truly dense packed like a two dimensional crystal. However, since the film is deposited from the surface of an aqueous solution and molecules in the film may retain flexibility and mobility the hydrodynamic radius may more closely reflect the space occupied by the molecule. This would clearly lead to a less dense film.

2.2 Experimental section

2.2.1 Material used in this experiment

(1) Glucose Oxidase (*Aspergillus niger*) was used as received from Sigma (type X-S), The product sheet specified a content of 78% protein, traces of other enzymatic impurities such as galactose oxidase (0.85% of GO activity), maltase (0.38% of GO activity) and catalase (0.6 Sigma units/mg protein) were identified as present in the product. All concentrations reported in this chapter are based on the nominal weight of samples. They are not corrected for the 78% protein content unless stated.

(2) Reagent grade (grade 2) glutaraldehyde (25% in H₂O) was obtained from Sigma. It was stored at 5 °C and was used as received. The properties of the glutaraldehyde have an effect on the product distribution, as well as on the

activity of LB films formed from the modified enzyme. Distilled glutaraldehyde, pure grade 1 glutaraldehyde shipped by Sigma on dry ice, and grade 2 Sigma glutaraldehyde were studied by Sun *et al.* in this lab [15]. The results show that only the impure grade 2 glutaraldehyde provides modified glucose oxidase with high activity electrochemically. The grade 2 glutaraldehyde was used exclusively in this study.

(3). Methanol (reagent grade) was doubly distilled. Two distillations proved to be necessary for cleanliness. Methanol was used to prepare all the solutions of both native and modified glucose oxidase and to clean the silicon and platinum substrates.

(4). Water: Distilled, deionized water was redistilled from alkaline permanganate, discarding the first 20% fraction and retaining the next 50%. It is also called double distilled, deionized water.

(5) A pH=7.4 phosphate buffer solution (PBS) was prepared from sodium phosphate salts (ionic strength 0.05 M) with sodium benzoate (5 mM) and ethylenediamine tetraacetic acid (1 mM) as preservatives and NaCl (0.1 M) as electrolyte.

(6) Silicon substrate: Silicon slides (1 cm x 4 cm) were prepared by scribing a 3 inch diameter test grade n-type silicon wafer, 100 orientation, with a resistivity of 1 to 2 Ω cm. It was provided by the Alberta Microelectronic Centre.

All slides were cleaned before deposition of LB films. Slides were sonicated for 15 minutes in 5% aqueous Sparkleen (Fisher), replacing the solution every 5 minute, then sonicated in distilled methanol for 15 minutes,

replacing the methanol every 5 minutes, and then sonicated in distilled water for 25 minutes, replacing the water every 5 minutes. After sonicating, the silicon slides were dried in an oven at 100 °C for 5 minutes. This gave uniformly hydrophilic silicon substrates.

2.2.2 Glucose oxidase modification reaction

Glucose oxidase cross-linked with glutaraldehyde was prepared by dissolving about 40 mg of glucose oxidase in 2 ml of double distilled deionized water and adding 1 ml of 25% glutaraldehyde (10,000:1 mole fraction of glutaraldehyde to glucose oxidase) [15], then 1 ml of double distilled deionized H₂O. This solution was allowed to stand for 5 minutes and then diluted with 2 ml double distilled methanol and double distilled deionized H₂O to 10 ml. After dilution, the solution was allowed to react for 24 hours at room temperature. This gave a solution of about 4 mg/ml of glucose oxidase, 25% glutaraldehyde.

By subsequent separation of the glutaraldehyde treated glucose oxidase using ultrafiltration, the distribution of molecular weight of the products formed by glutaraldehyde cross-linking can be controlled. Ultrafiltration using an XM-300 Diaflo Ultrafilter (Amicon. Inc.) with a molecular cutoff of 300,000 at a pressure of 5-10 psi, was used to reduce the fraction of higher portion oligomers. The XM-300 filter was rinsed to remove all residual protein after use, then was stored in a 10% ethanol/water solution in the refrigerator for reuse.

2.2.3 Langmuir Trough

A Joyce-Loebel Langmuir Trough (Model 6-11-4025) with a subphase volume of 4 Litre was controlled with an IBM-PC-XT and interface electronics and software provided by Joyce-Leobel. A Wilhelmy Plate (Whatman 1 CHR Chromatography paper) was used to measure changes in surface tension. In order to reduce the effect of vibration, the trough was mounted inside an arborite box supplied by Joyce-Leobel and on a Technical Manufacturers Micro-g air-table with a steel laminate top plate. A Schematic diagram is shown in Figure 2.2.

The trough components were cleaned by rinsing with Sparkleen (Fisher) detergent (2 - 5 % w/w in water) and distilled H₂O. Before use the surface of the subphase was cleaned by repeatedly removing the top layer with a Pasteur pipet attached to a vacuum aspirator when the barrier was compressed, and then replacing the lost volume when the barrier was fully open. When the surface tension remained constant as the barrier was compressed from 1000 to 100 cm² surface area, the subphase was taken to be clear. enzyme spreading solution was introduced using a Pipetman (Gilman) pipet to slowly and carefully deliver solution dropwise. When delivering enzyme spreading solution, the pipet tip was kept as close to the surface as possible, without contact with the surface.

Initial formal surface concentrations before compression were in the range of 2 to 18 mg/m². Typical values were about 8 mg/m² for native glucose oxidase and 4 mg/m² for modified glucose oxidase. Substrate coatings were deposited using a subphase containing about 1 g/L BaCl₂. A

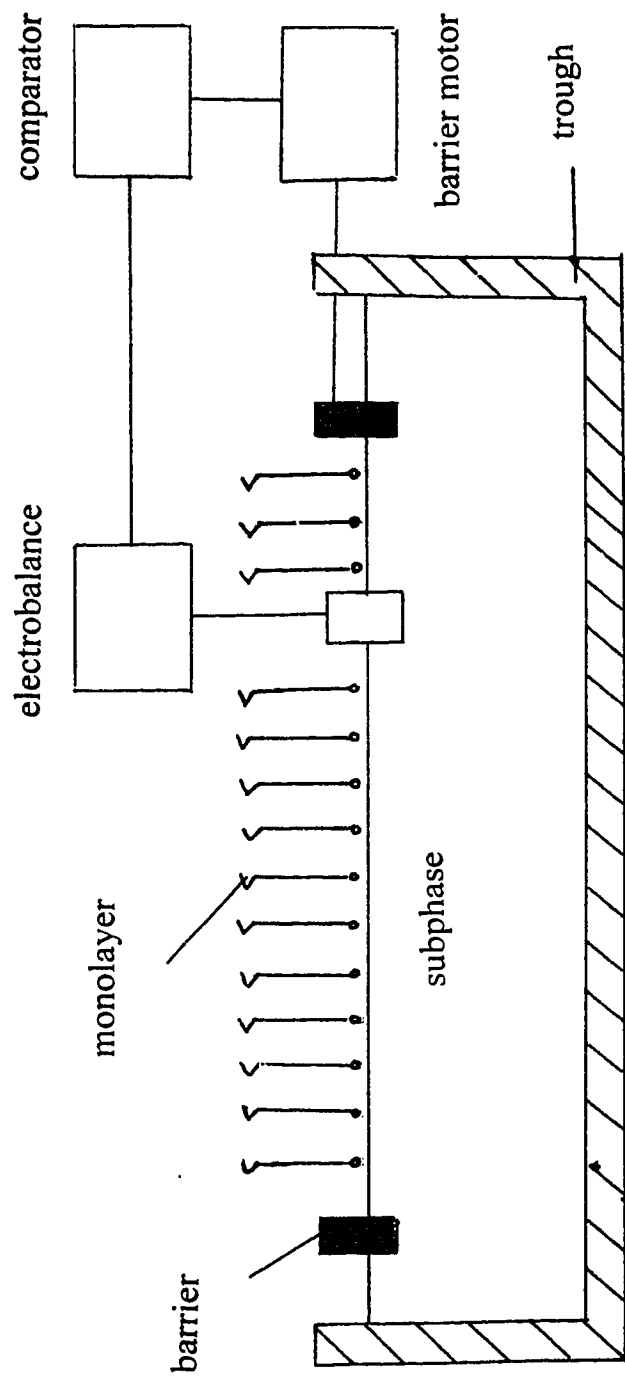


Figure 2.2 Schematic diagram of Langmuir trough.

constant surface pressure from 5 to 30 mN/m was maintained during deposition of the film. Only two to three layers of enzyme could be deposited at these pressures of 5 to 30 mN/m with a dipping speed of 20 mm/min. Beyond this number the film stripped off again as the slide reentered the subphase, as evidenced by an increase in trough surface area at constant surface pressure. To alleviate this problem, a two-stage process was used. While the substrate was submerged in the subphase, a surface pressure between 5 and 30 mN/m was established by compression of the surface area and then maintained as the substrate was withdrawn at 10 mm/min. If multiple coatings were performed, the substrate was then allowed to air dry for about 8 min., and before it reentered the subphase at 48 mm/min the surface area was expanded to give a surface pressure of 0 mN/m. After the substrate was submerged, the barrier was recompressed to give 20 or 30 mN/m for the next withdrawal. This allowed films of up to 10 layers to be deposited and was used since enzyme was deposited only on the upward stroke under all deposition conditions tried. These procedures described above were used for coating on clean Si, Pt, and Au coated QCM surfaces.

2.2.4 Film thickness measurement

A Gaertner L125B two-wavelength ellipsometer equipped with a rotating analyzer was used to measure the thickness of LB films. Data acquisition and ellipsometer control were done with an IBM- PS-2 system and software provided by Gaertner. Microspot optics gave a sampled area of

0.002 mm² at a 70° incident angle and 0.001 mm² at a 50° incident angle. The 6328 Å source was employed and an angle of 70° was most commonly used.

A Single Layer Absorbing (SLA) program was used to measure the thickness of the uncoated regions of sample silicon slides. This measurement determines the native oxide (SiO₂) thickness t , which is typically 20 to 30 Å. Using the Two Layer Non-Absorbing (TLNA) program with the following parameters: Si substrate $n_s=3.850$, $k_s=0.020$, oxide (SiO₂) layer $n=1.46$ (fixed), t =measured thickness from uncoated region (thickness of SiO₂), the thickness for LB film coated regions was then analyzed assuming a two-layer coating of enzyme/SiO₂/Si:substrate. Single or multiple layers of glucose oxidase were deposited on the Si slides. For LB film thickness greater than 150 Å, both thickness and refractive index could be determined from the data.

An average value of $n_{LB}=1.50$ was obtained for the deposited enzyme and this value was used as a fixed parameter for calculating the thickness of films less than 150 Å thick.

2.2.5 Quartz Crystal Microbalance

A 9-MHz quartz crystal microbalance (International Crystal Manufacturing Co., Inc., Oklahoma) was used to evaluate the mass of enzyme transferred to the crystal in a single dip coating. The crystal was driven with a circuit based on several inverters, and the frequency was measured with an HP Model 5335A universal counter. A schematic diagram is shown in Figure 2.3a and Figure 2.3b [22] of the oscillation circuit used in this study to control the QCM oscillation. The oscillator circuit was made by the electronic shop,

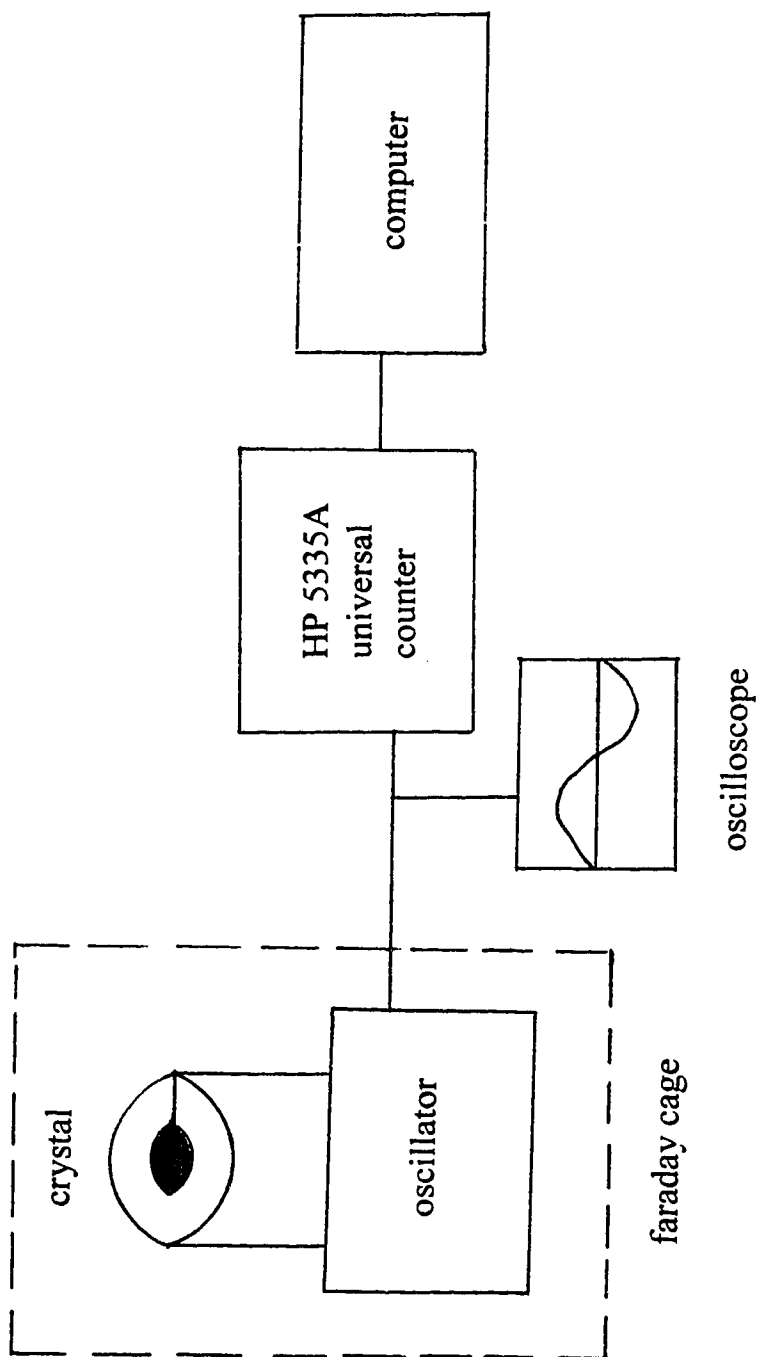


Figure 2.3a Schematic diagram of quartz crystal microbalance.

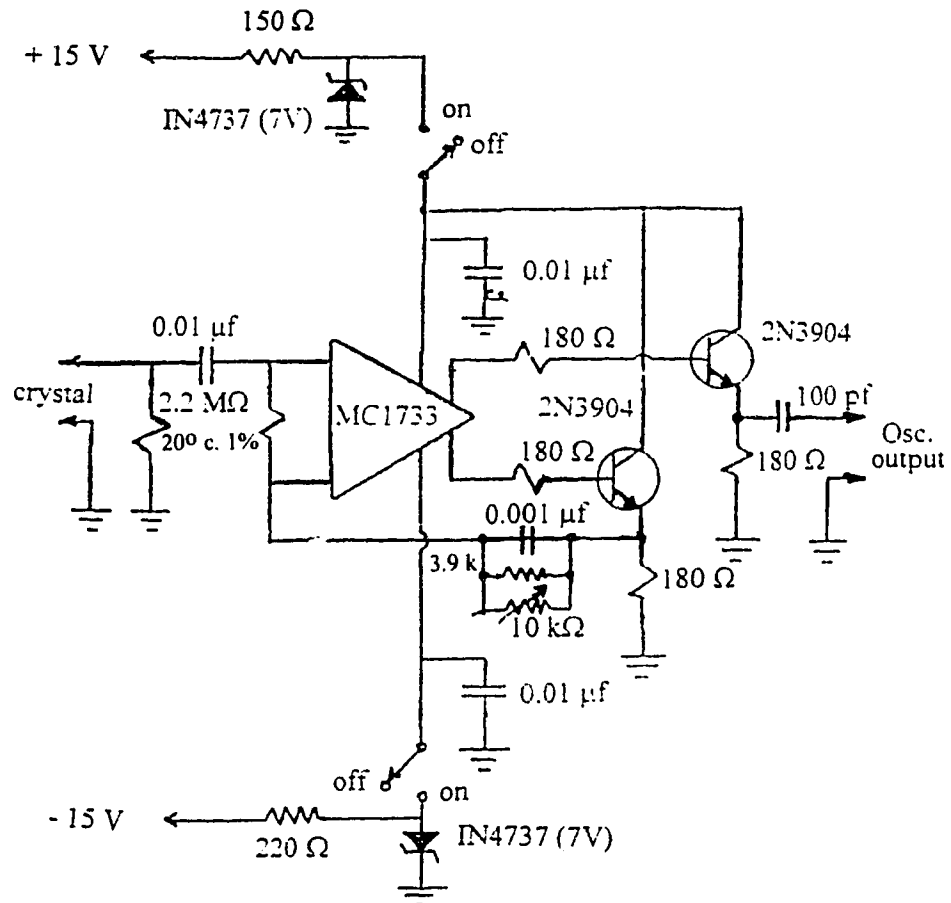


Figure 2.3b Modified oscillator circuit of QCM [22].

University of Alberta. Its original design is from Meltroy *et al.*'s paper [22], but the circuit was modified to allow it to work in the fundamental, third, or fifth harmonic modes.

The Quartz crystals were cleaned with 0.5% Terg-A-Zyme (Fisher) solution in distilled water at 50 °C, then rinsed thoroughly with distilled water. Before the frequency measurement, the crystal was rinsed with doubly distilled methanol, then doubly distilled, deionized H₂O and baked at 70 °C in an oven for 20 minutes. The crystals were repeatedly dipped into doubly distilled, deionized water using the Langmuir trough at a dipping and withdrawing speed of 10 mm/min. Then the crystal was baked in an oven at 70 °C for 20 to 40 minutes. When a reproducible oscillation frequency was obtained over several dipping-baking cycles, the crystal was dipped into the subphase through a Langmuir film of enzyme and baked using the same method. The dipping procedure for coating glucose oxidase onto the crystal is the same as for silicon slides. A single layer coating was performed for all QCM experiments under surface pressures ranging from 5 to 30 mN/m. Single layer coating is possible since enzyme is deposited only on the upward stroke. Crystals with deposited enzyme were baked at 70 °C in an oven for 20 minutes and then the frequency was measured after allowing the crystal to cool. The mass changes were calculated using equation (2.2) and the area per molecule values were calculated from equation (2.3).

2.2.6 Activity Measurement

The activity of LB films was determined quantitatively by electrochemical methods. The Pt substrate was cleaned with Sparkleen solution first, then it was cycled in 0.5 M H₂SO₄ at - 0.26 to +1.1 V vs a saturated calomel electrode (SCE) for 5 min. and anodized at +1.9 V for 5 min., followed by cycling at -0.26 to 1.1 V vs SCE for 15 min. again, and rinsing with doubly distilled, deionized H₂O. The electrode was air dried before the enzyme film deposition. The Pt substrates were dipped into the Langmuir trough using the same conditions as for silicon substrates.

Films coated on Pt electrodes were immersed in 50 ml of 0.1 M phosphate buffer at pH=7.4. The solution was magnetically stirred with a stir bar and an 89055A air-driven cell stirring module (Hewlett-Packard). The electrode was potentiostated at +0.7 V versus a saturated calomel electrode (SCE) with a Pine RDE-4 bipotentiostat, and the current was recorded with a Kipp and Zonen Model BD 90 X-Y recorder equipped with a time base. The current was allowed to stabilize in a glucose free solution, at which point an aliquot of 0.1 M glucose solution (pH=7.4, Phosphate buffer) was added and the change in signal recorded. The current density was calculated according to the measured current and the area of the Pt substrate.

2.3 Results and discussion

2.3.1 Film thickness measured by ellipsometry

The Langmuir films on the subphase can be transferred to a number of different solid substrates such as Pt, Au, Si, and glass using the Langmuir-Blodgett technique. We used Si substrates in the measurement of film thickness, TEM and AFM studies, and Pt substrates to test the activity of the films. A measurement of film thickness and comparison to the above dimensions should provide some information on the state and geometry of the deposited film.

A "Z-type" LB film deposition is observed under all conditions for both native glucose oxidase and modified glucose oxidase; that is, enzyme is transferred to the substrate only on the upward stroke as the substrate exited the subphase, and no deposition occurred on entering the subphase. This result was independent of substrate.

The film thickness of both native glucose oxidase and modified glucose oxidase was determined by ellipsometry. Data are listed in Table 1, which includes all thicknesses measured for native glucose oxidase, modified glucose oxidase prepared by ultrafiltration, and modified glucose oxidase prepared without ultrafiltration. All Langmuir-Blodgett films were deposited on Si substrate at a surface pressure of 30 mN/m. The average thickness of 45 Å per monolayer for modified glucose oxidase is significantly larger than the 34 Å per monolayer for native glucose oxidase. The film thicknesses measured by Sun *et al.* [15] are 48 Å per monolayer of modified glucose

Table 1. Native & modified GO thickness by ellipsometry of glucose oxidase LB films

Type of coating	coating layers	surface pressure mN/m	thickness, Å			thickness per layer, Å	average thickness, Å
			1*	2*	3*		
native GO	10	30	321	302		31.2	33.8 ± 1.7
	10	30	328	380	295	33.4	
	3	30	102	102	115	35.3	
	1	30	34	35	32	33.7	
	1	30	33	39	34	35.3	
modified GO, ultrafiltered	10	30	376	436	570	46	44.7 ± 1.5
	10	30	409	436		42.3	
	6	30	187	270		45.7	
	1	30	44	44	45	44.3	
	1	30	43	47	46	45.3	
modified GO, not ultrafiltered	1	30	63	74	69	68.7	69.2 ± 0.7
	1	30	66	75	68	69.7	

* 2 or 3 spots were measured by ellipsometry on the same silicon substrate

oxidase and 30 Å per monolayer of native glucose oxidase. The thicknesses obtained in our study are in good agreement with the previous values measured by Sun *et al.* The expected thickness for a monolayer of glucose oxidase is in the range of 50 to 80 Å at a surface pressure of 30 mN/m, depending on the packing geometry. From the thickness data measured by ellipsometry, the value of modified glucose oxidase is close to 50 Å. This suggests the minor axis of the enzyme ellipsoid is oriented perpendicular to the silicon substrate surface.

The thickness that we measured for native glucose oxidase is much lower than the expected range, while the thickness of modified glucose oxidase is close to the expected value. This suggests that the native enzyme is partially denatured during the LB film formation process. There may be a partial loss of the tertiary structure since a totally denatured film of protein is known to be about 10 Å thick. These results are consistent with previous studies of native enzyme films [23, 24, 25].

Since the film thickness measurements may be interpreted as indicating unfolding of native glucose oxidase and both partial and complete unfolding of proteins at the air-water interface is known to occur, a method to prevent or reduce this effect via intermolecular cross-linking of the enzyme was necessary. Glutaraldehyde is a well-known cross-linking reagent which is used to inter-molecularly link proteins, and was used in this study. Sun *et al.* [15] tested the glutaraldehyde modified glucose oxidase by electrophoresis. Treatment of glucose oxidase with glutaraldehyde clearly cross-links enzyme molecules, as evidenced by the higher molecular weight units observed in the

experiment. An increase in the integrity of quaternary structure of the enzyme is also apparent, since the modified glucose oxidase significantly resists breakdown into its 80,000 Dalton subunit under chemically denaturing conditions. Such denaturing is known to disrupt the bonds linking the two subunits in the native glucose oxidase and cause changes in the tertiary structure of the protein. The increased durability of the modified glucose oxidase most likely arises from intramolecular cross-linking via reactive sites on the enzyme that links together the two subunits through covalent bonds. This cross-linking would also be expected to impart resistance to unfolding as well.

From the measured thickness determined by ellipsometry, the increase of thickness from 34 Å for native enzyme to 45 Å for modified glucose oxidase is most likely due to the greater resistance of the modified enzyme to unfolding at the air-water interface. This is consistent with the chemical denaturing resistance discussed above.

The thickness of modified glucose oxidase without ultrafiltration is about 69 Å by ellipsometry measurement. It is significantly larger than the 45 Å for modified glucose oxidase with ultrafiltration. Previous SEM studies of such films by Sun *et al.* [15] showed large islands of excess enzyme are deposited when it is not filtered. Consequently, the increased film thickness must be a result of the increase in deposited enzyme mass.

2.3.2 Area per molecule from pressure-area isotherms

A typical isotherm of surface pressure *versus* area is shown in Figure 2.4a for native glucose oxidase (GO) in 20% double distilled methanol spread on a subphase of 2 g BaCl₂ in 4 L of water (distilled, deionized water was redistilled from alkaline permanganate). The pH of the subphase was adjusted to about 5 with HCl. The pH was tested with pH paper, and normally the subphase made as above gave a pH between 4.6 to 5.3. An aliquot of 0.2 ml of 4.376 mg/ml native glucose oxidase solution was delivered to the subphase. Figure 2.4b is an isotherm of modified glucose oxidase prepared on the same type of subphase as native glucose oxidase. The amount of modified glucose oxidase solution delivered was 1.5 ml of 0.3375 mg/ml. These volumes gave an initial formal concentration of 8.75 mg/m² for native glucose oxidase and 5.06 mg/m² for modified glucose oxidase.

The shape of the isotherms for native glucose oxidase and modified glucose oxidase is about the same, as shown by representative data given in Figure 2.4a and 2.4b, but they have different slopes at surface pressures in the range of 5 to 30 mN/m. The native glucose oxidase isotherm is steeper than is modified glucose oxidase. The apparent area per molecule values are extrapolated to a surface pressure of 0 mN/m from the linear portion of the compression curve, as illustrated in Figure 2.4a. Because the isotherm for native glucose oxidase is generally steeper than for modified glucose oxidase, extrapolation to 0 mN/m generally gives smaller area per molecule values for native glucose oxidase.

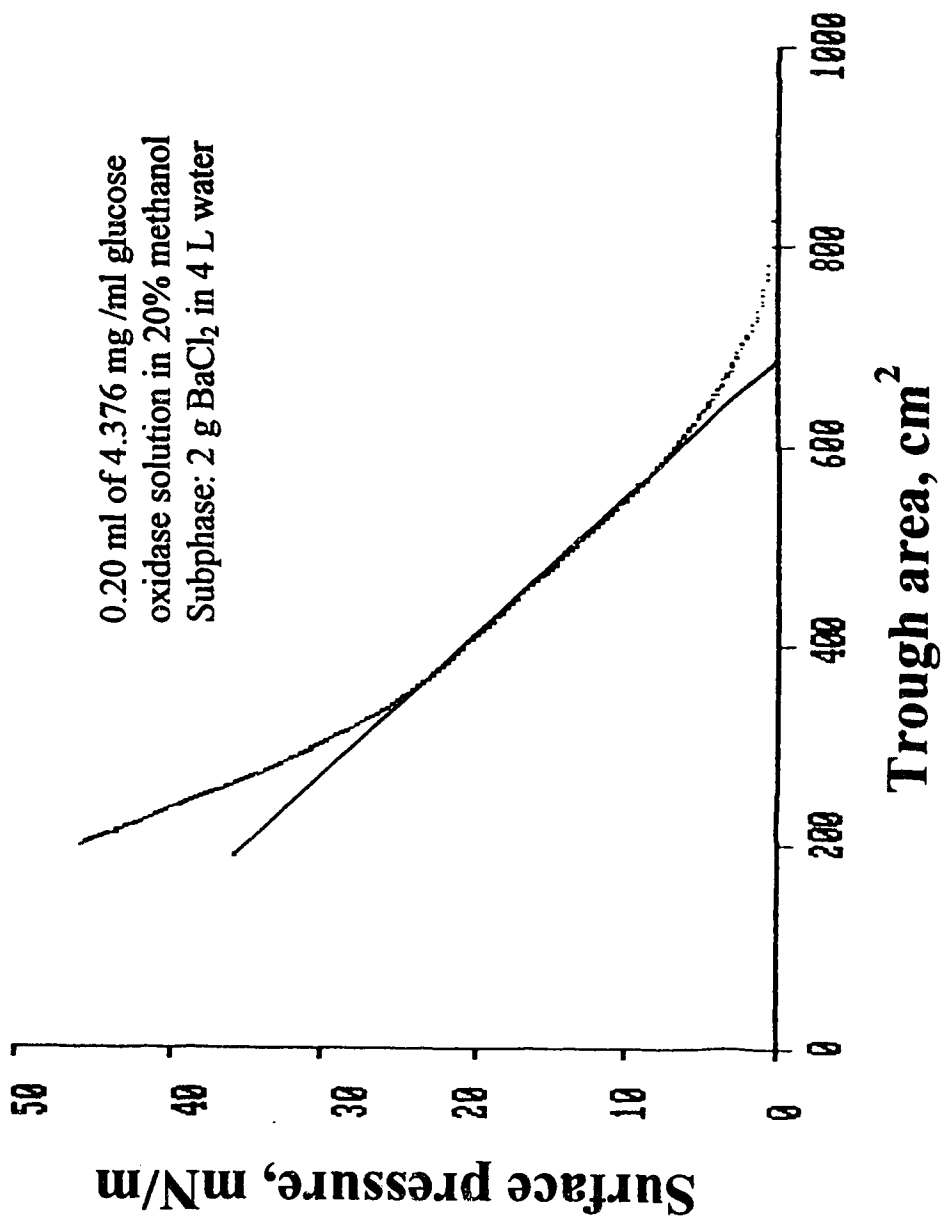


Figure 2.4a Isotherm of native glucose oxidase. The straight line shows extrapolation to a surface pressure of 0 mN/m.

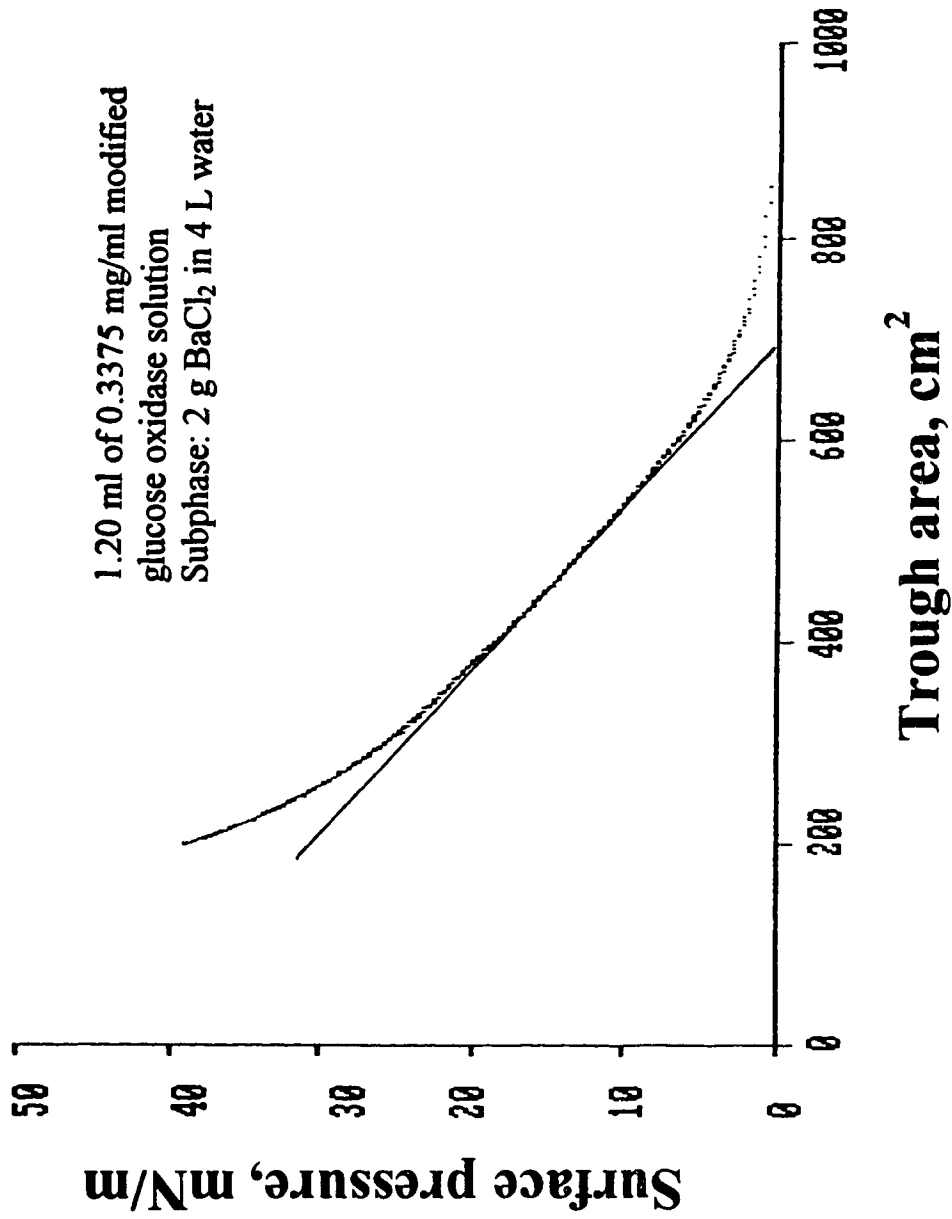


Figure 2.4b Isotherm of modified glucose oxidase. The straight line shows extrapolation to a surface pressure of 0 mN/m.

Different initial concentrations of both native glucose oxidase and modified glucose oxidase were spread on the subphase to make Langmuir films and the isotherms were recorded. The surface area per molecule values were obtained from various pressure-area isotherms, and are reported at various surface pressures. The data are listed in Table 2 for native glucose and Table 3 for modified glucose oxidase. As will become clear in the discussion, the apparent area/molecule measured by the pressure-area curve method is unreliable. It depends on initial concentrations, time, and delivering method.

In order to determine the concentration of modified glucose oxidase, a calibration curve was made by measuring the absorbance at 450 nm of glucose oxidase standard solutions. Figure 2.5 is the calibration curve of measured absorbance *versus* concentration of glucose oxidase, the data are listed in Table 4. The concentration of modified glucose oxidase after ultrafiltration is calculated through a measurement of solution absorbance at 450 nm and the calibration curve.

We found that the concentration of modified glucose oxidase after ultrafiltration decreased to about 1/10 of the initial native glucose oxidase solution used for the modification. For example, a concentration of 0.3806 mg/ml was obtained from a 4.10 mg/ml glucose oxidase solution, after reaction with glutaraldehyde and ultrafiltration. This is confirmed by the Langmuir film isotherms. For modified glucose oxidase, much more solution needed to be delivered to the subphase to get about the same trough area at a given surface pressure as compared to native glucose oxidase solution. The

Table 2. Area/molecule, Å², extrapolated from isotherms of native glucose oxidase

Slide #	101	102	103	104	201	202	203	301	302	303
GO concentration. (mg/ml)	4.376	4.376	4.376	4.376	4.376	4.376	4.376	4.376	4.376	4.376
Volume (ml)	0.40	0.40	0.40	0.40	0.30	0.30	0.30	0.20	0.20	0.20
Surface concentration (mg/m ²)	17.50	17.50	17.50	17.50	13.13	13.13	13.13	8.75	8.75	8.75
Extrapolate range (mN/m)	25--15	25--15	25--15	25--15	25--15	25--15	25--15	25--15	25--15	25--15
Area/molecule at 0 (mN/m)	1163.3	1054.9	1034.2	985.8	1430.5	1320.3	1262.8	1388.7	1341.6	1314.1
Area/molecule at 30 (mN/m)	515.6	444.2	459.1	421.8	602.2	551.3	539.1	640.9	607.7	612.2
Area/molecule at 25 (mN/m)	608.6	533.0	523.1	488.2	755.0	647.6	627.7	728.9	694.0	702.3
Area/molecule at 20 (mN/m)	718.2	635.2	622.7	588.7	884.5	776.0	746.1	853.5	812.0	815.3
Area/molecule at 15 (mN/m)	832.8	740.6	721.5	685.8	1026.3	913.3	877.5	991.3	953.1	944.8
Area/molecule at 10 (mN/m)	978.1	866	831.2	786.3	1190.1	1058.4	1015.2	1157.4	1105.9	1077.7
Area/molecule at 5 (mN/m)	1180.8	1024.6	958.2	905.1	1461.4	1252.1	1196.8	1423.2	1321.8	1278.7

- * 1. Concentrations are based on weighed amounts of enzyme, not corrected for the fact that only 78% of mass is protein.
- 2. Each column is for a single isotherm experiment, in each case several isotherms were run consecutively, and are listed in consecutive columns. Each isotherm was separated by about 15 to 30 minutes.

Table 3. Area/molecule, λ^2 , extrapolated from modified glucose oxidase isotherms

Silicon slide #	103	101	102	104	105	106	107	108	109	110
GOG concentration (mg/ml)	0.3806	0.3806	0.3806	0.3375	0.3375	0.3375	0.3375	0.3375	0.3375	0.3375
Volume (ml)	0.6	0.9	0.9	1.2	1.2	1.5	1.5	1.95	2.4	2.7
Surface concentration, (mg/m ²)	2.284	3.425	3.425	4.05	4.05	5.062	5.062	6.581	8.1	9.112
Extrapolation range (mN/m)	7--5	20--8	20--8	20--8	20--8	24--8	24--8	24--10	24--10	24--10
Area/molecule at 0 (mN/m)	3113.6	757.6	2781.7	2581.2	2565.9	2404.5	2378.9	2178.9	2100.1	2005.1
Area/molecule at 30 (mN/m)								894.2	828.9	752.7
Area/molecule at 20 (mN/m)			1590	1471.1	1499.8	1331.9	1360.6	1249.8	1182.4	1103.7
Area/molecule at 15 (mN/m)		1828.5	1866.7	1704.4	1740.3	1587.5	1599	1477.3	1406.7	1325.4
Area/molecule at 10 (mN/m)		2142.5	2180.7	2009.5	2023.8	1880.3	1874.6	1726.6	1656.1	1566.2

* 1. Concentrations are based on weighed amounts of enzyme, not corrected for the fact that only 78% of mass is protein.

2. Each column is for a single isotherm experiment, in each case several isotherms were run consecutively, and are listed in consecutive columns. Each isotherm was separated by about 15 to 30 minutes.

Table 4. Data of absorbance measured for native glucose oxidase solutions

Conc. of GO, mg/ml	4.380	3.220	2.220	1.610	0.875	0.438
Absorbance @ 450nm	0.5292	0.3623	0.2575	0.1904	0.097	0.0294

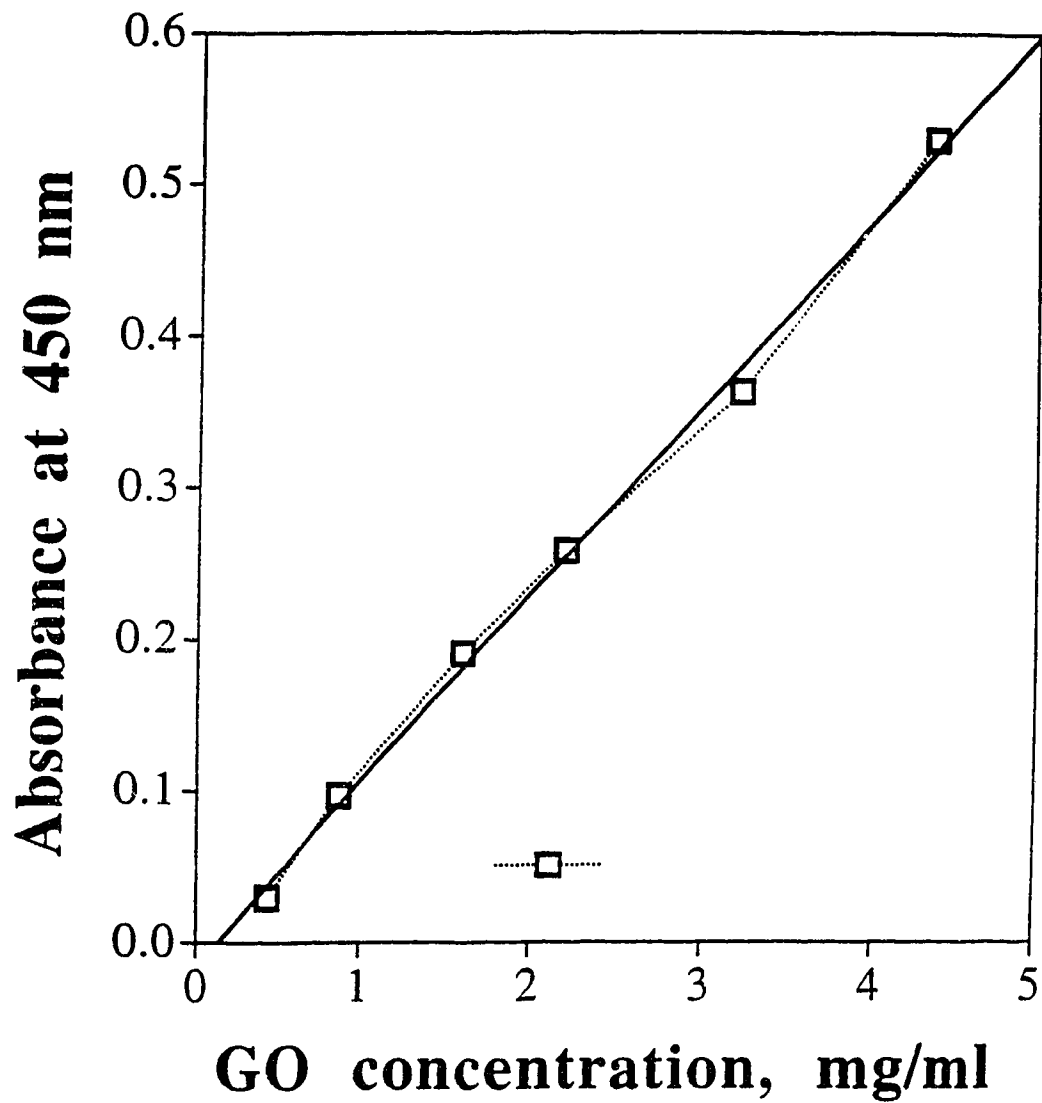


Fig.2.5 Plot of absorbance at 450 nm vs concentration of native glucose oxidase. Equation of the line is $y = 0.123x - 0.016$.

range of delivered volume of modified glucose oxidase was 1 to 3 ml, while for native glucose oxidase it was only 0.2 to 0.5 ml.

The area per molecule extrapolated to 0 mN/m for both the native and modified glucose oxidase Langmuir film decreases as the initial surface concentration increases. From Figure 2.6, we see the area per molecule value of native glucose oxidase decreases very fast at high initial surface concentration and much slower at low initial surface concentration. At surface concentrations lower than about 13.1 mg/m², the area per molecule of native glucose oxidase is a constant value. For modified glucose oxidase, the area per molecule keeps decreasing in the experimental range. The area per molecule value of modified glucose oxidase is larger than that for native glucose oxidase at about the same initial surface concentration. Table 2b is presented to provide an easy comparison between the two types of glucose oxidase prepared at similar surface concentration. The data from Table 2 are average values for native glucose oxidase, corrected for the 78% purity of protein. For modified glucose oxidase, the values are from Table 3 and corrected for the enzyme purity too.

Table 2b Area/molecule from pressure-area isotherms

	Native GO	Modified GO
surface concentration (mg/m ²)	8.75	9.11
surface pressure: SP=0 (mN/m)	1728 ± 48 Å ²	2571 Å ²
SP=30 (mN/m)	795 ± 23 Å ²	965 Å ²

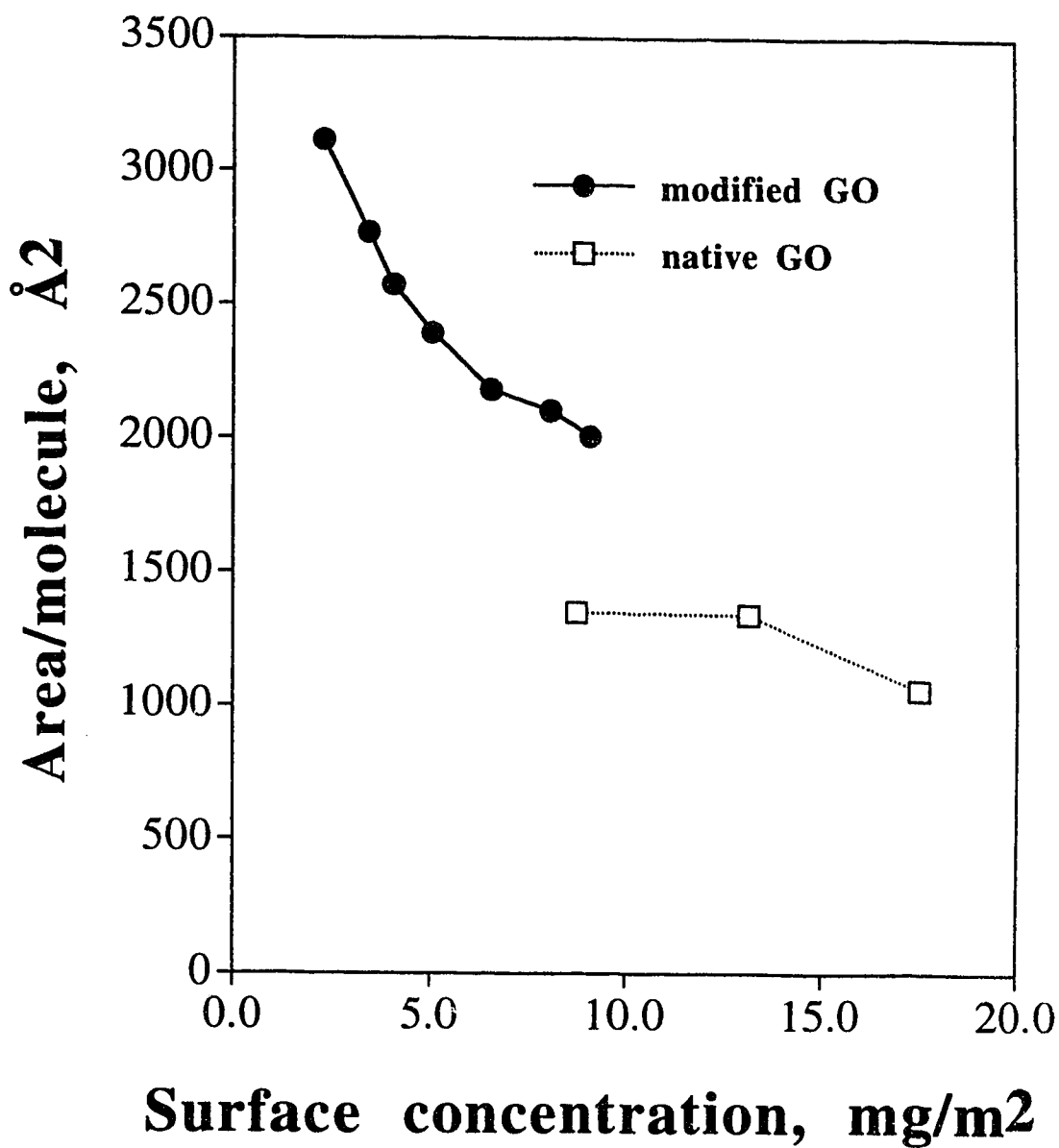


Figure 2.6 Area/molecule vs surface concentration of native and modified GO from pressure-area curves.

The area per molecule value of our experiment is much smaller than the predicted range. This could result either from folding and stacking of molecules at the air-water interface giving a multilayer structure or from loss of enzyme to the subphase. The loss of enzyme to the subphase is suggested by the increased area per molecule as the initial surface concentration is decreased. Since the surface pressure - area isotherm is a recording of the area change during compression, loss of enzyme to the subphase or film stacking results in fewer molecules of protein on the subphase. At low surface pressure, loss to the subphase is probably less than at high surface pressure. Consequently, the area per molecule might be expected to decrease well below the expected value as the trough is compressed. This is consistent with the data in Table 2 and Table 3. This interpretation is also supported by the slow decrease in trough area when the surface pressure is held constant over a period of 5 - 30 minutes.

A similar loss of enzyme adsorbed at the air-water interface to the subphase was elegantly demonstrated by Adams *et al.* using a radiotracer technique [26]. From Table 2 and Table 3, we also see that the area per molecule decreases with each subsequent isotherm for both native glucose oxidase and modified glucose oxidase. The later the isotherm experiment was performed, the smaller the area per molecule obtained.

The data listed above shows that the area per molecule value of modified glucose oxidase falls in the predicted range of 2000 to 2750 Å² from ellipsoidal shape penicillium vitale strain, while the measured value for native glucose oxidase is smaller than this range. However, this value is for

an uncompressed film, where a much larger area would be expected. The area per molecule values of the compressed films, at 30 mN/m, are far smaller than the predicted area, indicating a problem with the pressure-area isotherm data.

2.3.3 Area per molecule from mass-area isotherms

The mass of enzyme transferred to a gold substrate as a function of surface pressure was obtained by using a quartz crystal microbalance (QCM). Both native and modified glucose oxidase were measured with a 9-MHz QCM (International Crystal Manufacturing Co., Inc., Oklahoma). The data listed in Table 5 are the surface pressure and the area per molecule calculated from the measured mass change, Δm . Surface pressure *versus* area per molecule plots determined in this way are shown in Figure 2.7a and Figure 2.7b for both native and modified glucose oxidase. The concentration of native glucose oxidase was 4.376 mg/ml in 20% doubly distilled methanol. The modified glucose oxidase solution was making by ultrafiltering this solution, and the concentration determined from the calibration curve was 0.3375 mg/ml.

At a surface pressure of 30 mN/m, the measured area/molecule is 5723 \AA^2 for native glucose oxidase and 5611 \AA^2 for modified glucose oxidase. The measured hydrodynamic radius of glucose oxidase predicts an area per molecule of 5800 \AA^2 . The area per molecule values measured by Quartz Crystal Microbalance for both native and modified glucose oxidase

Table 5. Area per molecule of native and modified GO measured by QCM

	Initial surface conc., mg/m ²	surface pressure, mN/m				
		30	20	15	10	5
Area/molecule of native GO, Å ²	17.5	7051	9141	17308	21138	24362
		5093	7193	16048	22875	17873
		5225	8339	13478	18351	23146
		5124	7416	18283	19412	22438
		6120	8700	18625		
Average, Å ²		5723 ± 855	8158 ± 833	16748 ± 2084	20444 ± 1986	21955 ± 2835
Area/molecule of modified GO, Å ²	8.1	4680	11011	13478	21607	17432
		6638	10638	18113	16460	21370
		4934	8724	16323	15616	19145
Average, Å ²	16.88	6140	9452	14632	20259	
		5611 ± 930	9956 ± 1057	15636 ± 2022	18486 ± 2900	19316 ± 1974

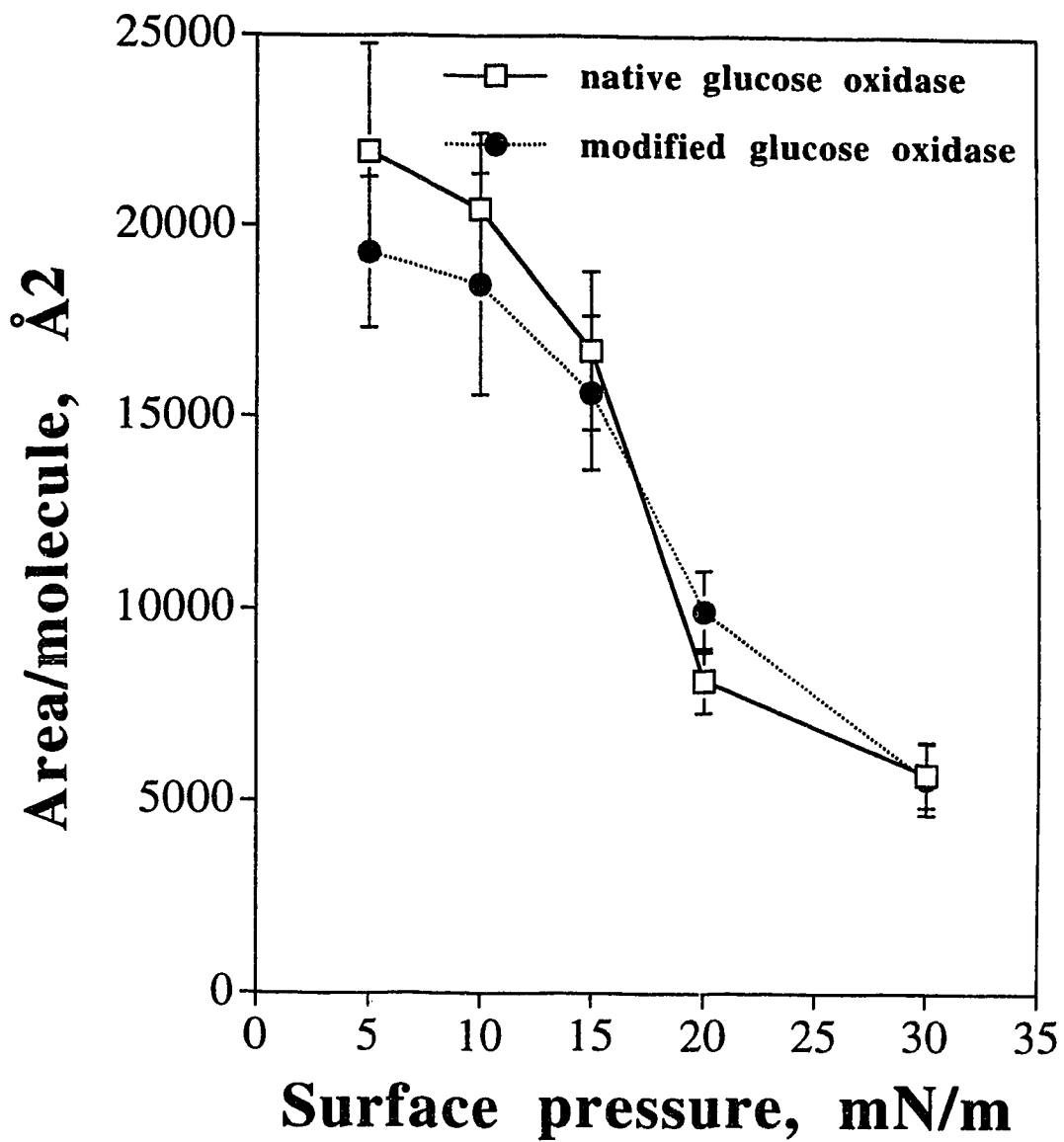


Figure 2.7a Area per molecule measured by QCM as a function of surface pressure.

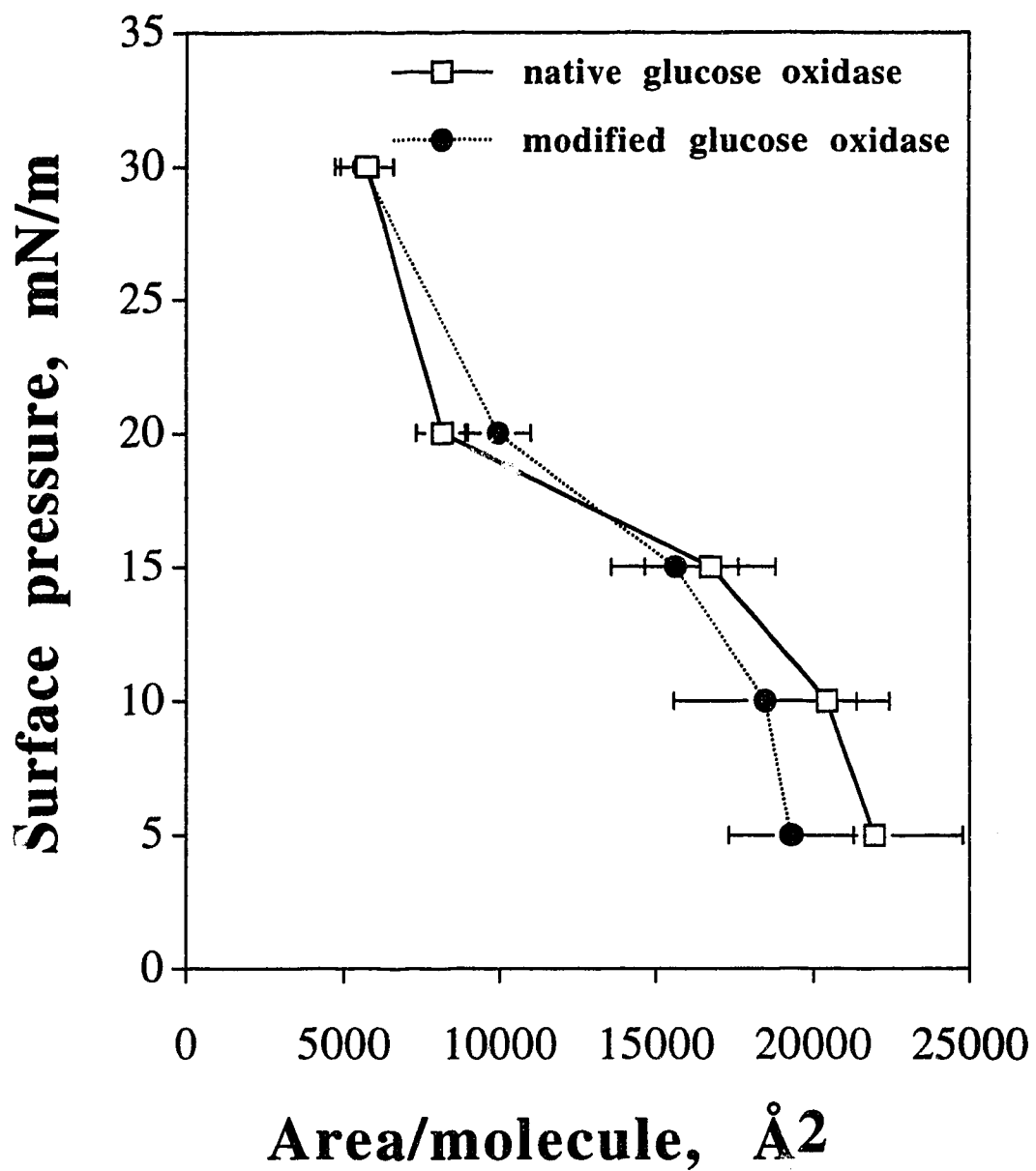


Figure 2.7b Plot of surface pressure *versus* area/molecule.

at surface pressures of 30 mN/m are in good agreement with the predicted value from the hydrodynamic radius.

Comparing the area per molecule of enzyme obtained by the surface pressure *versus* trough area isotherms and mass isotherms of quartz crystal microbalance, the area per molecule measured by QCM on a gold substrate is much larger than that extrapolated from the pressure-area isotherms. For native glucose oxidase, these data were obtained from initial surface concentrations of 8.75 to 17.5 mg/m² *versus* 17.50 or 21.88 mg/m² for the pressure-area *versus* QCM studies, respectively. For modified glucose oxidase the surface concentrations were 2.28 to 9.11 mg/m² *versus* 8.10 or 16.88 mg/m² for pressure *versus* QCM studies, respectively. The values in the following table for pressure-area isotherms are corrected for the 78% purity of glucose oxidase.

Table 3b Summary of area/molecule from pressure-area isotherms and pressure-mass isotherms

Isotherm (Si)		
Surface concentration of native GO, 8.75 to 17.5 mg/m ²	Area/molecule at SP=30 mN/m 541 to 785 Å ²	Area/molecule at SP=0 mN/m 1263 to 1781 Å ²
Surface concentration of modified GO, 2.28 to 9.11 mg/m ²	965 to 1146 Å ²	2571 to 3992 Å ²
QCM (gold)		
Surface concentration of native GO, 17.50 mg/m ² and 21.88 mg/m ²	Area/molecule at SP=30 mN/m 5790 Å ² 5622 Å ²	Area/molecule at SP=5mN/m 21794 Å ² 22438 Å ²
Overall Average	5723 ± 855 Å ²	21955 ± 2835 Å ²
Surface concentration of modified GO, 8.10 mg/m ² and 16.88 mg/m ²	5659 Å ² 5562 Å ²	19401 Å ² 19145 Å ²
Overall Average	5611 ± 930 Å ²	19316 ± 1974 Å ²

As mentioned before, the smaller value of area per molecule extrapolated from the pressure isotherms is caused by either folding and stacking of molecules at the air-water interface to give a multilayer structure,

or from loosing enzyme to the subphase. The area per molecule from the QCM experiment is in good agreement with the predicted hydrodynamic value of 5800 \AA^2 per molecule. This indicates the enzyme deposited on a gold substrate at a surface pressure of 30 mN/m is on average a relatively compact monolayer for both native and modified glucose oxidase. However, the crystal structure data [1] indicates the film could be denser if crystal-like packing was obtained in the film. The area per molecule of modified glucose oxidase from the pressure-area isotherms is larger than that of native glucose oxidase at surface pressures of both 30 and 0 mN/m . For contrast, the areas per molecule are about the same as determined from the QCM at a surface pressure of 30 mN/m , while a smaller value is found for modified glucose oxidase prepared at 5 mN/m .

2.3.4 Activity of Langmuir-Blodgett film of modified glucose oxidase

The activity of modified glucose oxidase LB films was determined electrochemically, by deposition of the films on Pt and measurement of the current for H_2O_2 oxidation. The measured current density with glucose concentration data is listed in Table 6 and Figure 2.8 is a plot of current density in units of $\mu\text{A/cm}^2$ versus concentration of glucose for a two monolayer deposition at surface pressures of 30 mN/m and 20 mN/m . The modified glucose oxidase films prepared at 30 mN/m and 20 mN/m surface pressure show a glucose response curve that follows Michaelis-Menton kinetics and is linear up to about 5 mM glucose in an air saturated solution.

Table 6. Current density with glucose concentration

Concentration of glucose, mM	Current density, $\mu\text{A}/\text{cm}^2$			
	Electrode #1 at 30 mN/m	Electrode #2 at 30 mN/m	electrode #1 at 20 mN/m	electrode #2 at 20 mN/m
0.990	0.638	0.833	0.172	0.244
1.961	1.355	1.665	0.301	0.448
2.913	2.152	2.264	0.430	0.652
4.762	3.428	3.130	0.644	0.978
6.542	4.464	4.196	0.859	1.264
8.257	5.341	4.995	1.031	1.468
11.504	6.776	6.394	1.332	1.834
14.530	7.892	7.326	1.590	2.161
17.355	8.768	8.125	1.805	2.446

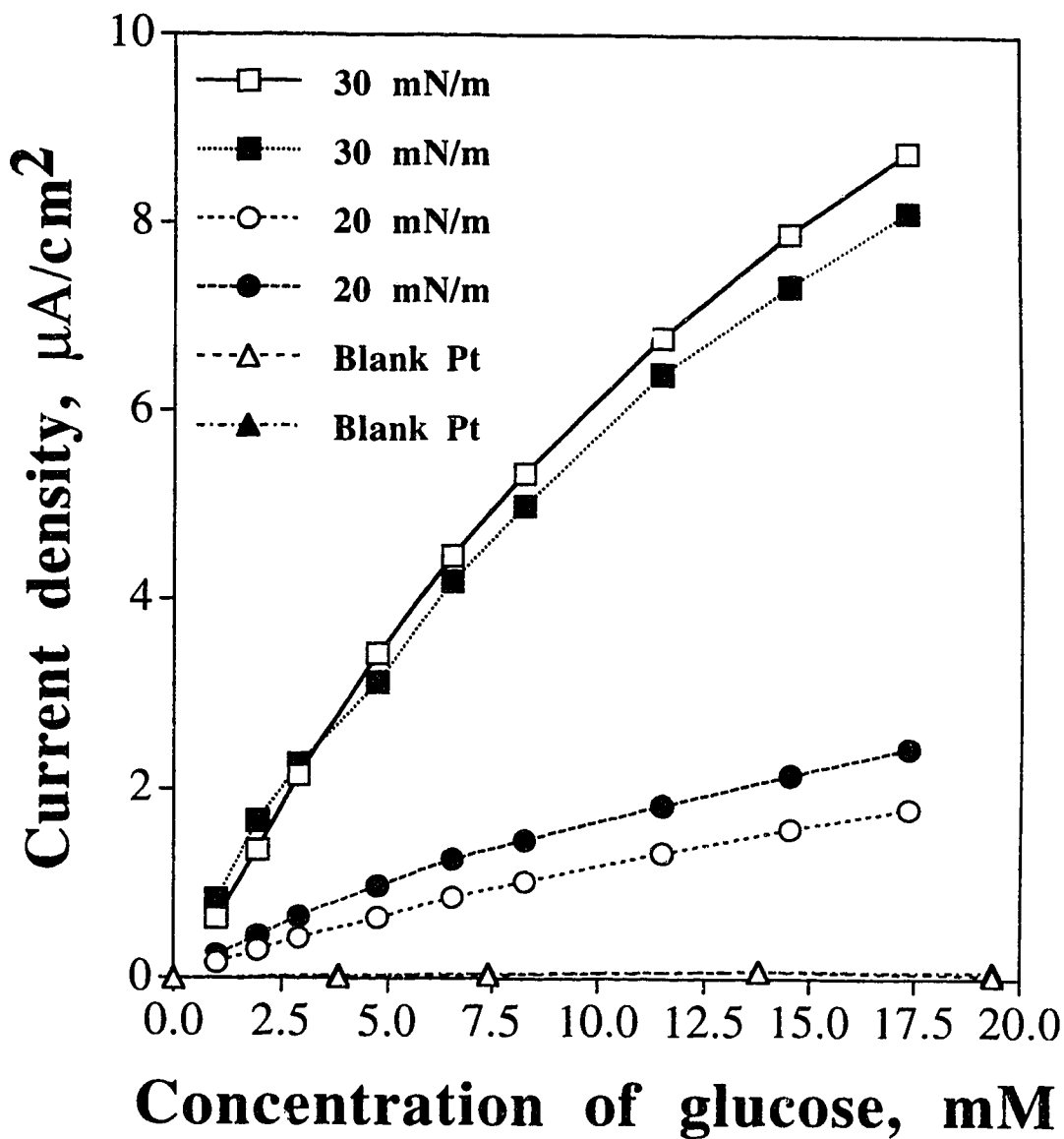


Figure 2.8 Current density as a function of glucose concentration for two Pt electrodes shown as open and filled symbols, respectively. Two layers of modified GO was deposited at indicated surface pressure.

From the QCM experiment, the area per molecule of modified enzyme at 20 mN/m is 9944 \AA^2 and is about twice that (5715 \AA^2) at 30 mN/m surface pressure. This data was measured by QCM at an initial surface concentration of 16.88 mg/m^2 . This indicates that twice as much modified enzyme is deposited on the substrate at a surface pressure of 30 mN/m compared to that at 20 mN/m. The measured activity of the modified enzyme film deposited at a surface pressure of 30 mN/m is about 4 times that for the film formed at surface pressure of 20 mN/m. Apparently, the higher activity of a Langmuir-Blodgett film of modified glucose oxidase prepared at higher surface pressures is not simply due to an increase in the mass of enzyme deposited. This observation also provides evidence for improved orientation of the enzyme in the more densely packed film. However, it does not tell us whether the enzyme is more accessible to the substrate, or if it is less unfolded at higher pressures, so as to be more active.

A blank Pt electrode activity was tested under the same conditions as a modified glucose oxidase, LB film coated, Pt electrode. The response to glucose is only 0.25 \mu A/cm^2 maximum at 15 mM glucose concentration. This result confirms that the glucose response is due to the enzyme films and not due to the catalytic activity of the Pt.

The activity of the LB film of modified glucose oxidase can be compared semiquantitatively to a conventional BSA immobilized glucose oxidase film on Pt. For the BSA film an activity of 166 \mu A/mg of glucose oxidase per mM glucose was measured by Sun *et al.* [15], based on the film composition and the quantity deposited on the electrode. The

normalized current density in units of $\mu\text{A}/\text{mM}$ glucose is 0.648 for a modified glucose oxidase film prepared at a surface pressure of 30 mN/m and 0.162 $\mu\text{A}/\text{mM}$ for a film formed at 20 mN/m. Taking the area per molecule value of 5611 \AA^2 measured by QCM for a modified glucose oxidase film prepared at 30 mN/m, the activity will be 675 ($\mu\text{A}/\text{mg}$)/mM, while for the film formed at 20 mN/m the activity will be 303 ($\mu\text{A}/\text{mg}$)/mM with a measured area per molecule value of 9944 \AA^2 by QCM. The relative enzyme activity of Langmuir-Blodgett films of modified glucose oxidase is about 4 times higher than the conventional BSA immobilized film. Clearly, the modified glucose oxidase films transferred by the Langmuir-Blodgett technique has much better sensitivity than a conventional BSA immobilized film.

2.4 Conclusions

In this study some of the work done by Sun *et al.* was repeated, some of that work was further extended, and new mass-based isotherms were obtained. Five points are summarized below.

(1) The Langmuir-Blodgett technique is a powerful means of transferring active glucose oxidase films to a substrate without the need for any added lipid component. As Sun *et al.* [15] showed, the cross-linking reagent, glutaraldehyde, greatly increases the activity of the enzyme films. The most likely role of the glutaraldehyde is to intra-molecularly link base residues on the enzyme in such a way as to increase its quaternary and tertiary

structural rigidity and resistance to denaturing forces. Up to at least 10 monolayers of enzyme have been transferred to a substrate by using the LB technique without any difficulty. This method results in films with much increased sensitivity and improved response time for glucose determination when compared to lipid glucose oxidase films prepared by Langmuir-Blodgett techniques. The studies reported here reconfirm all of Sun *et al.*'s earlier results.

(2) The LB film thickness measured by ellipsometry shows a significantly increased thickness of cross-linked glucose oxidase films compared to the native glucose oxidase films. An average of 34 Å for native glucose oxidase and 45 Å for modified glucose oxidase at 30 mN/m are similar to the results of 30 Å for native enzyme and 48 Å for the modified enzyme obtained by Sun *et al.* The small differences are likely due to experimental errors. The LB films of modified glucose oxidase are much thicker than the native glucose oxidase. This result shows the cross-linking reagent, glutaraldehyde must stabilize the structure of glucose oxidase LB films.

(3) A detailed data set of pressure-area and mass-area isotherms was presented. The initial surface concentration affects the area per molecule value from pressure-area isotherm. The area per molecule obtained from pressure-area isotherm are about 1728 Å² and 2571 Å² at 0 mN/m for native and modified glucose oxidase, respectively at a surface concentration of 8.75 mg/m² and 9.11 mg/m². This is well outside the value predicted by the hydrodynamic radius, 5800 Å² per molecule. The area per molecule obtained

from the QCM mass isotherms, of 5723 \AA^2 and 5611 \AA^2 for native and modified glucose oxidase, are in reasonable agreement with the known hydrodynamic radius of the enzyme. This shows the film is, on average, a closely packed monolayer. This study confirms that the surface pressure-area isotherms are unreliable, and that total mass deposited, as measured by the QCM gives more reliable data.

(4) From the measurement of film thickness by ellipsometry and area per molecule by QCM, the modified glucose oxidase film transferred by the Langmuir-Blodgett technique appears to give a reasonably compact monolayer at a surface pressure of 30 mN/m. The experimental results are not really in agreement with the area predicted by the X-ray crystallographic dimensions of the dimer, which are $60 \text{ \AA} \times 52 \text{ \AA} \times 77 \text{ \AA}$ for glucose oxidase derived from *Aspergillus niger*. Instead the hydrodynamic radius gives a better prediction of the area per molecule indicating the film is less dense than a two dimensional crystal of glucose oxidase would be.

(5) With same amount of glucose oxidase, the relative activity of modified glucose oxidase at 30 mN/m is about 4 times that of conventional BSA film. The electrochemical activity measurement shows that the surface pressure of LB films affects the relative enzyme activity, since the activity/molecule is twice as high at 30 mN/m as it is at 20 mN/m. This effect may suggest that distortion of the enzyme structure is greater in the less dense film, which might decrease the activity. Alternatively, there may be better orientation of the enzyme for glucose oxidation when prepared in densely packed form.

2.5 References

1. Hecht, H. J.; Kalisz, H. M.; Hendle, J.; Schmid, R. D.; Schomburg, D., *Crystal structure of Glucose Oxidase from Aspergillus niger Refined at 2.3 Å Resolution, J. mol. Biol.*, **1993**, *229*, 153-172.
2. Pazur, J. H., Kleppe, K., Cepure, A., *Arch. Biochem. Biophys.* **1965**, *111*, 351-357.
3. Hayashi, S., Nakamura, S., *Biochem. Biophys. Acta*, **1981**, *657*, 40-51.
4. Takegawa, K., Fukiwara, K., Iwahara, S., Yamamoto, K., Tochikura, T., *Biochem. Cell Biol.*, **1989**, *67*, 460-464.
5. Takegawa, K., Fukiwara, K., Iwahara, S., Yamamoto, K., Tochikura, T., *Agric. Biol. Chem.*, **1991**, *55*, 883-884.
6. Kalisz, H. M., Schmid, R. D., Hecht, H. J., Schomburg, D., *Biochim. Biophys. Acta*, **1991**, *1080*, 138-142.
7. Pazur, J. H., Kleppe, K., *Biochemistry*, **1964**, *3*, 578-583.
8. Adams, E. C., Jr. Mast. R. L., Free, A. H., *Arch. Biochem. Biophys.* **1960**, *91*, 230-234.
9. Gibson, Q. H., Swoboda, B. E. P., Massey, V., *J. Biol. Chem.*, **1964**, *239*, 3927-3934.
10. Bright, H. J., Gibson, Q. H., *J. Biol. Chem.*, **1967**, *242*, 994-1003.
11. Bright, H. J., Appleby, M., *J. Biol. Chem.*, **1969**, *244*, 3625-3634.
12. Duke, F. R., Weibel, M., Phage, D. S., Bulgrin, V. G., Luthy, J., *J. Amer. Chem. Soc.*, **1969**, *91*, 3904-3909.
13. Weibel, M. K., Bright, H. J., *J. Biol. Chem.*, **1971**, *246*, 2734-2744.

14. Bright, H. J., Porter, D. J. T., In *The Enzymes* 3rd edit. (Boyer, P. D., ed.), **1975**, pp. 421-505, Academic Press, New York, San Francisco and London.
15. Sun, S.; Ho-Si, P. H.; Harrison, D. J., *Langmuir*, **1991**, *7*, 727-737.
16. Laylin, K. J.; Leroy, G. A., *Advances in Enzymology*, **1966**, *28*, 1-39.
17. Gaines, G. L., *Insoluble Monolayers at Liquid-Gas Interfaces*, **1966**, Chapter 4, New York, Interscience Publishers.
18. Buttry, D. A., In *Electroanalytical Chemistry*, Bard, A. J., Ed., Marcel Dekker: New York, **1991**, *17*, 1-85.
19. Nakamura, S.; Hayashi, S.; Koga, K.; *Biochem. Biophys. Acta* **1976**, *445*, 294.
20. Vainshtein, B. K.; Kiselev, N. A.; Kaftonova, A. S., *Mol. Biol.*, **1974**, *10*, 19.
21. Jones, M. N., Manley, P., Wilkinson, A., *Biochem. J.*, **1982**, *203*, 285-291.
22. Melroy, O.; Kanazawa, K.; Gordon II, J. G.; Buttry, D., *Langmuir*, **1968**, *vol. 2, No. 6*, 697-700.
23. Miller, I. R.; Bach, D., *Surf. Colloid Sci.* **1977**, *7*, 185.
24. James, L, K.; Augenstein, L. G., *Adv. Enzymol. Relat. Subj. Biochem.* **1966**, *28*, 1.
25. Adamson, A. W., *Physical Chemistry of Surfaces*, 4th ed.; J. Wiley: New York, **1982**; *Chapter 3*.
26. Adams, D. J.; Evans, M. T. A.; Mitchell, J. R.; Phillips, M. C.; Rees, P. M., *J. Polym. Sci., Part C: Polym. Symp.* **1971**, *34*, 167.

CHAPTER 3

TRANSMISSION ELECTRON MICROSCOPY (TEM) AND ATOMIC FORCE MICROSCOPY (AFM) STUDY OF GLUCOSE OXIDASE FILMS

3.1 Introduction

Knowledge of the microstructure of materials was markedly advanced with the advent of the optical and later the electron microscopes. While the unaided eye can resolve features no smaller than about 0.1 mm in size, the optical microscope allows perception of textures 1/500 of this limit. The electron microscope provides a similar improvement in imaging power over even the most advanced optical microscopes. In fact electron microscopic resolutions approaching interatomic distances of some solids (2-3 Å) have frequently been demonstrated. The electron microscope has been shown to be an indispensable investigative tool [1].

Images produced in an electron microscope arise from the interaction of a high-energy electron beam with a thin-film specimen. This interaction manifests itself in various forms of electron scattering that are primarily dependent on material characteristics, e.g., thickness, density, and crystallinity.

Soft organic materials have been studied by TEM, and polymer science in particular benefited. Applications of TEM in polymer science include determining molecular weight of single molecules [2], and performing quantitative structure analysis of single crystal polymers [3]. TEM also helped establish an understanding of chain folding and molecular packing, aided the study of crystallization of polymers from the melt [4], and the study of microfibrillar of oriented polymers [5]. Polyethylene is perhaps the most widely studied polymer in this area. The study of Langmuir-Blodgett films by TEM has been more limited. H. E. Ries *et al.* reported the electron micrographs of monolayers of a synthetic lecithin by using Langmuir-Blodgett techniques to transfer monolayer samples [6]. A number of investigators have employed the electron microscope to study deposited fatty acid monolayers [7]. Unfortunately, electron microscopy of organic polymers or biological compounds is somewhat hampered by the low-contrast image they produce. Special specimen preparation techniques are required. Shadowing is one of the techniques which greatly improves the image contrast.

Atomic force microscopy (AFM) of biological structures is progressing rapidly, due to its fast speed of analysis and the fact it is not limited by poor electrical conductivity. P. J. Mulhern *et al.* used AFM to study a cell sheath [8]. H. G. Hansma *et al.* reported AFM images of DNA covalently and non-covalently bound to a Langmuir-Blodgett film of polymerizable fatty acid transferred onto a mica substrate [9]. The AFM obtains images fast enough (a few seconds per image) to observe many biological and chemical processes in real time [10].

The TEM images of both modified and native glucose oxidase LB films coated at a surface pressure of 30 mN/m are presented in this Chapter. AFM imaging of modified glucose oxidase film, transferred by the LB method to a silicon substrate with and without Pd/Pt coating was performed. No satisfactory AFM images were obtained for the uncoated glucose oxidase films due to the fact the soft enzyme adsorbed on the tip and was pushed out of the scan area. Data is reported for the alloy coated films.

3.2 Experimental

3.2.1 Preparation of glucose oxidase LB films

All films for TEM and AFM study were prepared using the Langmuir-Blodgett technique to deposit coatings on silicon substrates as described in Chapter 2. In this study, glucose oxidase modified with glutaraldehyde films (with and without ultrafiltration) and native glucose oxidase films were transferred onto silicon substrate at a surface pressure of 30 mN/m.

For native glucose oxidase, the original glucose oxidase solutions were prepared by dissolving about 40 - 60 mg of glucose oxidase in 8 ml of double distilled, deionized water and 2 ml of double distilled methanol, giving a concentration of about 0.4 to 0.5 mg/ml. The modified glucose oxidase was prepared by adding 1 ml of 25% glutaraldehyde to the above solution, and allowing it to react for more than 24 hours at room temperature. The solution was then ultrafiltered using an XM-300 Diaflo ultrafilter (Amicon. Inc.) The

concentration of modified glucose oxidase solution after filtration was determined by absorbance measurements using the calibration curve technique discussed in Chapter 2.

When preparing LB films of native glucose oxidase, about 0.5 ml of solution was delivered to the subphase to ensure that there was enough material for coating a few silicon slides. For modified glucose oxidase solution, delivering 2 to 3 ml was necessary since the concentration was decreased after filtration. Before silicon substrate dipping into the subphase, the Langmuir trough was fully opened to maintain a minimum surface pressure, then a surface pressure of 30 mN/m was maintained by compression of the surface area during substrate withdrawal at 10 mm/min. For all TEM and AFM samples, a 20 mm length of silicon substrate was dipped into the subphase and single layer coating was performed.

A Gaertner L125B two-wavelength ellipsometer equipped with a rotating analyzer was used to measure the thickness of LB films. Data acquisition and ellipsometer control were done with an IBM- PS-2 system and software provided by Gaertner. Microspot optics gave a sampled area of 0.002 mm^2 at a 70° incident angle and 0.001 mm^2 at a 50° incident angle. The 6328 \AA source was employed and an angle of 70° was most commonly used.

A single layer absorbing (SLA) program was used to measure the thickness of the uncoated regions of sample silicon slides. This measurement determines the native oxide (SiO_2) thickness t , which is typically 20 to 30 \AA . Using the Two Layer Non-Absorbing (TLNA) program with the following parameters: Si substrate $n_s=3.850$, $k_s=0.020$, oxide (SiO_2) layer $n=1.46$

(fixed), t =measured thickness from uncoated region (thickness of SiO_2), the thickness for LB film coated regions was then analyzed assuming a two-layer coating of enzyme/ SiO_2 /Si:substrate. For an LB film thickness greater than 150 Å, both thickness and refractive index could be determined from the data. An average value of $n_{\text{LB}}=1.50$ was obtained for the deposited enzyme and this value was used as a fixed parameter for calculating the thickness of films less than 150 Å thick. As discussed in Chapter 2, the average thickness of native glucose oxidase LB film is 34 Å, while it is 45 Å for a modified glucose oxidase film.

3.2.2 Preparation of TEM specimen

A) Silicon substrates coated with enzyme or without an enzyme layer (blank slides) were shadow coated with Pd/Pt (10/90) alloy (about 1 nm thick) at about a 15 to 30° degree angle, by using a vacuum evaporation coater operated under high vacuum (10^{-6} Torr, Denton Vacuum DV-502A). A layer of carbon film (about 100 nm thick) was then coated under the same conditions, but the sample was rotated. A schematic diagram of shadowing is shown in Figure 3.1 [1].

B) Floating the carbon coated films: First, the silicon slides coated with Pd/Pt and carbon layers were put into 30% KOH solution for 10 minutes, then transferred to pure double distilled water. A few drops of 1% Sparkleen solution helped to float larger pieces of film on the surface of the water. The floated films were put onto the TEM grids by capturing them with a grid from underneath.

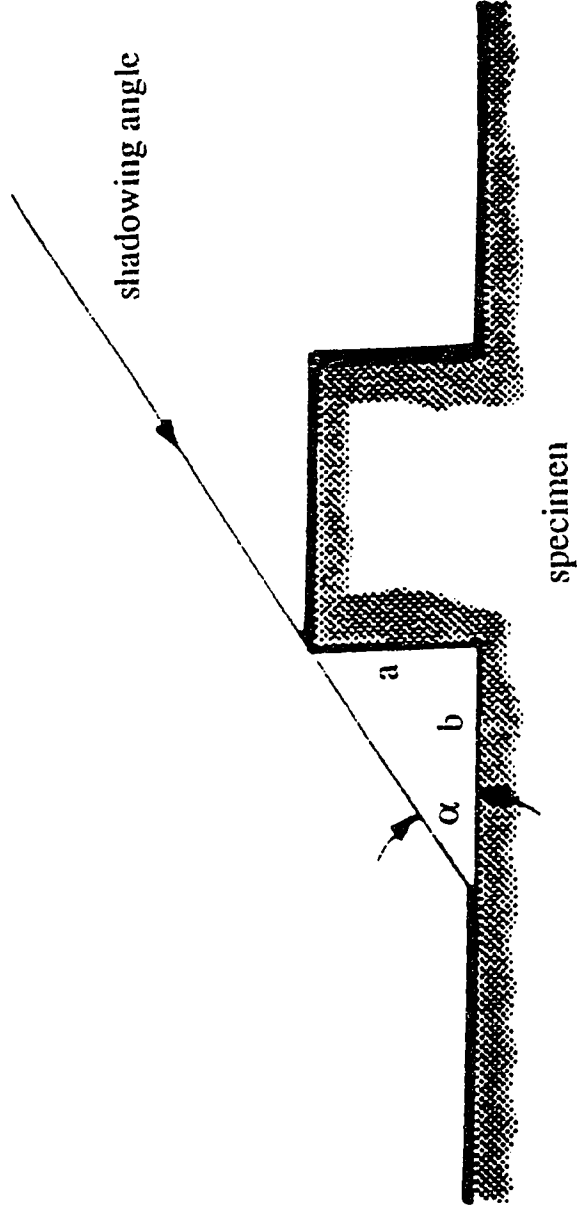


Figure 3.1 Shadowing used to determine thickness, $a = b \tan \alpha$ [1].

3.2.3 Preparation of AFM sample

Two types of AFM samples were prepared in this study. They were LB films of modified glucose oxidase without a Pd/Pt alloy coating and with a Pd/Pt coating. The coating used the same procedures as for the TEM specimens. These were air dried and kept in a clean plastic container.

3.2.4 TLM and AFM equipment

The TLM system used in this study was a HITACHI H-7000 (Med/Dent EM lab. University of Alberta). In this study, experimental conditions of #3 objective lens and acceleration voltage of 75 KV were used to obtain the TEM images. The film used for the HITACHI H-7000 was Kodak Eastman Fine Grain Release Positive Film (5302).

The AFM images were taken from a Topometrix TMX-2000 (Canada Centre for Mineral and Energy Technology, CANMET, DEVON) and data acquisition was accomplished by using SPM Lab V3.04 program. Image analysis was done with a newer version of SPM Lab V3.06. We used silicon nitride (Si_3N_4) cantilevers with Si_3N_4 integrated tips and constant force mode to obtain topography images in air. A scan rate of 5 $\mu\text{m/s}$ was used and data reported were after levelling analysis. In our study, contact (conventional topography) mode of AFM was performed and the force between sample and the tip was repulsive.

3.3 Results and discussions

3.3.1 Blank silicon substrate TEM images

Figure 3.2 shows TEM images of a silicon substrate blank which was not dipped in the subphase. The magnification in Figure 3.2a is 234,000 and in Figure 3.2b it is 27,000. Figure 3.3a and Figure 3.3b show the TEM images of a blank silicon substrate dipped into the subphase with no enzyme present, with magnifications of 31,000 and 234,000, respectively.

The silicon substrate prepared without dipping into the subphase shows a flat, smooth surface at a magnification of 27,000. When the silicon substrate was dipped in the subphase the surface was also smooth, but some spots and big clumps appeared in the TEM image, as shown in Figure 3.3a. These artifacts were introduced from the subphase [7]. At the higher magnification of Figure 3.2b and Figure 3.3b, both the blank substrates show a similar surface morphology. They both appear uniform and featureless.

3.3.2 TEM images of modified glucose oxidase LB films

Figure 3.4 shows TEM images of a modified glucose oxidase LB film with a one layer coating, prepared at a surface pressure of 30 mN/m. Two separately prepared samples are illustrated, with a magnification of 234,000. The modified glucose oxidase solutions were made from either 55.4 mg or 42.0 mg of native glucose oxidase (Sigma, type X-S), followed by ultrafiltration after modification with glutaraldehyde.

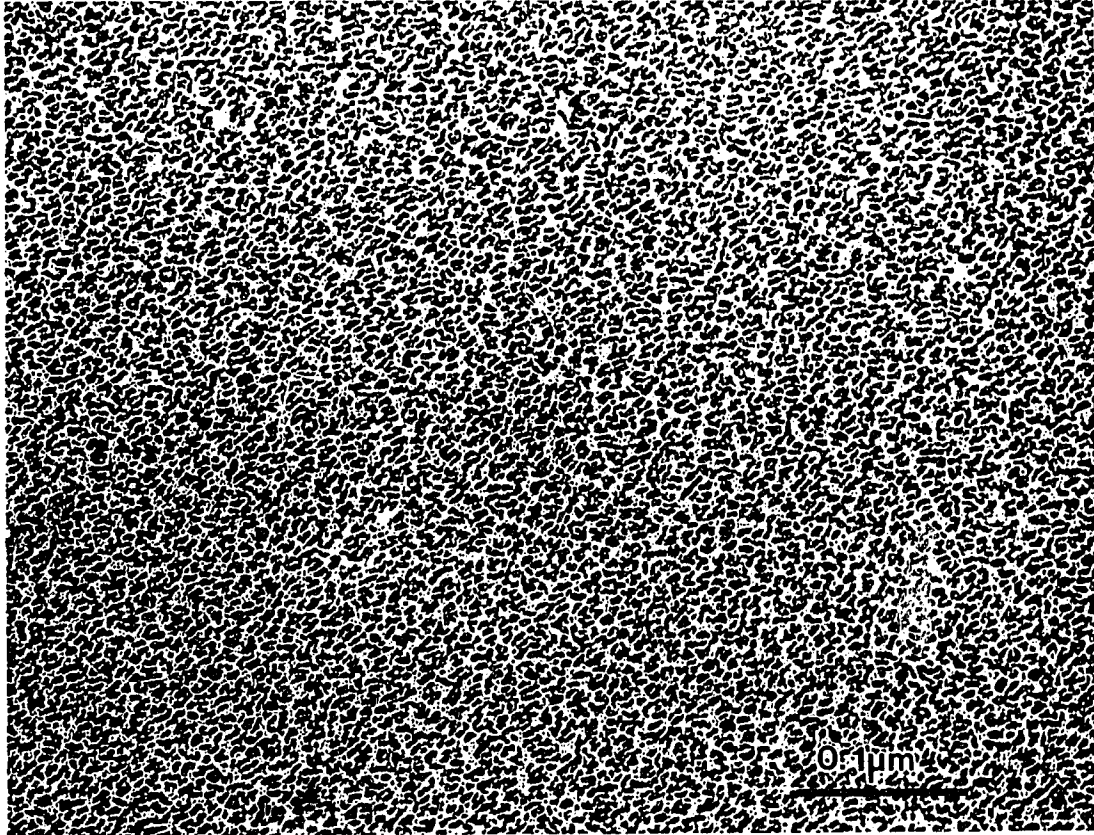


Figure 3.2a TEM image of silicon substrate. It was not dipped in the subphase. The magnification is 234,000.

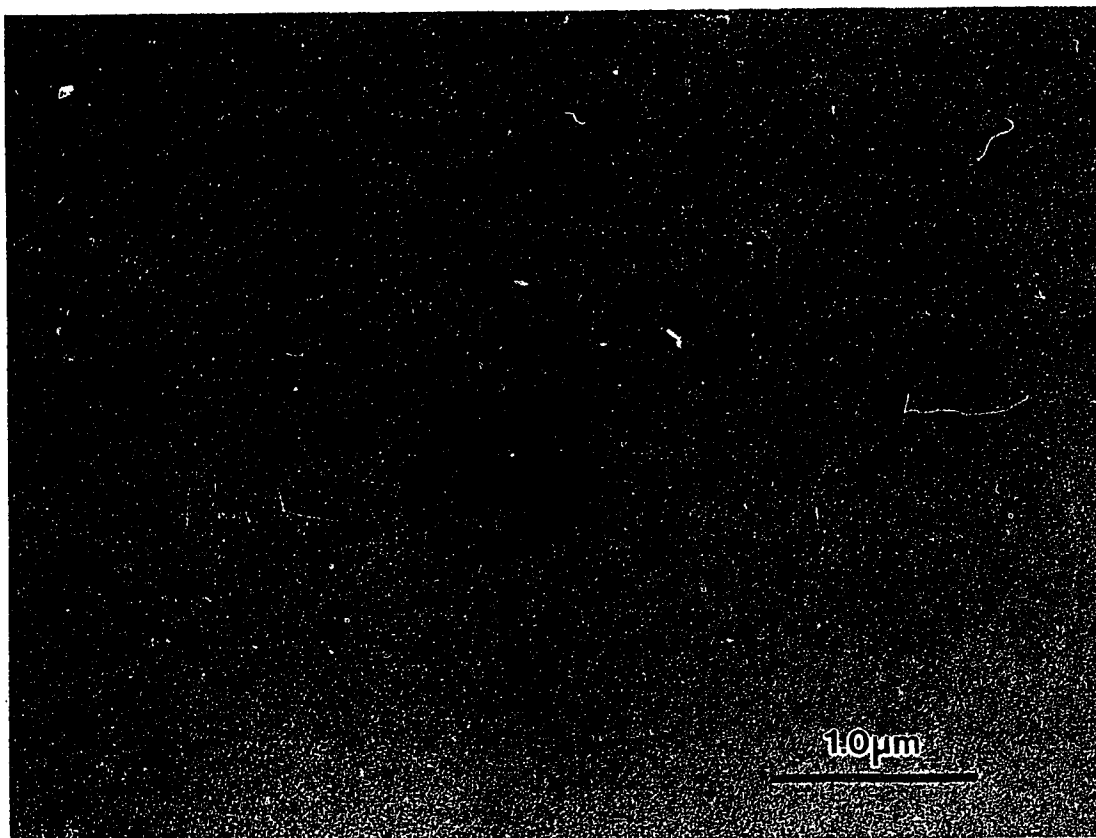


Figure 3.2b TEM image of the same silicon substrate as in Figure 3.2a with a magnification of 27,000.

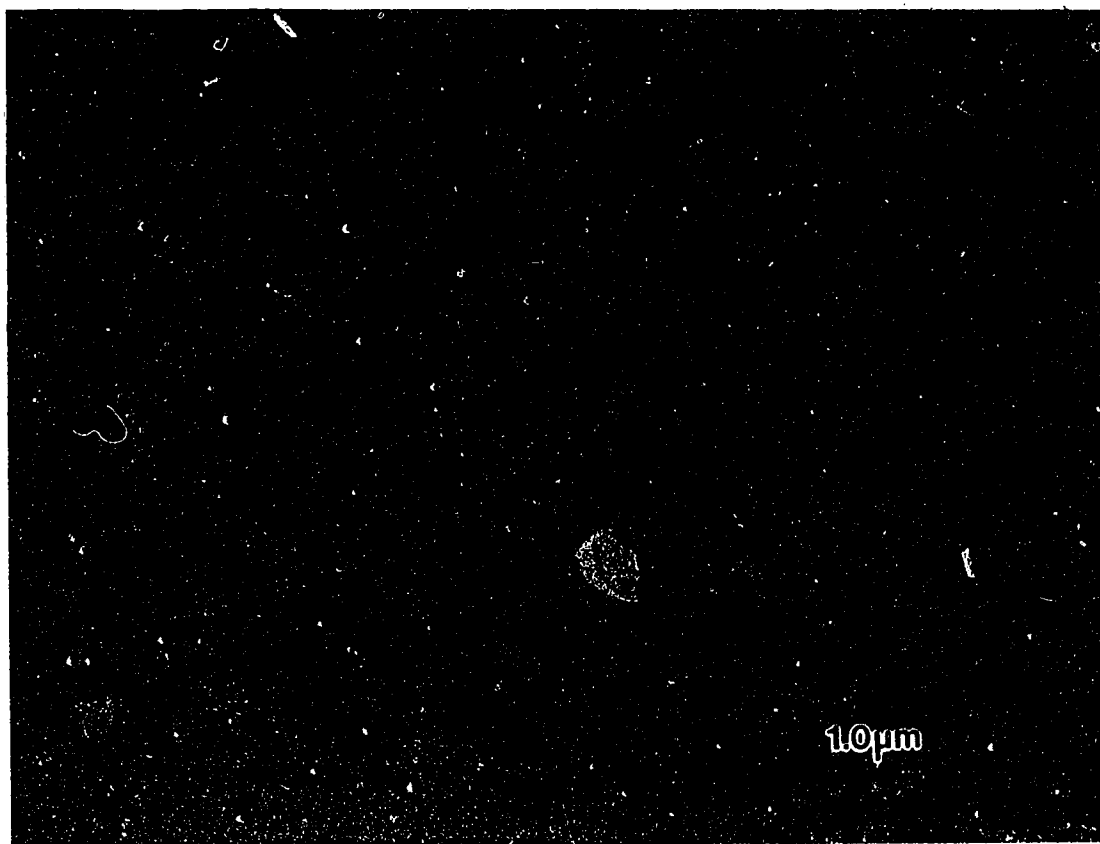


Figure 3.3a TEM image of silicon substrate dipped in the subphase with a magnification of 31,000.

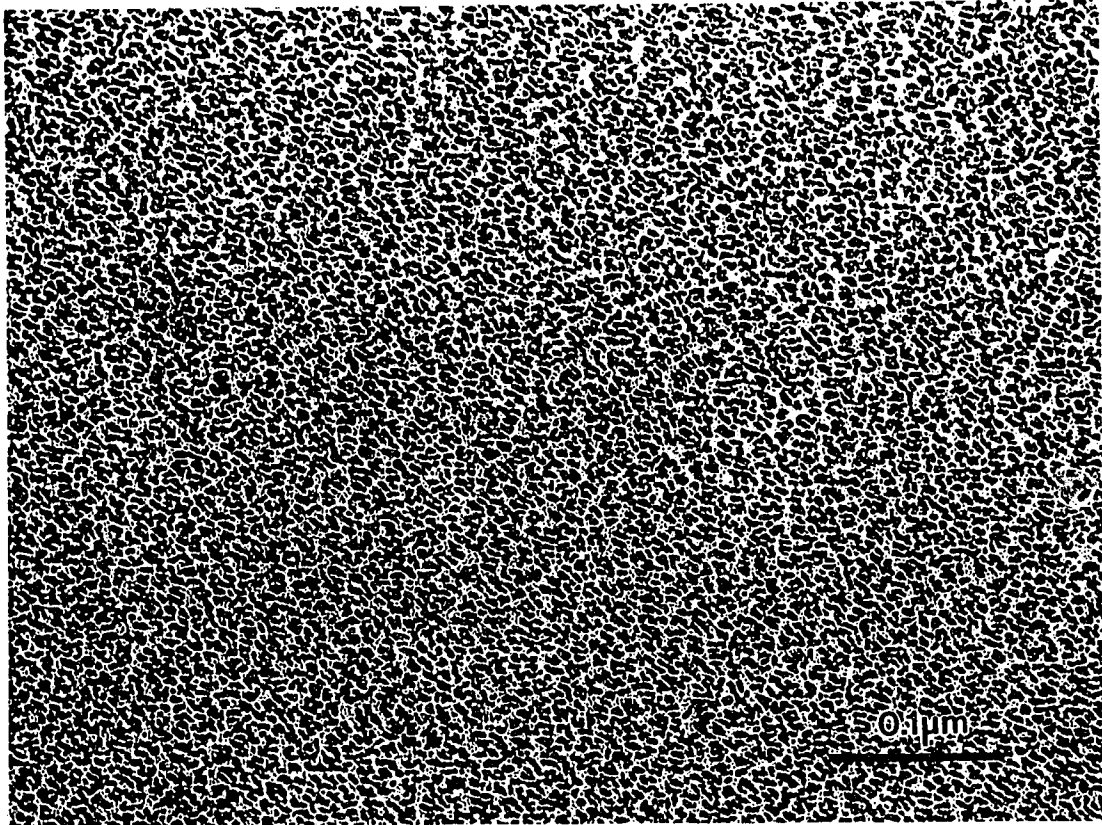


Figure 3.3b TEM image of silicon substrate dipped in the subphase with a magnification of 234,000.

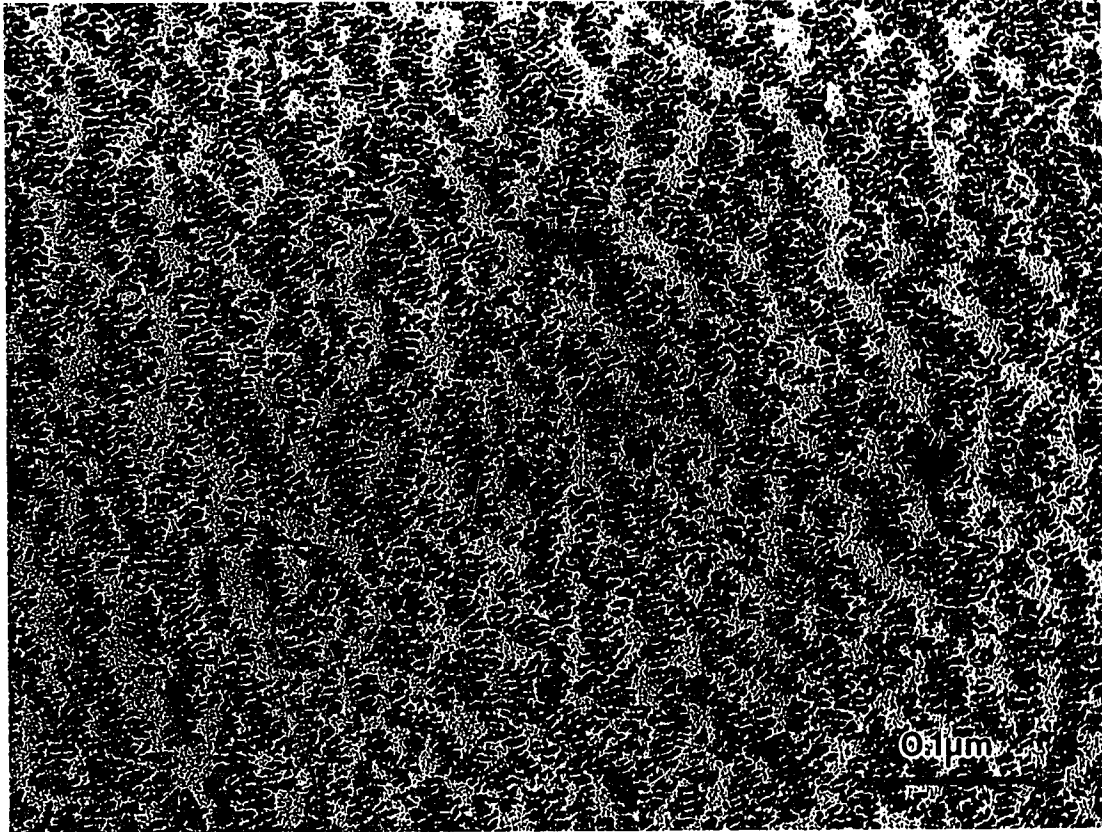


Figure 3.4a TEM image of one layer modified glucose oxidase LB film coated at a surface pressure of 30 mN/m. The solution was 55.4 mg/ml and ultrafiltered. The magnification is 234,000.

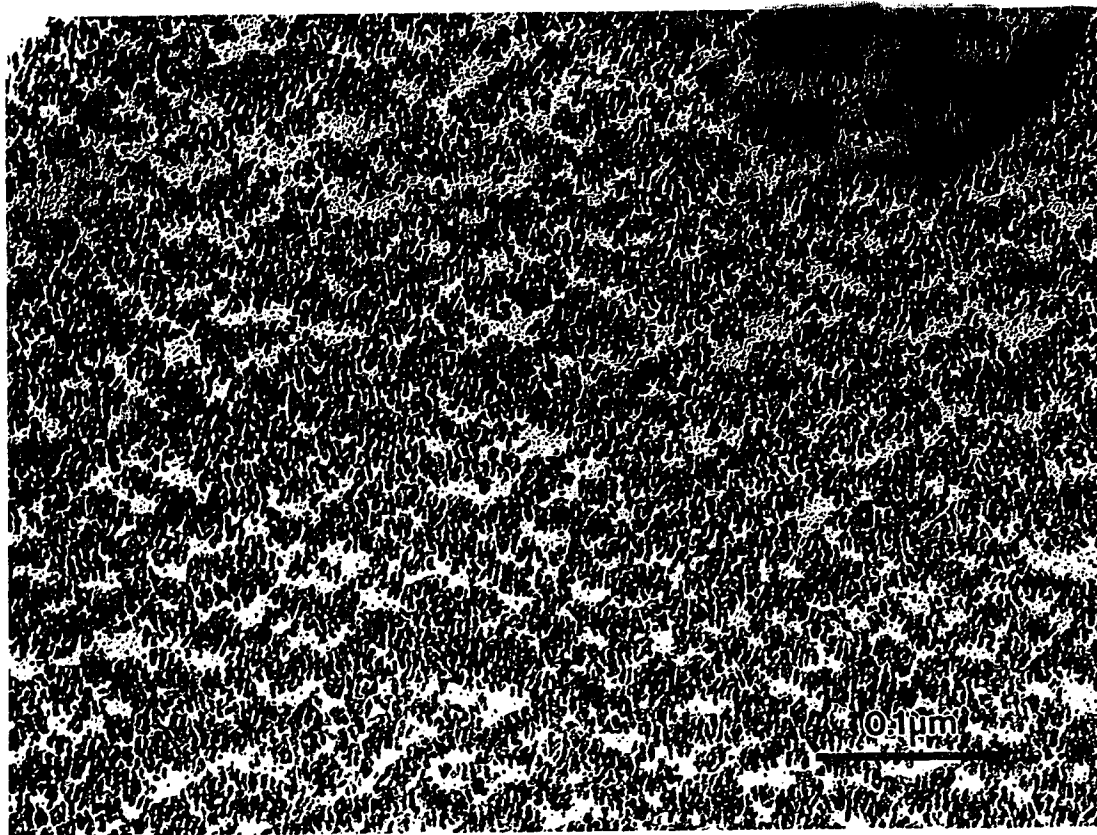


Figure 3.4b TEM image of one layer modified glucose oxidase LB film coated at a surface pressure of 30 mN/m. The solution was 42.0 mg/ml and ultrafiltered. The magnification is 234,000.

The two samples in Figure 3.4a and 3.4b show a similar surface pattern. The dark regions are the Pd/Pt alloy coated areas, which represent high regions in the topography of the protein coating. The light areas are the regions in shadow during the Pt/Pd coating and represent low valleys in the topography of the deposited enzyme. The width of the high regions is in the range of about 128 Å to 342 Å. The shape is predominantly a continuous long stranded snake, with some short branches attaching different strands to each other. There appears to be local order, with a parallel pattern, however, over large areas the pattern becomes fairly random.

The gaps in the image are in the range of about 85 Å to 170 Å wide. The shadowing produces a very highly scattering layer, which greatly improves contrast. Applied at an angle, shadowing also accents surface topography. If the angle is known, the technique provides a means for determining thickness as shown in Figure 3.1 [1].

$$\mathbf{a = b \tan \alpha} \tag{3.1}$$

where a is the film thickness in Å, b is the gap in the topography in Å, and α is the shadowing angle.

In our experiment, the shadowing angle is about 30°. Taking b as the gap we measured and using equation 3.1, the calculated thickness is in the range of 49 Å to 98 Å. The thickness measured by ellipsometry is 45 Å, but it is an average value across a much larger area than studied by TEM. The TEM data shows there are gaps and high points, consistent with an average

thickness value measured by ellipsometry being lower than the thickness measured by TEM. The 98 Å thickness probably indicates enzyme molecules are stacked up on each other, although given a maximum diameter of 77 Å from the crystal structure this is not a definitive conclusion.

The TEM image of the same specimen as in Figure 3.4a is shown in Figure 3.5 with a smaller magnification of 31,000. This Figure shows that on the largest scale, the overall film shows a continuous and homogeneous pattern for the modified glucose oxidase films. However, the coarseness of the coating is still apparent.

Figure 3.6a and Figure 3.6b are the TEM images of modified glucose oxidase LB films formed after and before ultrafiltration, respectively. They are at the same magnification of 109,000. The original glucose oxidase solution was 5.71 mg/ml before filtering. A 0.5 ml aliquot was delivered to the trough for the unfiltered solution and 2 ml for the filtered solution. Comparing Figure 3.6a and Figure 3.6b, we conclude that the film formed from a filtered, modified glucose oxidase solution shows a much more uniform and smooth surface than does a film formed from an unfiltered solution.

3.3.3 TEM images of native glucose oxidase

The TEM images of one layer of native glucose oxidase LB films coated at a surface pressure of 30 mN/m are shown in Figure 3.7a and 3.7b, with magnifications of 109,000 and 26,000, respectively. The concentration

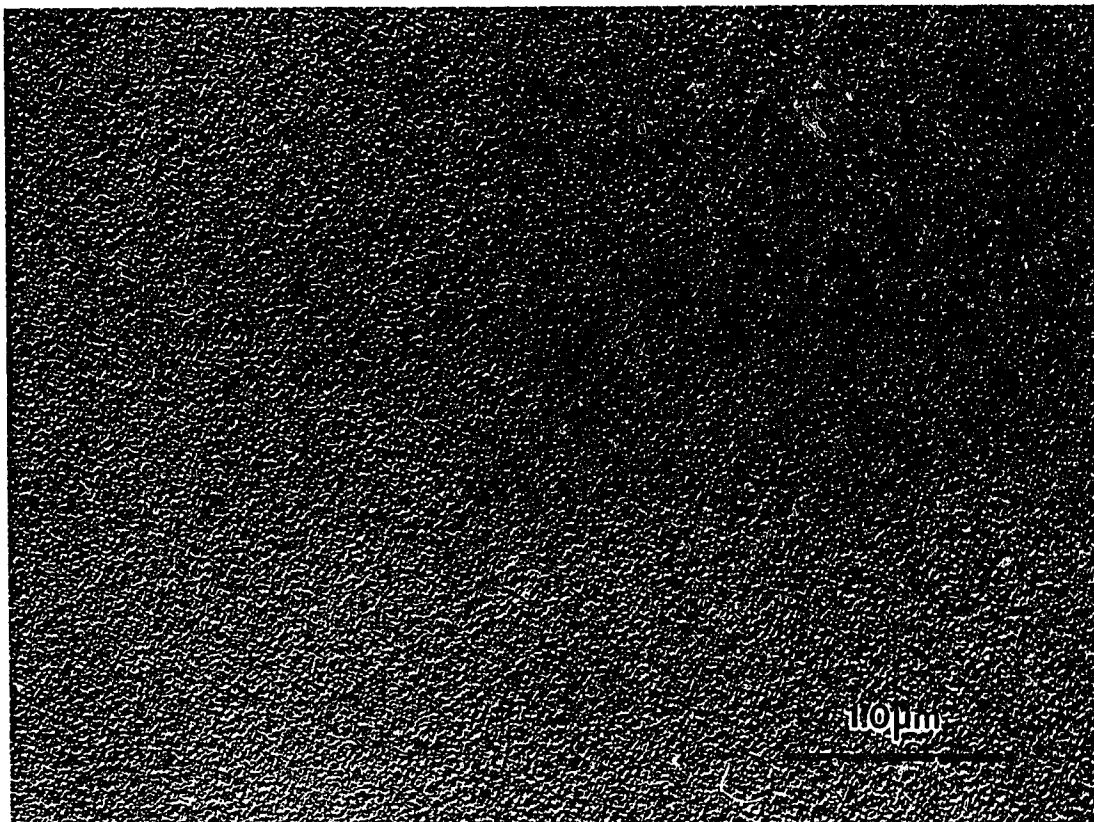


Figure 3.5 TEM image of one layer modified glucose oxidase LB film coated at a surface pressure of 30 mN/m. The solution was 55.4 mg/ml and ultrafiltered. The magnification is 31,000.

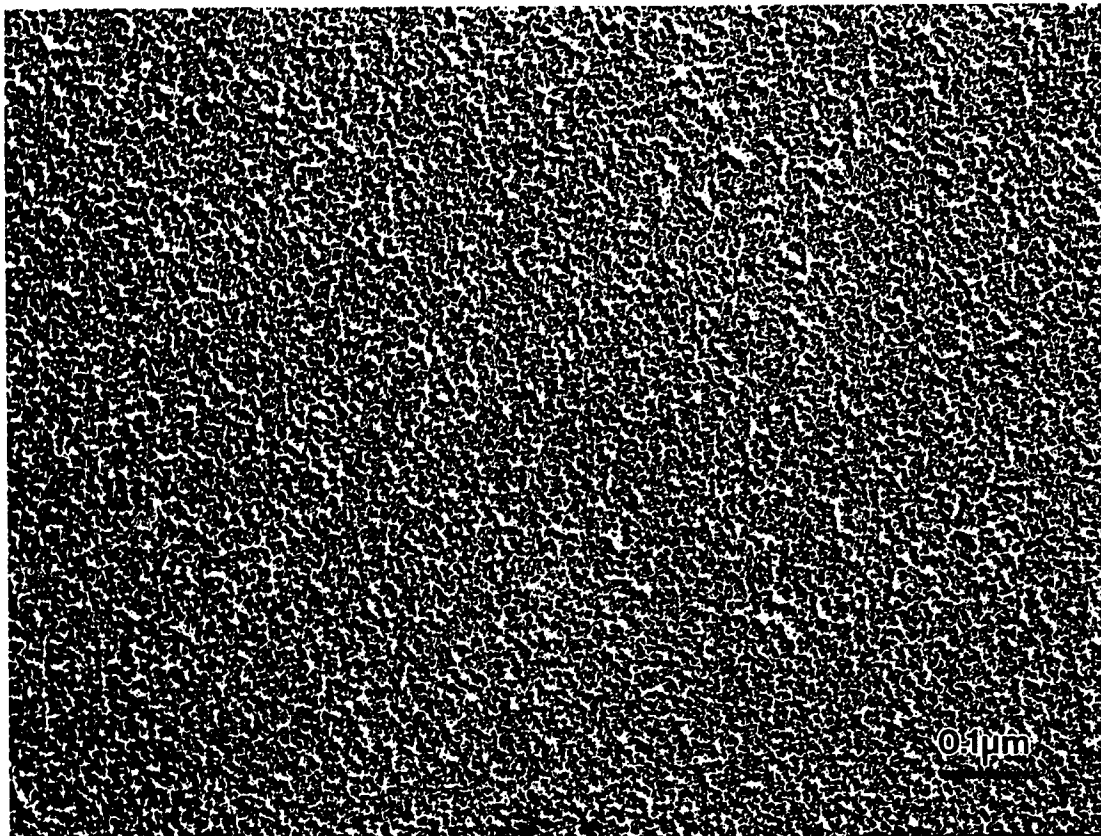


Figure 3.6a TEM image of one layer modified glucose oxidase LB film coated at a surface pressure of 30 mN/m. The solution was 57.1 mg/ml and ultrafiltered. The magnification is 109,000.

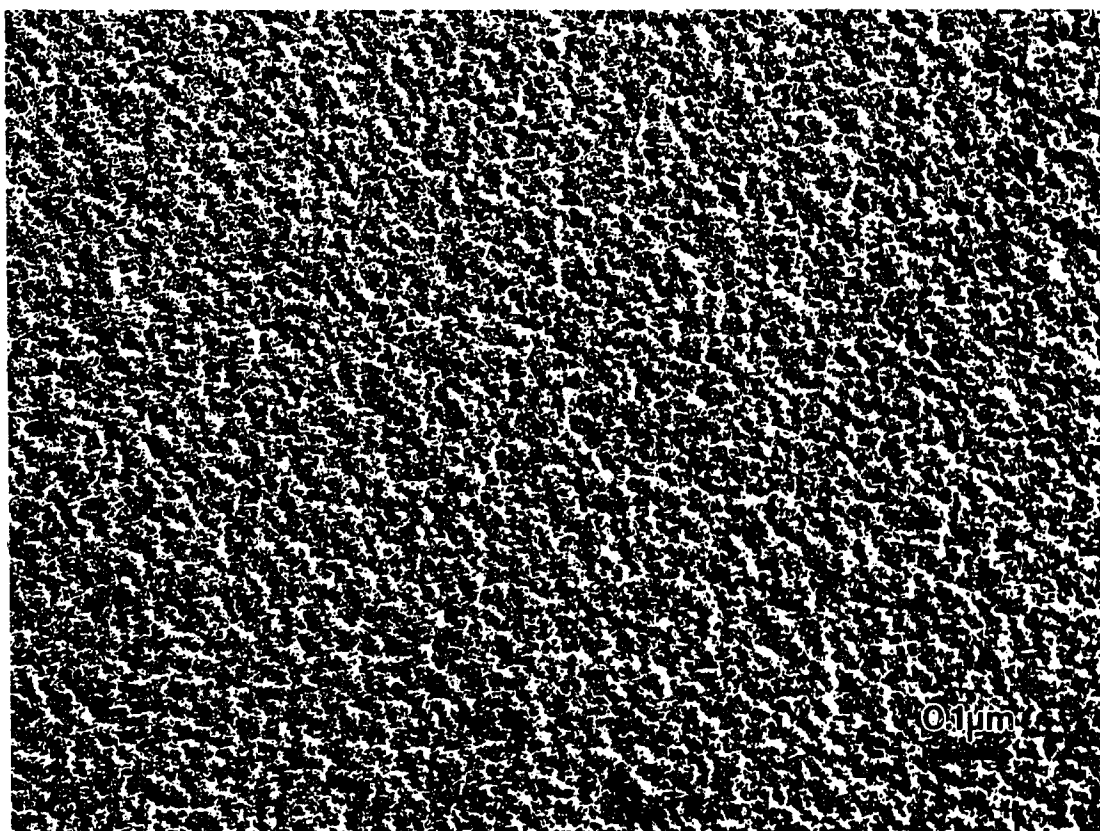


Figure 3.6b TEM image of one layer modified glucose oxidase LB film coated at a surface pressure of 30 mN/m. The solution was not filtered. The magnification is 109,000.

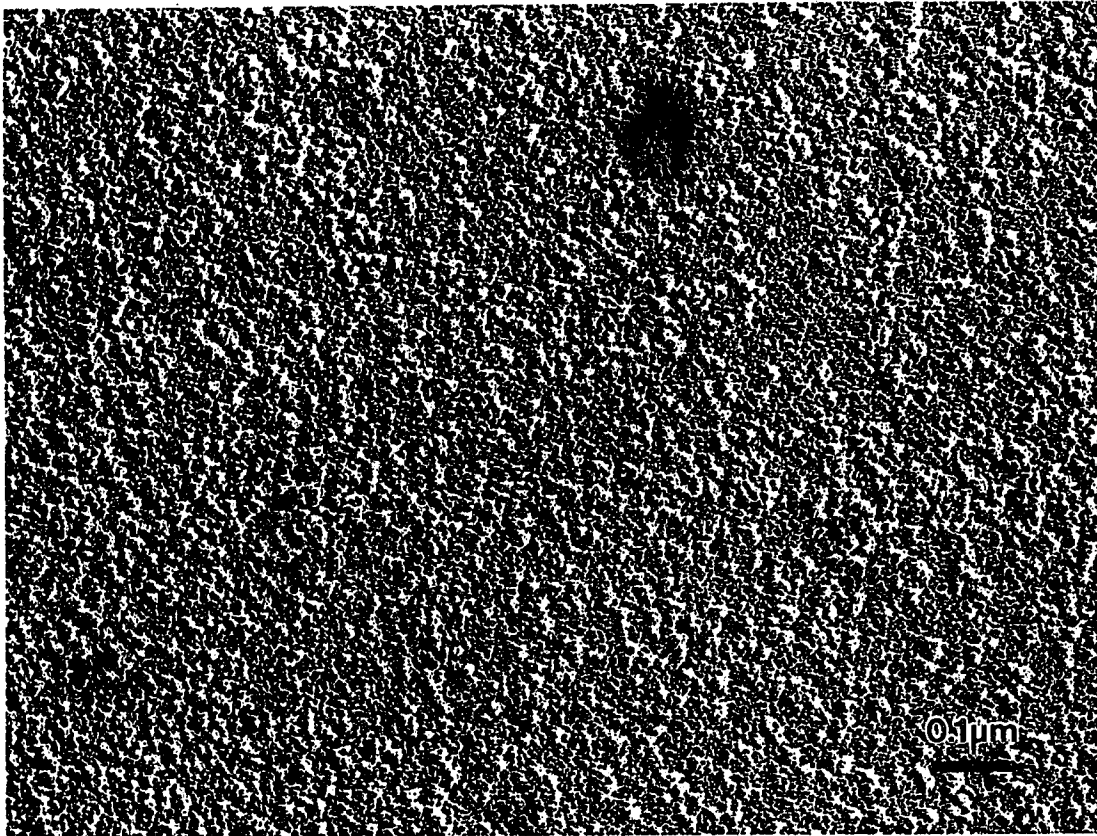


Figure 3.7a TEM image of one layer native glucose oxidase LB film coated at a surface pressure of 30 mN/m. The concentration of solution was 4.01 mg/ml. The magnification is 109,000.

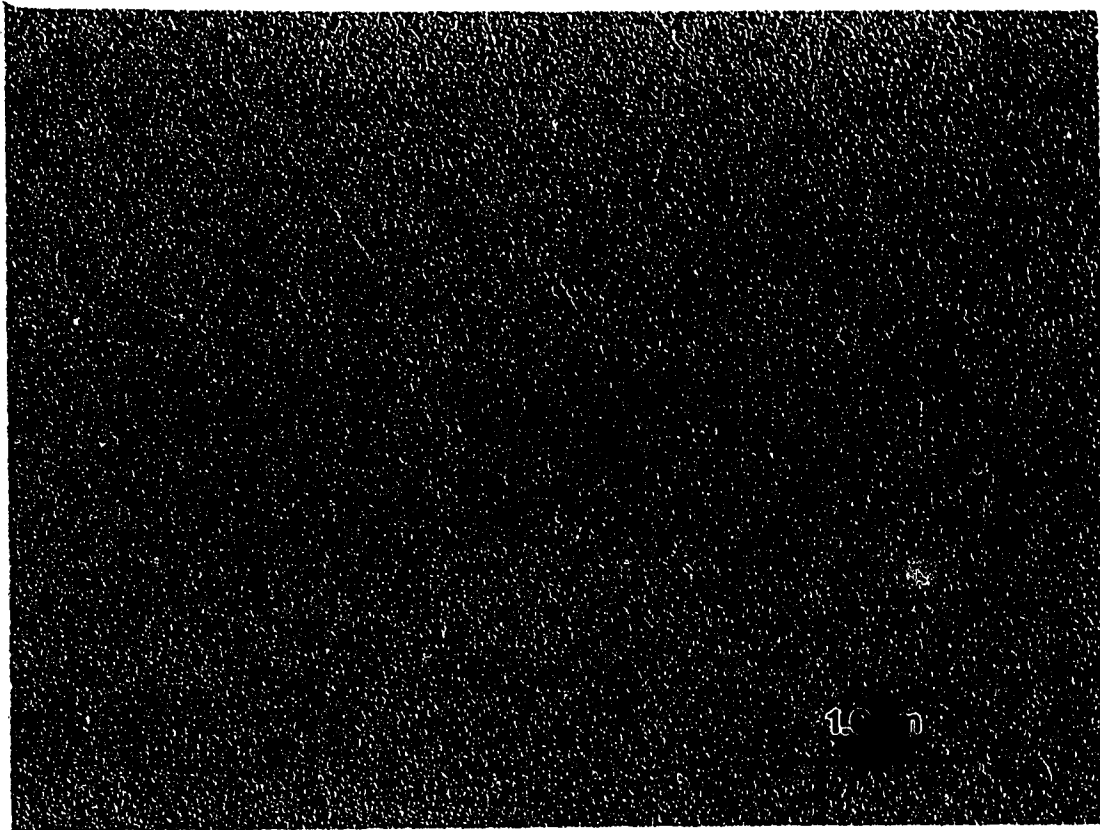


Figure 3.7b TEM image of one layer native glucose oxidase LB film coated at a surface pressure of 30 mN/m. The concentration of solution was 4.01 mg/ml. The magnification is 26,000.

of the native glucose oxidase solution was 4.01 mg/ml. The film was made by initially delivering 0.5 ml of solution to the subphase, then transferring to a silicon substrate at a constant surface pressure of 30 mN/m.

Figure 3.7 shows a much less locally ordered pattern for native glucose oxidase than is seen for the modified enzyme. The white regions (valleys) tend to be more isolated, and roughly spherical. The dark regions (either patches of protein or else large area uncoated regions) are larger and more aggregated than for the modified glucose oxidase. The deposition pattern thus differs for native versus modified protein, consistent with the differences in coating thickness. The exact nature of the films is hard to discern from these images, but is clear they are not uniform, dense packed monolayers. Instead there is some local order and a large number of defects, making the films quite porous.

3.3.4 AFM images of modified glucose oxidase

The AFM image of one layer of modified glucose oxidase LB film prepared at a surface pressure of 30 mN/m is shown in Figure 3.8 with a scan area of 900 nm x 900 nm. Figure 3.8a and 3.8b show the top and two dimensional view, respectively. The coating procedure was the same as for preparing TEM samples. The modified enzyme solution was prepared by ultrafiltering a 55.4 mg/ml native glucose oxidase (Sigma, type X-S) solution after reaction with glutaraldehyde for 24 hours at room temperature. A 2 ml aliquot was delivered to the subphase and then transferred to a silicon substrate at a constant surface pressure of 30 mN/m.

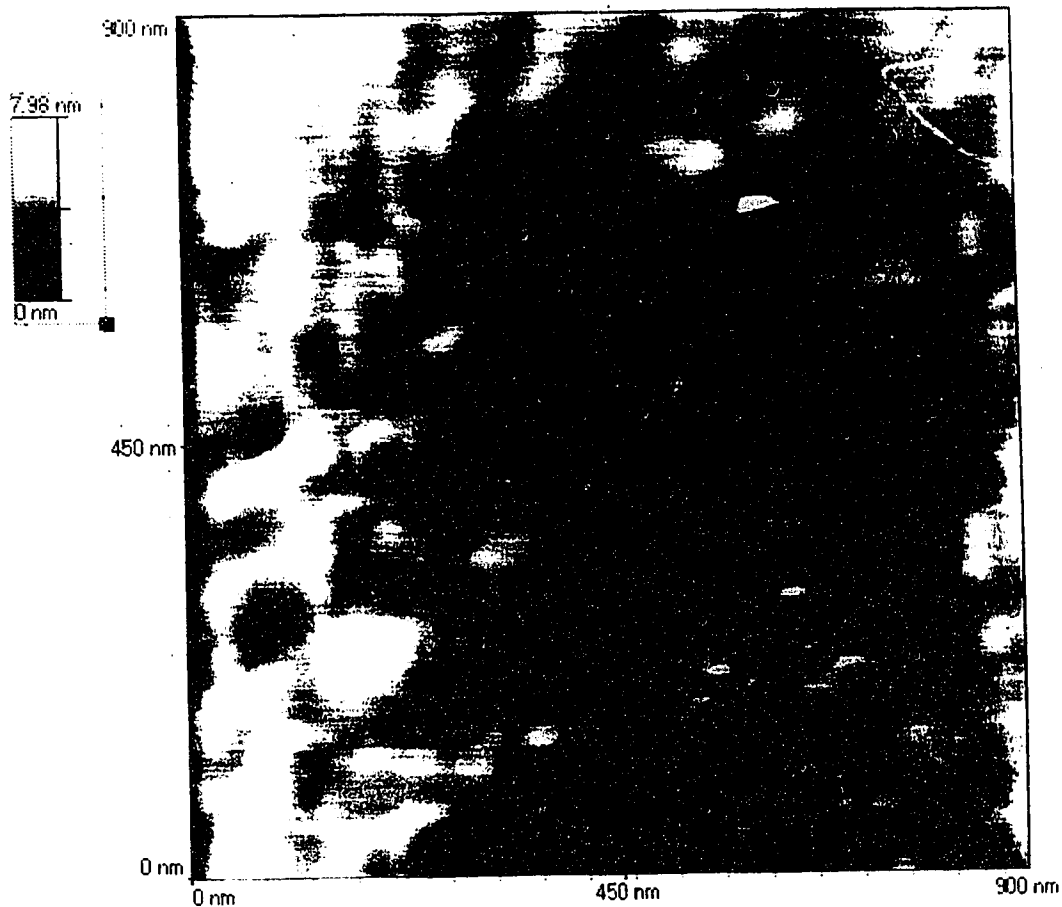


Figure 3.8a Top view AFM image of one layer of modified glucose oxidase LB film coated at a surface pressure of 30 mN/m. A scan rate of 5 $\mu\text{m/s}$ was used for the constant force (repulsive force) mode AFM imaging. The solution of modified GO was ultrafiltered.

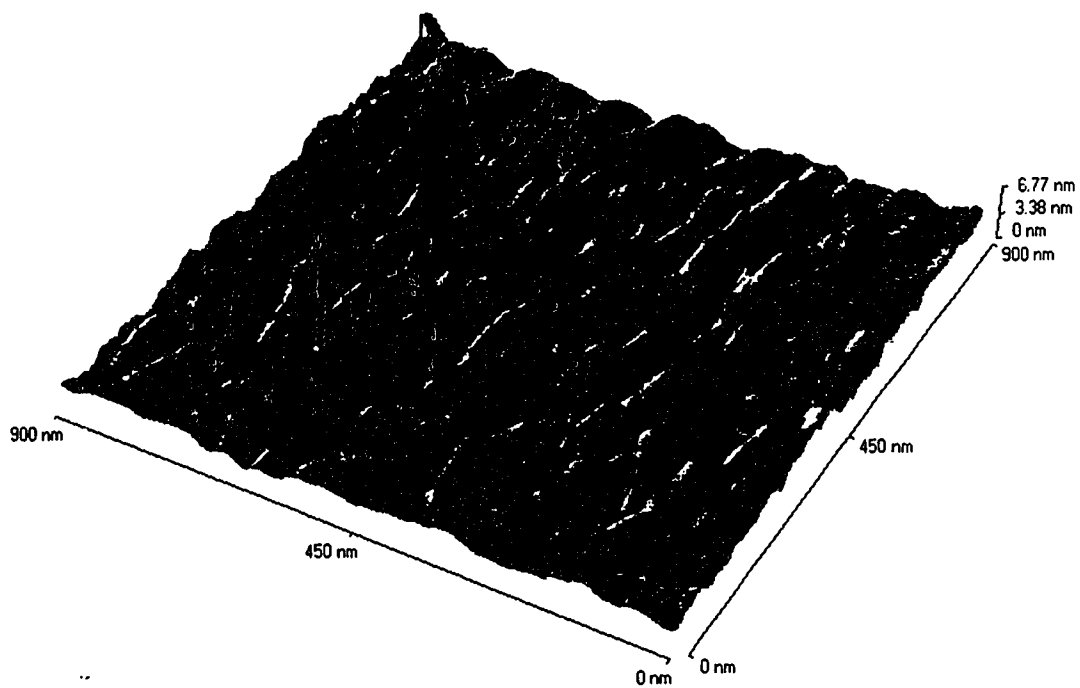


Figure 3.8b Two dimensional view AFM image of one layer of modified glucose oxidase LB film coated at a surface pressure of 30 mN/m. A scan rate of 5 $\mu\text{m/s}$ was used for the constant force (repulsive force) mode AFM imaging. The solution of modified GO was ultrafiltered.

In the AFM image the light areas represent the high regions of enzyme coated areas and the dark areas are the regions without or with less enzyme coating. Similar observations were obtained as with the TEM images. Both AFM and TEM images show a local order, with a parallel pattern and this pattern becomes random on a large scale.

From the AFM image, we see fewer valley regions. The high regions consist mostly of long narrow strands with two dimensions (a and b) in the range of 150 Å to 300 Å for a and 760 Å to 1450 Å for b. We also see that quite a few long strands are attached to each other. The size of the the attached strands is about 610 Å x 1450 Å.

The roughness of the surface topography can be determined from the AFM data. The SPM Lab V3.06 software gives an average surface roughness range of 45 Å to 52 Å. The discrepancy from TEM analysis may arise due to the AFM tip, causing change to the film by pushing it around as it gets too close, and might also be due to the AFM tip not sticking all the way down into the valleys. Alternatively, errors in the angle of shadow coating could lead to errors in the peak to valley ratio seen by TEM. It is interesting to compare the range seen by AFM to the total average thickness measured by ellipsometry, 45 Å. The good agreement suggests that the valleys we see are truly open space, not significantly coated by enzyme.

Figure 3.9 shows an AFM image of a silicon substrate without enzyme coating but coated with Pd/Pt alloy. Figure 3.9a is a top view picture and Figure 3.9b is a two dimensional picture at a scan rate of 5 μm/s. It shows a flat, uniform surface, and featureless topography. The area roughness analysis

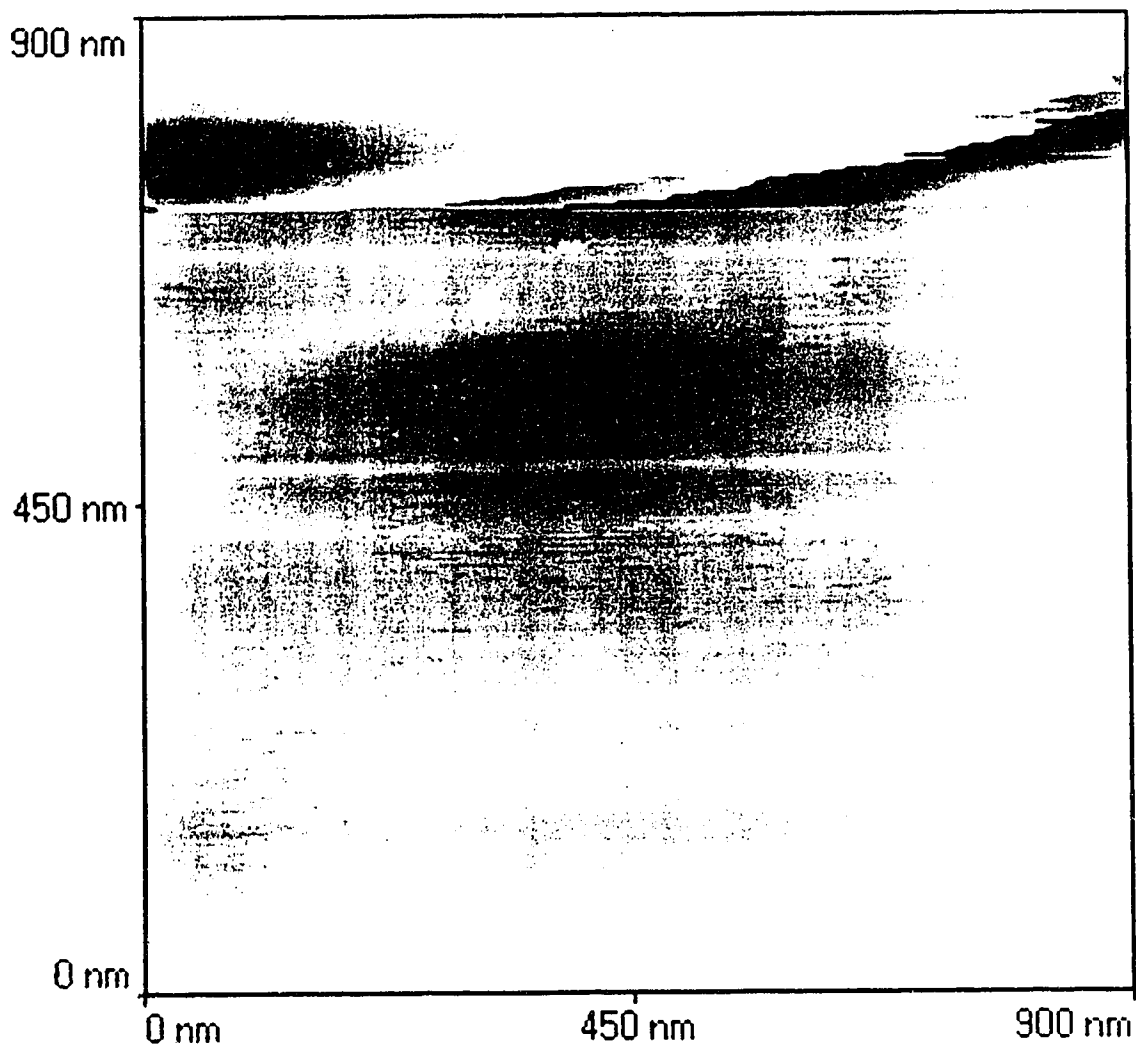


Figure 3.9a Top view AFM image of blank silicon substrate shadow coated with Pd/Pt alloy. A scan rate of 5 $\mu\text{m/s}$ was used for the constant force (repulsive force) mode AFM imaging.

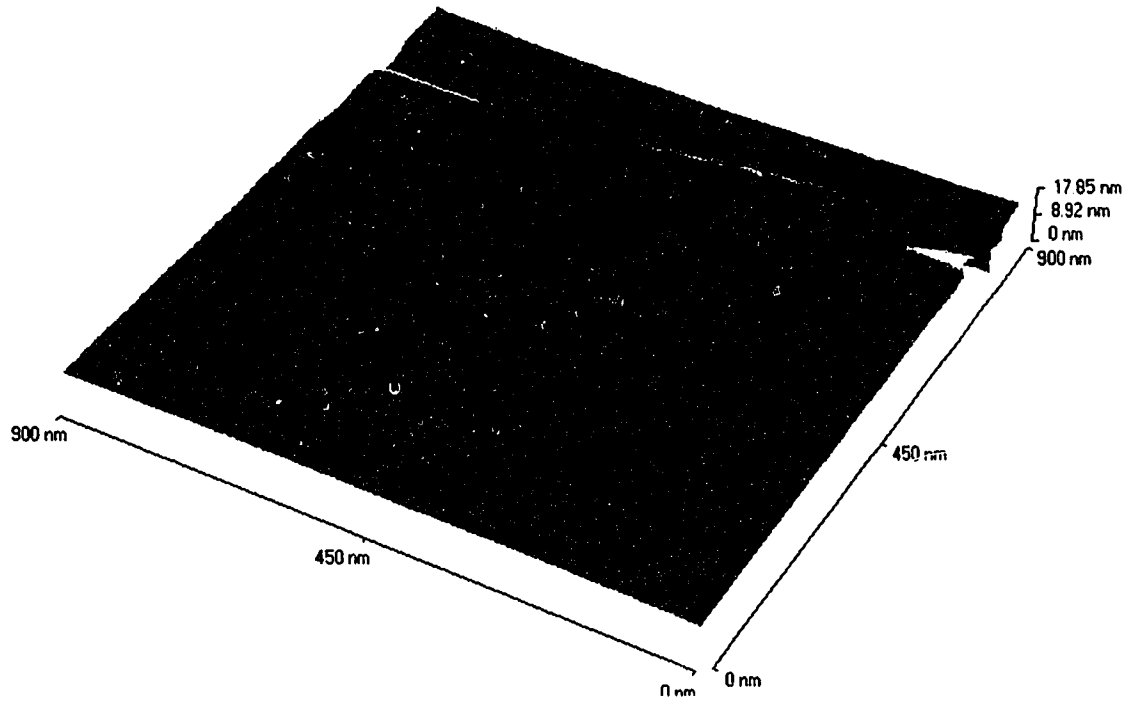


Figure 3.9b Two dimensional view AFM image of blank silicon substrate shadow coated with Pd/Pt alloy. A scan rate of 5 $\mu\text{m/s}$ was used for the constant force (repulsive force) mode AFM imaging.

gave a value of 15 Å to 20 Å. This is close to the average thickness for SiO₂ as we measured by ellipsometry, 18 Å. It is also close to the size of the metal islands, which probably are the source of the variation.

3.4 Conclusions

In this Chapter, we presented TEM images of both native and modified glucose oxidase LB films. The shape of the modified enzyme in the film is that of a continuous, long stranded snake, with some short branches attaching different strands to each other. There appears to be local order, with a parallel pattern, however, over large areas the pattern becomes random. On the larger scale, the overall film shows a continuous and homogeneous pattern for the modified glucose oxidase LB films. However, the roughness of the coating is still apparent.

The TEM images of native glucose oxidase shows a much less locally ordered pattern. The dark regions are larger and more aggregated than for the modified enzyme. This indicates that the film of native enzyme is not a truly uniform, dense packed monolayer.

Both TEM and AFM images of blank silicon substrate show a flat, smooth surface and appear uniform and featureless. This difference from the enzyme coated substrate is proof that we are observing the deposited glucose oxidase on the silicon substrate.

The same surface conformation as seen in the TEM images was observed again with the AFM technique, for modified glucose oxidase. The remarkable point of the AFM technique is that the roughness of the glucose oxidase LB film, 45 Å to 51 Å, obtained from the area roughness analysis is in good agreement with the thickness value measured by ellipsometry, 45 Å.

The thickness of the modified enzyme film estimated from TEM is in the range of 49 Å to 98 Å. The 98 Å thickness probably indicates glucose oxidase molecule are stacked up on each other. However, since the thickness measured by ellipsometry is an average value and across a much larger area, it is still consistent with the thickness measured by ellipsometry being lower on average. All of the data concur, that the film is locally ordered, but somewhat porous, and can not be regarded as a densely packed monolayer. However, the film is certainly close to a monolayer in thickness.

3.5 References

1. Vadimsky, R. G.; *Electron Microscopy, Polymers*, **1980**, Vol. 16, Part B, 185-235.
2. Furuta, M., *J. Polym. Sci., Polym. Phys. Ed.* **1976**, 14, 479.
3. Bassett, D.C.; Keller, A., *Philos. Mag.*, **1962**, 7, 1533.
4. Keith, H.D.; Padden, Jr. F. J.; Vadimsky, R. G., *J. Polym. Sci.*, **1966**, Part A-2 4, 267.
5. Tarin, P. M.; Thomas, E. L., *Polym. Eng. Sci.*, **1978**, 18 (6), 472.

6. Ries, H. E., Matsumoto, M.; Uyeda, N.; Suito, E., *Monolayers*, **1975**, American Chemical society, Washington D. C., 286 - 293.
7. Gaines, G. L., *Insoluble Monolayers at Liquid-Gas Interfaces*, **1966**, Chapter 8, 332 -333, New York, Interscience Publishers.
8. Mulhern, P. J.; Blackford, B. L.; Jericho, M. H., *AIP conference Proceedings 241*, 200 - 208, **1991**, New York.
9. Hansma, H. G.; Sinsheimer, R. L.; Gould, S. A. C.; Weisenhorn, A. L.; Gaub, H. E.; Hansma, P. K., *AIP conference Proceedings 241*, 136 - 143, **1991**, New York.
10. Drake, B.; Prater, C. B.; Weisenhorn, A. L.; Gould, S. A. C.; Albrecht, T. R.; Quate, C. F.; Cannell, D. S.; Hansma, H. G.; Hansma, P. K., *Imaging Crystals, Polymers, and Processes in Water with the Atomic Force Microscope*, *Science*, **1989**, Vol. 243, 1586-1589.

CHAPTER 4

CONCLUSIONS

4.1 Summary of the study on the LB films of glucose oxidase

A method of preparing active glucose oxidase film was demonstrated in Chapter 2. The Langmuir-Blodgett technique was shown to be a successful means of transferring active glucose oxidase films to a substrate without the need for any added lipid component. Up to at least 10 monolayers of enzyme have been transferred to a substrate by using the LB technique without any difficulty.

This method results in films with much increased sensitivity and improved response time for glucose determination when compared to lipid glucose oxidase films. The activity of the LB film of modified glucose oxidase can be compared semiquantitatively to a conventional BSA immobilized glucose oxidase film on Pt. For the BSA film an activity of 166 $\mu\text{A}/\text{mg}$ of glucose oxidase per mM glucose was measured by Sun *et al.* [1], based on the film composition and the quantity deposited on the electrode. The relative enzyme activity of Langmuir-Blodgett films of modified glucose

oxidase, $675 (\mu\text{A}/\text{mg})/\text{mM}$, is about 4 times higher than the conventional BSA immobilized film. Clearly, the modified glucose oxidase films transferred by the Langmuir-Blodgett technique has much better sensitivity than a conventional BSA immobilized film. The electrochemical activity measurement shows that the surface pressure of LB films affects the relative enzyme activity, since the activity/molecule is twice as high at 30 mN/m as it is at 20 mN/m. This effect may suggest that distortion of the enzyme structure is greater in the less dense film, which might decrease the activity. Alternatively, there may be better orientation of the enzyme for glucose oxidation when prepared in densely packed form.

The LB film thickness measured by ellipsometry shows a significantly increased thickness of cross-linked glucose oxidase films compared to the native glucose oxidase films. An average of 34 Å for native glucose oxidase and 45 Å for modified glucose oxidase at 30 mN/m were obtained. This result shows the cross-linking reagent, glutaraldehyde must stabilize the structure of glucose oxidase LB films. The cross-linking reagent, glutaraldehyde, greatly increases the activity of the enzyme films. The most likely role of the glutaraldehyde is to intra-molecularly link base residues on the enzyme in such a way as to increase its quaternary and tertiary structural rigidity and resistance to denaturing forces.

A detailed data set of pressure-area and mass-area isotherms was presented. The initial surface concentration affects the value of area per molecule obtained from pressure-area isotherm. The area per molecule obtained from pressure-area isotherm are about 1728 \AA^2 and 2571 \AA^2 at 0

mN/m for native and modified glucose oxidase, respectively at a surface concentration of 8.75 mg/m^2 and 9.11 mg/m^2 . This is well outside the value predicted by the hydrodynamic radius, 5800 \AA^2 per molecule. The area per molecule obtained from the QCM mass isotherms, of 5723 \AA^2 and 5611 \AA^2 for native and modified glucose oxidase, respectively, are in reasonable agreement with the area predicted from the known hydrodynamic radius of the enzyme. This study confirms that the surface pressure - area isotherms are unreliable, and that total mass deposited, as measured by the QCM gives more reliable data. From the measurement of film thickness by ellipsometry and area per molecule by QCM, the modified glucose oxidase film transferred by the Langmuir-Blodgett technique appears to be a reasonably compact monolayer at surface pressure of 30 mN/m . The experimental results are not really in agreement with the X-ray crystallographic dimensions of the dimer, which are $60 \text{ \AA} \times 52 \text{ \AA} \times 77 \text{ \AA}$ for glucose oxidase derived from *Aspergillus niger*. Instead the hydrodynamic radius is a better prediction of the area per molecule indicating the film is less dense than a crystal structure of glucose oxidase would be.

In Chapter 3, we presented TEM images of both native and modified glucose oxidase LB films and AFM image of modified glucose oxidase LB film. Both TEM and AFM images of modified glucose oxidase show a similar surface conformation. The shape of the modified enzyme in the film is that of a continuous, long stranded snake, with some short branches attaching different strands to each other. There appears to be local order, with a parallel pattern, however, over large areas the pattern becomes random. On a larger

scale, the overall film shows a continuous and homogeneous pattern for the modified glucose oxidase LB films. However, the roughness of the coating is still apparent.

The TEM images of native glucose oxidase shows a much less locally ordered pattern. The dark regions are larger and more aggregated than for the modified enzyme. This indicates that the film of native enzyme is not a uniform, dense packed monolayer.

The roughness of the surface topography can be determined from the AFM data. The SPM Lab V3.06 software gives an average surface roughness range of 45 Å to 52 Å. This range is smaller than that seen by TEM. The discrepancy may be due to the AFM tip, causing change to the film, pushing it around as the tip gets too close to the film. Alternatively, errors in the angle of shadow coating could lead to errors in the peak to valley ratio seen by TEM. It is interesting to compare the range seen by AFM to the total average thickness measured by ellipsometry, 45 Å. The good agreement suggests that the valleys we see are truly open space, not significantly coated by enzyme. The thickness of the modified enzyme film estimated from TEM is in the range of 49 Å to 98 Å. The 98 Å thickness probably indicates glucose oxidase molecule are stacked up on each other. However, since the thickness measured by ellipsometry is an average value and across a much larger area, it is still consistent with the thickness measured by ellipsometry being lower on average.

The results in the previous Chapters provide a general picture of the LB film of glucose oxidase, that the film is locally ordered, but somewhat

porous, and can not be regarded as a truly dense packed monolayer. However, the film is certainly close to a monolayer in thickness.

4.2 Future research directions

It is likely that the approach in this study would be useful in stabilizing other enzymes at the air-water interface, although a different choice of cross-linking agent would be necessary with enzymes that are denatured by glutaraldehyde. Even with glucose oxidase it could prove valuable to develop an alternate means of cross-linking the enzyme that is better characterized than the glutaraldehyde reaction [1].

The AFM image shows reasonable resolution of the Pd/Pt coated glucose oxidase LB film, but no successful image was obtained for the enzyme uncoated with Pd/Pt. The enzyme molecules were pushed by the tip out of the scan area due to the soft nature of biological structures. A good tip profile is much more important for imaging of biological structures than it is for atomic resolution of hard inorganic surfaces. In practice it may not be possible to avoid having several microtips in close proximity and high resolution imaging may only be obtainable if the imaging forces are reduced (i. e. imaging under water to eliminate capillary effects) or if the sample stiffness is increased (i. e. cooling samples to low temperatures) [2]. A continuing challenge for the AFM, as for other microscopes, is developing new sample preparation techniques. In the near future, the AFM provides images of larger

proteins with sufficient detail to allow computer simulations to converge on their three-dimensional structure [3].

4.3 References

1. Sun, S.; Ho-Si, P. H.; Harrison, D. J., *Langmuir*, **1991**, 7, 727-737.
2. Mulhern, P. J.; Blackford, B. L.; Jericho, M. H., *AIP conference Proceedings 241*, 200 - 208, **1991**, New York.
3. Drake, B.; Prater, C. B.; Weisenhorn, A. L.; Gould, S. A. C.; Albrecht, T. R.; Quate, C. F.; Cannell, D. S.; Hansma, H. G.; Hansma, P. K., *Imaging Crystals, Polymers, and Processes in Water with the Atomic Force Microscope*, *Science*, **1989**, Vol. 243, 1586-1589.